2011

Identification and Characterization of the Human Herpesviruses 6A and 6B Genome Integration into Telomeres of Human Chromosomes during Latency

Jesse Herbert Arbuckle
University of South Florida, arby09@netscape.net

Identification and Characterization of the Human Herpesviruses 6A and 6B Genome Integration into Telomeres of Human Chromosomes during Latency

by

Jesse Herbert Arbuckle

A dissertation submitted in partial fulfillment
of the requirements for the degree of
Doctor of Philosophy
Department of Molecular Medicine
College of Medicine
University of South Florida

Major Professor: Peter G. Medveczky, M.D.
Robert J. Deschenes, Ph.D.
Andreas Seyfang, Ph.D.
Alberto van Olphen, Ph.D., D.V.M.

Date of Approval:
April 26, 2011

Keywords: Human Herpesvirus 6, HHV-6, viral latency, genome integration, telomere, chromosome, germ-line transmission, recombination, viral reactivation, integrase, central nervous system diseases

DEDICATION

I would like to dedicate this dissertation to my mom Laura Smith, grandparents Ron and Peg Smith, brother Bart, sisters Heidi and Jennifer, uncles Mark and Brad Smith, aunts Susan and Beth Smith, great grandparents Kay and Herbert “Tink” Smith, grandfather Stan Arbuckle, and girlfriend Bernadette Marrero for all of their love and continued support of my short and long term goals.

ACKNOWLEDGMENTS

I would like to give a special thanks to my mentor Peter Medveczky who has guided me through the research of this dissertation project. I have appreciated the training in the fundamentals of molecular biology, and the skills of successful scientific writing, data analysis, and research conduct that are all necessary to become a principal investigator in academia. I have thoroughly enjoyed working in your laboratory as well as the support for presenting at international conferences. I would like to thank Maria Medveczky for her expertise in scientific techniques and for playing an integral role in the publication of our manuscripts. Both of you have been incredible mentors and friends, and for this I'm forever in debt to the both of you.

I would like to express my gratitude to Drs. Andreas Seyfang, Alberto Van Olphen, Robert Deschenes, and Philip E. Pellett for serving on my committee, imparting scientific advice, and guidance through the dissertation process.

I finally would like to acknowledge the Department of Molecular Medicine as well as the professors, staff, and students from the College of Medicine. Many of you have been played a vital role during my training at USF.

TABLE OF CONTENTS

LIST OF TABLES

LIST OF FIGURES

LIST OF ABBREVIATIONS

ALT	Alternative Lengthening of Telomeres
BAC	Bacterial Artificial Chromosome
cccDNA	Covalently Closed Circular DNA
CMV	Cytomegalovirus
CPE	Cytopathic Effect
DNA	Deoxyribonucleic Acid
DR_L	Left direct Repeat
DR_R	Right Direct Repeat
EBNA	Epstein-Barr Virus Nuclear Antigen
EBV	Epstein-Barr Virus
FISH	Fluorescent *in situ* Hybridization
GFP	Green Fluorescent Protein
HEK-293	Human Embryonic Kidney-293 Cells
HHV-6	Human Herpesvirus 6
HHV-6A	Human Herpesvirus 6A
HHV-6B	Human Herpesvirus 6B
HVS	Herpesvirus *saimiri*
iHHV-6	Inherited HHV-6
IPCR	Inverse PCR
IR	Inverted Repeats
KSHV	Kaposi's Sarcoma-associated Herpesvirus
LANA	Latency-Associated Nuclear Antigen
MDV	Marek's Disease Virus
MOI	Multiplicity of Infection
ORF	Open Reading Frame
PBMCs	Peripheral Blood Mononuclear Cells
PCR	Polymerase Chain Reaction
RNA	Ribonucleic Acid
RT	Room Temperature
STELA	Single Telomere Length Analysis
TERRA	Telomere-Repeat-Encoding RNA
TPA	12-O-Tetradecanoyl-13 Acetate
TR	Terminal repeats
TRF1	TTAGGG Repeat Factor 1
TRF2	TTAGGG Repeat Factor 2
TPE	Telomere Position Effect
TSA	Trichostatin-A
U	Unique
U_L	Unique Long
U_S	Unique Short

ABSTRACT

While the latent genome of most Herpesviruses persists as a nuclear circular episome, previous research has suggested that Human Herpesvirus 6 (HHV-6) may integrate into host cell chromosomes, and be vertically transmitted in the germ-line. Because the HHV-6 genome encodes a perfect TTAGGG telomere repeat array at the right end direct repeat (DR_R) and an imperfect TTAGGG repeat at the end of the left end direct repeat (DR_L), we established a hypothesis that during latency, the HHV-6A and HHV-6B genome integrates into the telomeres of human chromosomes through homologous recombination with the n(TTAGGG) viral repeats, and the integrated virus can be induced to lytic replication.

We sought, first, to definitively illustrate the *in vitro* and *in vivo* integration of HHV-6A and HHV-6B. Following infection of naïve Jjhan and HEK-293 cell lines by HHV-6A and Molt3 cell line by HHV-6B, the virus integrated into telomere of chromosomes. Next, peripheral blood mononuclear cells (PBMCs) were isolated from families in which several members, including at least one parent and child, had unusually high copy numbers of HHV-6 DNA per ml of blood. FISH confirmed that HHV-6 DNA co-localized with telomeric regions of one allele on chromosomes *17p13.3*, *18q23*, and *22q13.3*, while the integration site was identical among members of the same family. Partial sequencing of the viral genome identified the same integrated HHV-6A strain within members of families, confirming vertical transmission of the viral genome through the germ-line [inherited HHV-6 (iHHV-6)].

Amplification and sequencing of the HHV-6A and more recently HHV-6B viral-chromosome junction identified DR_R integrated into the telomere directly adjacent to the subtelomere of the chromosome. After mapping the DR_R of iHHV-6, we subsequently focused on determining if the DR_L was present in the integrated genome and whether the remaining telomere sequence of the chromosome was extended beyond the DR_L. Southern hybridization of PCR amplified HHV-6 integrated cell lines and iHHV-6 patients PBMCs indicate the presence of DR_L within the integrated viral genome. Moreover, the tandem array of telomere repeats [$(TTAGGG)_n$] at the end of chromosome was shown to extend beyond the DR_L of iHHV-6. Therefore, the genomic structure of the iHHV-6 is as follows: chromosome-subtelomere-$(TTAGGG)_{5-41}$-DR_R-U-DR_L-$(TTAGGG)_n$.

During latent integration, no circular episomes were detected even by PCR. However, trichostatin-A treatment of PBMCs and *in vitro* integrated HEK-293 cells induced the reactivation of iHHV-6 from its latent integrated state. We demonstrated the induction of integrated iHHV-6 with trichostatin-A lead to the excision of the integrated genome and generation of the U-DR-U junction which signifies circularization and/or concatemer formation of the viral genome through rolling-circle replication. Taken together, the data suggests that HHV-6A and HHV-6B are unique among human herpesviruses: they specifically and efficiently integrate into telomeres of chromosomes during latency rather than forming episomes, and the integrated viral genome is capable of producing virions.

INTRODUCTION

Classification of Human Herpesviruses

Human Herpesviruses are ubiquitous and belong to the family of *Herpesviridae* which features large enveloped virions. The Herpesvirus virion contains a single double stranded DNA (dsDNA) genome ranging from 150 to 230 kbp that is packaged in an icosahedral capsid (1). The viral nucleocapsid is surrounded by a proteinaceous tegument often consisting of proteins necessary for initiation of viral genome replication and degradation of cellular mRNAs. Following the capsid and tegument layers, the virion is encased by an envelope that is obtained from the host cell's plasma membrane or cellular organelles during the process of budding.

Human Herpesviruses can be subdivided into three major subfamilies characterized by their genome sequence and structure, as well as host cell range during lytic and latent infection (**Table 1**) (1). The Alphaherpesviruses: Herpes Simplex virus type 1 (HSV-1), HSV-2, and Varicella Zoster virus (VZV) infect and establish latency within neurons. The Gamaherpesviruses: Epstein-Barr virus (EBV) and the Kaposi's Sarcoma-associated Herpesvirus (KSHV) infect B-lymphocytes, while various malignant diseases can occur during latent infection. Betaherpesviruses: Human Herpesvirus 6A (HHV-6A), HHV-6B, HHV-7, and Cytomegalovirus (CMV) are characterized upon their ability to establish latent infection in monocytes and retain similarities in their genes and genomic structure amongst these viruses.

Table 1. Classification of Human Herpesviruses (1).

Designation	Common Name	Abbreviation	Subfamily	Genome Size (kbp)
HHV-1	Herpes Simplex virus 1	HSV-1	Alpha	152
HHV-2	Herpes Simplex virus 2	HSV-2	Alpha	155
HHV-3	Varicella-Zoster virus	VZV	Alpha	125
HHV-4	Epstein-Barr virus	EBV	Gamma	172
HHV-5	Cytomegalovirus	CMV	Beta	230
HHV-6A	Human Herpesvirus 6A	HHV-6A	Beta	159
HHV-6B	Human Herpesvirus 6B	HHV-6B	Beta	162
HHV-7	Human Herpesvirus 7	HHV-7	Beta	145
HHV-8	Kaposi's Sarcoma-associated Herpesvirus	KSHV	Gamma	170

Human Herpesvirus 6 (HHV-6) was initially recognized as Human B-Lymphotropic virus (HBLV) by Salahuddin *et al*. in 1986, given that the virus was isolated from B-lymphocytes of patients infected with HIV, HTLV, and lymphoproliferative disorders (2). However, through further molecular and clinical studies, as well as sequencing of the viral genome, the virus was found to include two different species; HHV-6A and HHV-6B (3-6). HHV-6A and HHV-6B have been shown to productively infect T-lymphocytes, monocytes/macrophages, human umbilical cord blood, and various cell lines (7-11).

Furthermore, in 1988 Yamanishi *et al.* established that HHV-6B primary infection in young children is the etiological agent of exanthema subitum (roseola infantum), which is characterized by high fever, diarrhea, and a mild skin rash along the trunk, neck, and face (5, 12). Serologic studies have found that by the age of two, 90% of children have acquired a primary HHV-6 infection (13, 14). As for HHV-6A, the virus has been associated with several adult diseases; including cofactor in AIDS progression, and

various neurological disorders including encephalitis, ataxia, seizures, and chronic fatigue syndrome, however the causal link between human disease and virus infection remains to be fully elucidated (6, 15-23).

Genome Organization of Human Herpesviruses

The genome of Human Herpesviruses are linear double-stranded DNA ranging in sizes from 150 to 230 kbp (1)**.** Human Herpesviruses also contain repetitive sequences longer than 100bp that vary among sequence, location, and complexity among the different species (**Fig. 1**). Terminal repeats (TR) and direct repeats (DR) located at the termini of herpesvirus genomes permit circularization. Several Human Herpesviruses also encode inverted repeats (IR) flanking the unique long (U_L) and unique short (U_S) portion of the viral genome. The IRs are essential for segment inversion during recombination, which generates multiple isomers of the viral genome. VZV has two isomeric forms, while HSV-1, HSV-2, and CMV have 4 isomeric forms. HHV-6A, HHV-6B, HHV-7, EBV, and KSHV lack IRs that permit recombination and thus only exist as one isomer.

Replication of Herpesviruses

The nine known Human Herpesviruses can replicate in various cell types depending on their unique features. However, the replication cycle of these Herpesviruses share several common features. During the course of lytic infection, the viral envelope of Herpesviruses fuse with the cell's plasma membrane and the nucleocapsid releases the linear viral genome into the nucleus (**Fig. 2**) (1). Subsequently the linear genome of Herpesviruses circularizes and initiates the expression of the so-called immediate early genes.

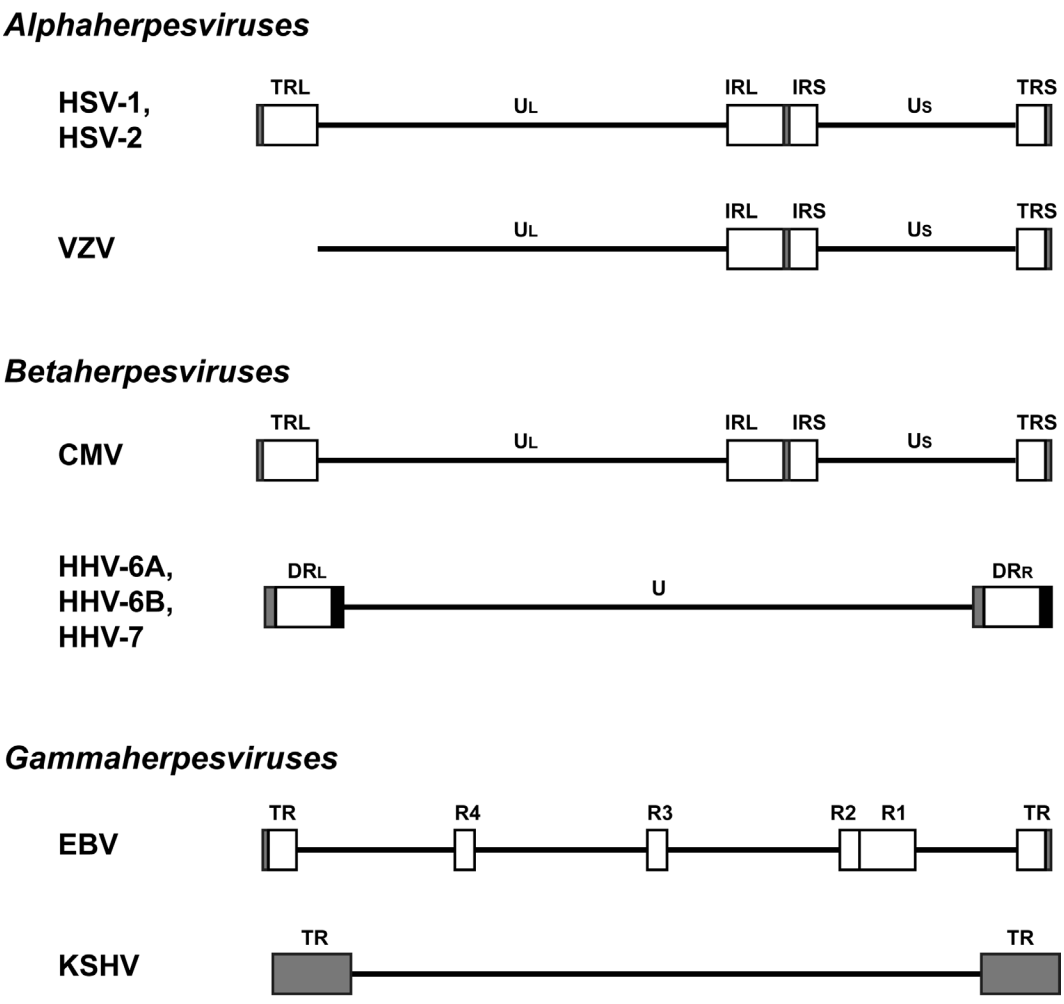

Fig. 1. Genome organization of Human Herpesviruses. The unique (U), unique long (U_L), and unique short (U_S) coding region of the viral genome (solid lines) is flanked by terminal (TR) and inverted repeats (IR) (box regions). The left direct repeat (DR_L) and right direct repeat (DR_R) of HHV-6A, HHV-6B, and HHV-7 encode perfect (black box) and imperfect (gray box) telomere TTAGGG repeats (1, 3, 4).

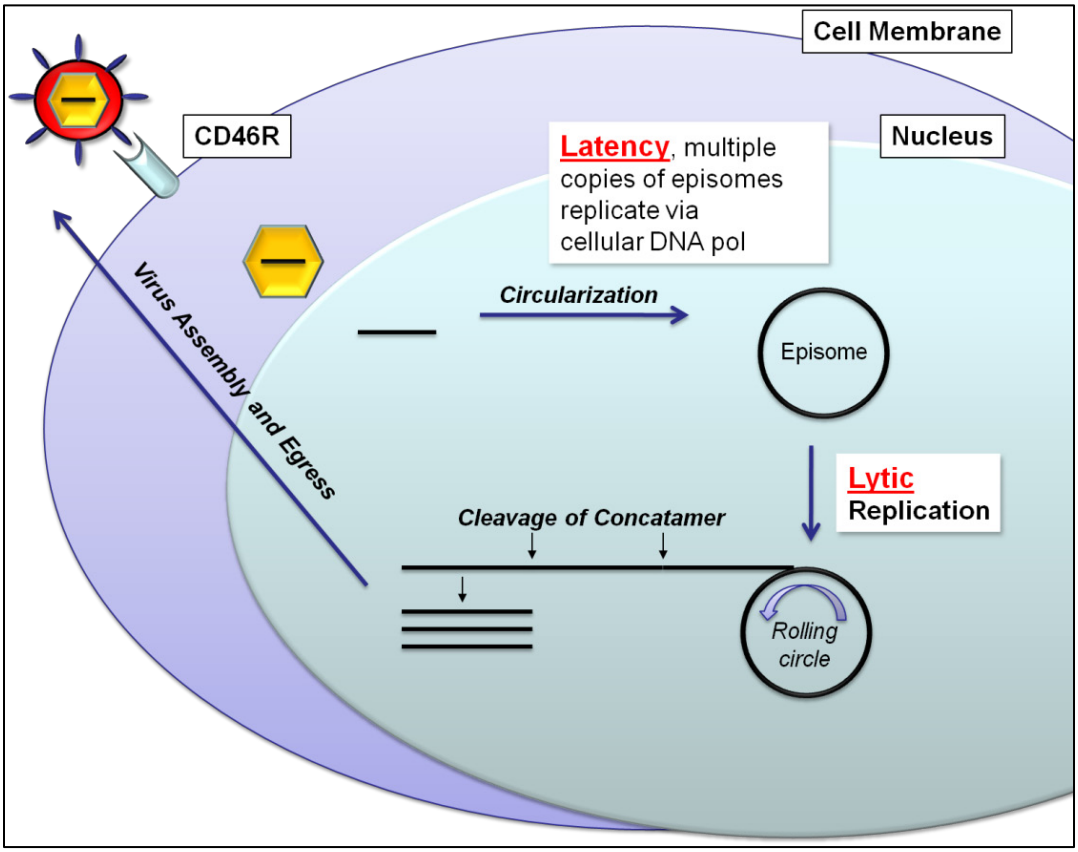

Fig. 2. Schematic representation of lytic and latent replication of Herpesviruses. During lytic infection, the HHV-6A and HHV-6B viral envelope fuses with the cell's plasma membrane through CD46R (24, 25). The nucleocapsid then enters the cell and releases the linear viral genome into the nucleus (1). Subsequently, the genome of Herpesvirus circularizes to form the viral episome and lytic or latent infection can proceed. Lytic infection results in rolling-circle replication of the viral genome, cleavage of concatemer, viral assembly, and egress. During latent infection, the genome replicates as multiple copies of episomes in the absence of virion maturation. However, the integration of HHV-6A and HHV-6B into the telomere of chromosomes during latency will be further discussed in subsequent sections.

The immediate early gene products activate the viral DNA polymerase and replication of the viral genome occurs via rolling-circle mechanism (26, 27). Rolling-circle replication leads to the formation of concatemers consisting of linear viral genomes linked in a head-to-tail conformation that are subsequently cleaved to give rise to single copies of the complete viral genome. During the last late stage of the replication cycle, various components of the virion are produced in large quantities, new virions are formed, and the infected cell dies.

Maintenance of Latent Herpesviruses Genomes by Episomal Replication

However, not all infections lead to immediate production of mature virions. Following primary infection, the genome of Herpesviruses can establish latency as a nuclear circular episome (**Fig. 2**) (1, 26, 27). The expression of latent viral genes allows the stable replication and persistence of the latent viral genome. During latency the cellular DNA polymerase and latency-associated viral genes promote genome replication of Herpesviruses without production of infectious virus, however the genomes of HSV-1 and HSV-2 do not replicate during neuronal latency. Therefore, the central dogma of Herpesvirus replication is that the viral genome establishes latency as a nuclear circular episome and reactivation occurs through rolling-circle DNA replication (1, 26, 27). However findings over the last two decades suggest this may not be the case as pertaining to latency of HHV-6A and HHV-6B latency (28-34).

Luppi *et al.* identified the HHV-6 genome linked to a high molecular weight cellular DNA in peripheral blood mononuclear (PBMCs) in three patients (34). The initial observation of HHV-6 integration into the human genome was confirmed by other laboratories (28-32); however the significance of this event, the location of viral

integration, and whether the integrated viral genome reactivates from its integrated state had not been fully characterized.

Results completed in this dissertation demonstrate the *in vivo* and *in vitro* integration of HHV-6A and HHV-6B into the telomeres of human chromosomes during latency (33). Moreover, HHV-6A and HHV-6B viral reactivation from its latent integrated state was demonstrated in patient PBMCs and *in vitro* integrated cell lines. This dissertation details the current knowledge of HHV-6 genome structure during latent infections, the viral and cellular genes that could perhaps mediate integration, and lastly discuss the cellular as well as the clinical impact of viral integration into the telomeres.

Integration of Herpesviruses and Retrotransposons into Chromosomes

Epstein-Barr Virus

During latency, the episomes of Herpesviruses associate with chromosomes through the expression of viral DNA binding proteins such as EBV nuclear antigen-1 (EBNA-1) and KSHV's latency-associated nuclear antigen (LANA) (35, 36). The binding of EBNA1 and LANA to chromosomes is not site-specific, but this association of EBV and KSHV episomes with chromosomes ensures each infected cell obtains multiple copies of the viral episome during cell division. However, in rare cases as shown by EBV, the full length genome infrequently integrates into random chromosome sites during latency (37, 38). The integration of EBV into chromosomes has been demonstrated during long-term passage of infected cell lines and the isolation of reactivated virus from these cell lines has not been established.

Marek's Disease Virus

Similar to the integration of iHHV-6A and iHHV-6B into telomeres of human chromosomes during latency (further discussed in subsequent sections) (33), the Gammaherpesvirus Marek's disease virus (MDV) frequently integrates into the telomere of chickens through telomeric repeats $(TTAGGG)_n$ encoded in the internal repeat short (IRS) of the viral genome (39-41). MDV is acquired through inhalation of virions released from the dander of infected chickens. During latency, the linear ~180 kbp dsDNA genome integrates into multiple telomeres of chickens in each cell. The expression of viral oncogenes Meq and viral telomerase RNA (vTR) induces transformation of T-cells and leads to the rapid formation of solid visceral tumors and T-cell lymphomas within two to six weeks.

Retrotransposon TRAS1

The sequence specific integration of the retrotransposable element TRAS1 (telomeric repeat-associated sequence) was found to frequently integrate within the $(TTAGG)_n$ telomere repeat of the silkworm, *Bombyx mori* (42). The method of integration occurs through cleavage of the telomere TTAGG sequence by the TRAS1 endonculease and the fusion with the TTAGG terminal repeats encoded in TRAS1 (43). In summary, the specific integration of iHHV-6A and iHHV-6B into telomeres during latency is a novel process for a Human Herpesvirus (33). However, the similar strategy of telomere integration is also employed by the avian herpesvirus MDV and the silkworm retrotransposon TRAS1 (39-43).

Genome of Human Herpesvirus 6A and 6B

In particular, the viral genome of HHV-6B is 162 kbp long, containing 119 unique open reading frames (ORF), while HHV-6A genome contains 119 unique ORF and is 159 kbp long (3, 4). The genomic architecture of HHV-6A and HHV-6B is organized into two major regions (**Fig. 1**). The unique (U) region of the genome which is ~143 kbp, contains seven major core gene blocks that are conserved amongst Herpesviruses. These conserved genes are responsible for replication, cleavage, and packaging of the viral genome into the capsid. Additionally, these viral genes include: DNA binding protein, DNA polymerase, capsid, tegument, glycoproteins, and proteinase. Also, the U region contains blocks of CMV related genes known as US22 family that are conserved amongst Betaherpesviruses.

The second major genomic regions of HHV-6A and HHV-6B is the ~8 kbp left and right direct repeats (DR) located at the termini of the U region (**Fig. 1**) (3, 4). Within the right end direct repeat (DR_R) and the left end direct repeat (DR_L) the HHV-6A/HHV-6B genome encodes a perfect TTAGGG telomere repeat array and an imperfect TTAGGG repeat. The viral TTAGGG repeat sequence is conserved with the telomere sequence of human chromosomes and also encoded within the DR of HHV-7 (44). Details about this telomere repeat region will be further discussed in subsequent sections.

The distinction between HHV-6A and HHV-6B can not only be classified by their differences in clinical disease association, but also differences in their restriction fragment length polymorphism and the nucleotide sequence of their genomes (3, 4, 33). The nucleotide sequence identity between HHV-6A and HHV-6B is 90%. The variation in nucleotide sequence is not only observed between HHV-6A and HHV-6B, but also between clinical isolates and laboratory strains of the virus. Variability in the number of

telomere repeats within the DR of clinical HHV-6A and HHV-6B isolates is observed in the range of 15 to 180 repeats (33, 45). Furthermore, preliminary experiments suggest that ORF U2 through U5 (46), as well as DR1 through the first exon of DR6 (47) are dispensable for *in vitro* viral replication. These examples demonstrate the plasticity of the HHV-6 genome as well as variability in the sequences of HHV-6A and HHV-6B which warrant consideration for these viruses to be classified as different herpesvirus species rather than merely a subtype distinction between “A” and “B” (48).

Pathologies and Unique Features of Human Herpesvirus 6B

Human Herpesvirus-6 (HHV-6) was initially recognized as Human B-Lymphotropic virus (HBLV) by Salahuddin *et al*. in 1986, given that the virus was isolated from B-lymphocytes of patients infected with HIV, HTLV, and lymphoproliferative disorders (2). However, through further molecular and clinical studies, as well as sequencing of the viral genome, the virus was found to include two different species; HHV-6A and HHV-6B (3-6). HHV-6A and HHV-6B have been shown to productively infect T-lymphocytes, monocytes/macrophages, human umbilical cord blood, and various cell lines (7-11).

Furthermore in 1988, Yamanishi *et al.* established that HHV-6B primary infection in young children is the etiological agent of exanthema subitum (roseola infantum), which is characterized by high fever, diarrhea, and a mild skin rash along the trunk, neck, and face (5, 12). Serologic studies have found that by the age of two, 90 % of children have acquired a primary HHV-6 infection due to a persistent level of HHV-6 DNA and antibodies detected in saliva (13, 14, 49). Few cases have also reported severe complications such as febrile seizures, encephalitis, hepatitis, thrombocytopenia, and hemophagocytic syndrome (12, 18, 50-52). Viral reactivation has also been shown

to induce graft rejection in solid organ and bone marrow transplantation, seizures, and encephalitis (6, 16-19, 53).

Pathologies and Unique Features of Human Herpesvirus 6A

The infection of multiple cell types by HHV-6B and HHV-6A occurs through attachment to the complement regulator receptor CD46 (24, 25). The diverse cell tropism and multiple disease associations with HHV-6A/HHV-6B are due, in part, to the expression of CD46 present on the surface of all nucleated cells. In particular, HHV-6A has been associated with several adult diseases; including cofactor in AIDS progression, and various neurological disorders including encephalitis, ataxia, seizures, and chronic fatigue syndrome (6, 15-23). However the causal link between human disease and virus infection remains to be fully elucidated.

Results supporting HHV-6A as a co-factor in AIDS progression are based upon several different lines of evidence. First, HHV-6A infection contributes to the killing of CD-4 lymphocytes (11, 20, 54). Second, HHV-6A and HIV co-infection of the CD4 lymphocytes has shown to enhance HIV replication through activation of the long terminal repeats (LTR) (21). However, the most compelling data was completed in a study by Lusso *et al*. in which dual infection of macaques with HHV-6A and simian immune virus (SIV) enhanced the progression to AIDS at a faster rate when compared to those macaques infected with SIV alone (20).

Additionally, HHV-6A has a greater neurotropism when compared to HHV-6B due to increased concentration of viral DNA present in the plaques of patients' brains with MS and its ability to establish latency in oligodendrocytes (6, 55-57). In particular, Goodman *et al.* obtained biopsies from 5 patients brain tissue containing acute lesions attributed to MS (56). *In situ* polymerase chain reaction detected HHV-6 DNA in

oligodendrocytes, microglia, and lymphocytes, while immunocytochemical staining identified viral antigens in microglia and astrocytes. Cermelli *et al.* utilized laser microdissection to selectively isolate MS plaques from normal appearing white matter (55). HHV-6 DNA was detected in 57.8 % of MS plaques and only in 15.9 % of normal appearing white matter. However, 26.8 % of healthy brain tissue and 21.7 % of brain tissue from patients with various neurological disease were positive for HHV-6, which indicates that HHV-6 may normally reside in the brain (58).

Several investigators reported an increase in anti-HHV-6 IgG and IgM antibody titers and HHV-6A DNA and RNA during clinical relapse of MS compared to controls (59-61). HHV-6 DNA was also detected in the CSF and brain tissues at higher levels than control individuals (55, 62). Interestingly, markers of HHV-6 infection increased during relapse and decreased during remission (60, 63). In summary, these reports suggest HHV-6A may have a role in MS progression; however the interpretation of these findings remains uncertain.

Chromosome Integration of the Human Herpesvirus 6 Genome

Primary infection of HHV-6 leads to an increase in viral copies present in peripheral blood of children and subsequent decrease in viral copies during latency (5, 12-14, 16). The genome of Herpesviruses forms a nuclear circular episome during latency and the minimal amounts of viral genes are expressed to allow the stable replication of the viral genome. However, in a select number of patients including adults and children, there are high copies of HHV-6 genome consistently detected in peripheral blood measuring greater than 1 million copies per ml or 1 copy of HHV-6 per cell (31, 33, 64, 65). Moreover, Jarrett *et al.* identified a patient with HHV-6 detected in multiple tissues which is suggestive of germ-line transmission (66). In 1993 Luppi *et al.* identified

a unique high molecular weight viral fragment present in PBMCs of three patients with elevated copies of HHV-6 (34). This high molecular weight fragment resolved by pulse field gel electrophoresis demonstrated one of the earliest observations of viral integration into the genome. Subsequently, several other labs have shown integration of HHV-6 into human chromosomes through fluorescent *in situ* hybridization (FISH) and PCR amplification allowed for the detection of HHV-6 sequences in hair follicles, lymph node, spleen, kidney, brain, liver and cardiac tissues (28, 29, 31, 66, 67). The FISH assay however, cannot distinguish non-covalent linkage of viral episomes from integration or establish the specific site of viral integration.

Despite previous publications (28-32, 34, 64-66), investigators lacked conclusive results supporting the integration of HHV-6 into chromosomes and whether the integrated viral genome represented a latent infection remained unanswered. Therefore, these questions will be addressed in subsequent sections.

Telomere Biology

The human telomere is a repetitive TTAGGG dsDNA sequence extended from the end of chromosomes (**Fig. 3**) (68-70). The telomere repeat is bound by a set of proteins that form the shelterin complex. TTAGGG repeat factor 1 (TRF1), TRF2, and protection of telomeres 1 (Pot1) directly bind to the telomeric TTAGGG repeat. The shelterin complex is then maintained through interaction with TRF1-Interacting Nuclear Factor 2 (TIN2), TPP1 (TINT1, PIP1, PYOP1), and Repressor Activator Protein 1 (RAP1). Until recently, telomeres were believed to be transcriptionally silent; however mammalian telomeres were shown to transcribe telomere-repeat-encoding RNA (TERRA) (71). TERRA stabilizes the shelterin complex and facilitates telomere heterochromatin formation through direct interaction with TRF1 and TRF2 (72).

Therefore, the repetitive TTAGGG telomere sequence, shelterin complex, and TERRA protect the ends of chromosomes from double stranded breaks, chromosome fusions, and inhibit telomerase mediated lengthening (68-72).

The telomere length in somatic cells is 5-15 kbp and after every cell division, 250-300 bp are lost from the end of telomeres due to the challenges encountered with the process of end replication (70). The Hayflick limit occurs when telomeres reach a critical length, and cells undergo replicative senescence or apoptosis (73). Telomeres can be lengthened by telomerase reverse transcriptase (TERT) through the addition of the TTAGGG repeat (70). Telomerase mediated telomere lengthening has been detected in germ-line cells, cancer cells, and stem cells (74).

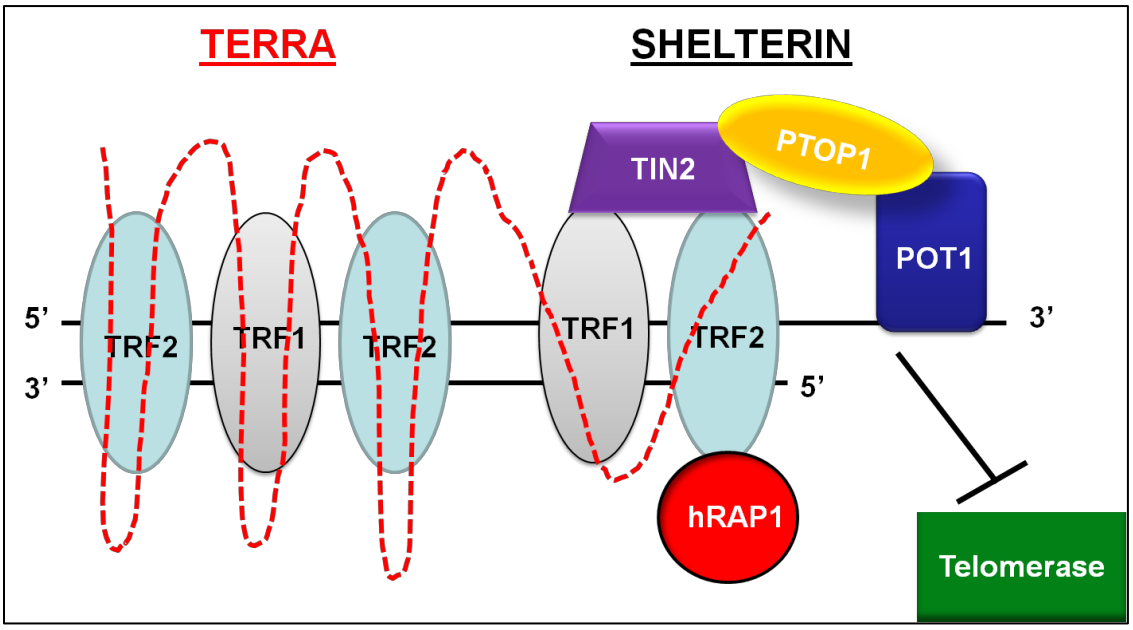

Fig. 3. Diagram of the shelterin complex and TERRA maintenance of telomere ends. The double stranded repetitive TTAGGG telomere sequence (black lines) is bound by the TRF1 and TRF2, while the interaction of POT1 with the 3' end of the telomere promotes strand invasion of the telomere duplex-loop (not shown) (68-70). TERRA (red line) stabilizes the shelterin complex and facilitates telomere heterochromatin formation through the direct interaction with TRF1 and TRF2 (72). Collectively, the shelterin complex inhibits telomerase mediated lengthening, double stranded breaks, and chromosome fusions (68-72).

Shay *et al.* estimated that 85 % of all malignant and transformed cells utilize telomerase to lengthen their telomeres to prevent telomere attrition (74). However, telomere length can also be maintained through the recombination mediated alternative lengthening of telomeres (ALT) (75, 76). The mechanism of ALT has yet to be fully characterized; however one method suggests that circular extrachromosomal telomeric repeats (T-circle) formed from the lost of the telomere-loop (T-loop) at the end of telomeres may serve as a template for telomere lengthening through rolling-circle replication (77-80). Similar to the replication of T-loops, the circular episome of herpesviruses also replicate through rolling-circle replication which leads to the formation of viral concatemers (**Fig. 2**) (26, 27).

The integration of HHV-6A and HHV-6B into telomeres is a newly identified form of human herpesvirus latency that will be discussed in this dissertation (33). The knowledge attained from the virus telomere biology may play a critical role in understanding the process of virus replication and integration.

Significance

HHV-6A and HHV-6B have been identified as cofactors in AIDS progression, graft rejection in transplants, as well as associated with MS and various neurological symptoms (6, 16-21, 53, 55-57). Furthermore, 90 % of the population has acquired a primary HHV-6 infection by three years of age (13, 14). The prevalence of high HHV-6 viral load (10^6-10^7 copies per ml of blood) has been described in several British cohorts (64, 65) attributed to chromosome integration of HHV-6. The prevalence of high viral loads in normal blood donors was 0.8 % (4/500) (64) and 1.0 % (57/5638) (81) . In contrast, prevalence of integrated HHV-6 in hospitalized patient cohorts was higher, 2.9 % (13/449) (64) and 3.3 % (6/184) (65). Therefore, it's essential that investigators

determine the overall clinical impact the integrated virus may have on hospitalized patients and disease progression. As a result, the significance of this dissertation is the characterization of the novel mechanism by which HHV-6A and HHV-6B integrates into telomeres of human chromosomes during latency and the reactivation of the integrated virus to lytic replication.

OBJECTIVES

HYPOTHESIS: During Latency, the Human Herpesviruses 6A and 6B Genome Integrates into the Telomeres of Human Chromosomes through Homologous Recombination with the n(TTAGGG) Viral Repeats, and the Integrated Virus can be Induced to Lytic Replication

AIM I. To Determine whether the Human Herpesviruses 6A and 6B Genome Integrates into Chromosomes of *in vitro* Infected Cell Lines

AIM II. To Determine that Human Herpesviruses 6A and 6B Genome Integrates into the Telomeres of Patients through Germ-Line Transmission

AIM III. To Determine if the Telomere Integrated Human Herpesviruses 6A and 6B Genome can Reactivate from Latency and Produce Infectious Virus

MATERIALS AND METHODS

Cell Lines, Primary Human T-cells, Media, and Virus Strains

Heparinized peripheral blood from four families with germ-line inherited HHV-6 (iHHV-6) was obtained by the HHV-6 Foundation (**Table 11**), after the subjects had given informed consent. PBMCs were isolated by diluting peripheral blood with an equal volume of RPMI-1640 and slowly pipetted onto isotonic density gradient of Lymphoprep™ (Axis-Shield, Oslo, Norway). Since Lymphoprep™ has a density of 1.077 g/ml, mononuclear cells can be isolated from the interphase while erythrocytes and granulocytes form a pellet (82). Samples were centrifuged for 30 min at 800 x g, 25°C. Mononuclear cells were isolated from the buffy coat located at interphase, resuspended in RPMI-1640, and centrifuged for 10 min at 250 x g, 25°C. The pellet of mononuclear cells was then resuspended in RPMI-1640 media containing 10 % FBS and 5 µg/ml PHA (Sigma-Aldrich, St. Louis, MS) for 72 hrs followed by culturing in 100 U/µl IL-2 medium to promote the expansion of primary T-cells.

T-cell lines Jjhan (HHV-6 Foundation), Molt3 (ATCC), and Burkitt's lymphoma cell line Raji (ATCC) were maintained in RPMI-1640 complete medium containing 10% FBS and 50 µg/ml gentamicin sulfate. Human embryonic kidney-293 cells (HEK-293) were maintained in DMEM supplemented with 10 % FBS and 50 µg/ml gentamicin sulfate. HHV-6A (U1102 strain) and HHV-6B (Z29 strain) viruses were supplied by P. Pellett (Wayne State University). HHV-6 integrated Burkitt's lymphoma cell line Katata was supplied by M. Daibata (Kochi Medical School, Japan) (83).

Human Herpesvirus-6 *in vitro* Integration and Infection of Cell Lines

To evaluate if HHV-6 frequently integrates in culture, we infected both T-cell lines and HEK-293 cells (**Table 2**). To begin, HEK-293 cells cultured at 50 % confluency were infected with HHV-6A (U1102) at 0.1 multiplicity of infection (MOI). The cultures were incubated for five days. Then the cells were washed to remove extracellular virus, and single cells were introduced in each well of a 96 well plate. Single HEK-293 cell clones were expanded and genomic DNA was isolated through Wizard® Genomic DNA Purification Kit (Promega, Madison, WI), while remaining cells were stored at -80 ºC in 10 % DMSO and FCS. To determine which clones were successfully infected with HHV-6A, the presences of the viral genome was determined by PCR for ORF U94 (**Table 6**) and agarose gel electrophoresis. Evaluation of *in vitro* HHV-6A integration was competed by FISH with HHV-6 cosimd probes (**Table 3**) (84) and inverse-PCR coupled with Southern blot hybridization (85).

Moreover, HHV-6A and HHV-6B infection and integration was evaluated in two T-cell lines (**Table 2**). In these experiments, the T-cell line Jjhan was infected with HHV-6A (U1102) and the T-cell line Molt3 was infected with HHV-6B (Z29). After removal of dead cells through Lymphoprep™ isotonic density gradient, 10^7 T-cells were infected with HHV-6A and HHV-6B at 1.0 MOI in 1 ml of RPMI-1640 complete for 2 hrs at 37°C. Unabsorbed virus was removed by centrifugation for 5 min at 1,500 rpm, 25°C. Cell pellet was resuspended to 10^6 cells/ml and incubated at 37 ºC, 5 % CO_2. DNA was prepared from cells at the peak of cytopathic effect (CPE) (5 – 14 days), containing ~10^3 infectious units/ml of virus. HHV-6A and HHV-6B viral integration into T-cell lines (Jjhan and Molt3) were evaluated by amplification of the viral genome-telomere junction using chromosome specific primers (**Table 8**). Southern blot hybridization and sequencing of

pCR®4-TOPO® (TOPO TA Cloning® Kit for Sequencing, Invitrogen, Carlsbad, CA) clones confirmed chromosome integration.

Table 2. HHV-6A and HHV-6B chromosome integrated cell lines.

Cell lines	Virus	Description
HEK-293	HHV-6A	Three single cell clones derived
Jjahn (T-cell)	HHV-6A	Mixed infection
Molt3 (T-cell)	HHV-6B	Mixed Infection
Katata [ref. (83)]	HHV-6B	$EBV^{Negative}$ Burkitt's lymphoma

Immortalization of Human Herpesvirus 6 Integrated T-cells using Herpesvirus *saimiri*

Immortalization of iHHV-6 positive patient T-cells (**Table 12**) with Herpesvirus *saimiri* (HVS) strain 484-77 was used to generate lymphoidblastoid cell lines (LCL) (86, 87). A semi-confluent monolayer of owl monkey kidney (OMK) cells in a 100 mm-dish was infected with about 10^6 pfu/ml (plaque forming units) of HVS strain 484-77. Once OMK cells presented CPE (2 – 3 days), media was collected, and HVS virus present in the supernatant was concentrated by high-speed centrifugation in a SW28 rotor for 1 hr at 20,000 rpm. Human PBMCs were then harvested through Lymphoprep™ isotonic density gradient followed by T-cell expansion through PHA and IL-2 stimulation. Patient T-cells (2×10^7) were then infected with HVS and cultured in AIM V medium (Gibco) supplemented with 20 U/ml IL-2. Lymphoidblastoid cell lines were achieved roughly after 3 months in culture and these cell lines continuously divided in the absence of IL-2.

Reactivation of Chromosome Integrated Human Herpesvirus 6

Human PBMCs were either harvested through Lymphoprep™ isotonic density

gradient or through incubating with RBC Lysis Solution (Bioworld Consulting Laboratories, LLC) according to manufactures' instructions. Reactivation of iHHV-6 was then achieved through culturing $1x10^6$ PBMCs per ml in RPMI-1640 medium supplemented with 10 % FCS, 20 ng/ml TPA, and $1x10^{-6}$ M hydrocortisone or 80 ng/ml TSA for 3 to 5 days. To isolate reactivated virus, $1x10^4$ Molt-3 cells were added to 10^6 PBMCs and cultured for 10 – 14 days. Reactivation was monitored for cell CPE (cell lysis and syncitia), Gardella gel, qPCR, and sequencing of ORF U94.

Isolation of Human Herpesvirus 6 Genomic DNA from Mammalian Cells

Isolation of cellular and iHHV-6 genomic DNA from mammalian cells began by centrifuging 5 min at 500 x g, 4°C to pellet cell suspension. Supernatant was discarded and cells were resuspended with 10 ml ice-cold PBS and centrifuged centrifuging 5 min at 500 x g, 4°C. PBS resuspension and centrifugation was repeated for a second time to remove any remaining contaminating material. Cell pellet was resuspended with 100 µl PBS followed by the addition of 1.0 ml of lysis buffer and incubated for 12 – 18 hrs at 50°C. Lysis buffer contained 100 mM NaCl, 10 mM Tris-HCl (pH 8.0), 25 mM EDTA (pH 8.0), 0.5 % SDS, and 0.1 mg/ml proteinase K. Genomic DNA was then extracted twice with an equal volume of phenol and centrifuged 10 min at 1700 x g, room temperature (RT). The aqueous phase was removed from the top layer and extracted with an equal volume of chloroform/isoamyl alcohol (24:1) and centrifuged for 10 min at 1700 x g, RT. The top aqueous phase was removed and DNA was precipitated by mixing 0.3 M ammonium acetate, 2.5 volumes of ice-cold 96 % ethanol, and incubating 20 min at -80°C. Precipitated DNA was then centrifuged for 20 min at 4000 x g, 4°C. Next, pellet was rinsed with 70 % ethanol, centrifuged for 5 min at 4000 x g, 4°C, and air dried for 10 – 20 min. DNA pellet was then dissolved in TE buffer and stored at 4°C.

Alternatively, genomic DNA was isolated from whole blood and PBMCs with the Wizard® Genomic DNA Purification Kit (Promega, Madison, WI) according to the manufacture instructions. DNA concentration and purity was determined by agarose gel electrophoresis compared to known concentration of *λHindIII* ladder or through spectrophotometer analysis of A_{260}:A_{280} absorbance ratio (NanoDrop Spectrophotometer, ND-1000, Thermo Scientific, Wilmington, DE). DNA samples with an A_{260}:A_{280} ranges of 1.8 – 2.0 were utilized for downstream experiments.

Identifying Chromosome Integrated Human Herpesvirus 6

Gardella Gel Analysis

The vertical agarose gel technique of Gardella *et al.* is capable of distinguishing cellular genomic DNA, covalently closed circular DNA (viral episomes), and replicating linear viral DNA (**Fig. 4**) (88). This occurs through the gentle release of DNA by *in situ* lysis within the loading well of the vertical agarose gel followed by the application of an electric current. To begin, living lymphoid cells were first isolated from dead cells through the isotonic density gradient of Lymphoprep™ (Axis-Shield, Oslo, Norway) as previously described. Following, 1×10^6 cells were resuspended in 80 µl of sample buffer (15 % Ficoll, 0.01 % bromophenol blue in TBE buffer) and could either be stored at -80°C or directly loaded into the wells of a 0.8 % vertical agarose gel. Cells were then lysed *in situ* by layering with cell lysis solution (5 % Ficoll, 1 % SDS, 1 mg/ml pronase) and electrophoresed 0.8 V/cm (22 V) for 3 hrs followed by 7.5 V/cm (70 V) for 14 hrs at 4°C in TBE buffer.

The DNA in the gel was visualized through ethidium bromide staining coupled with the Gel Doc™ XR+ system equipped with a CCD camera (Universal Hood II, Bio-Rad, Hercules, CA). Alternatively, to increase sensitivity, the gel was stained with 20 µl

of SYBERGreen™ Nucleic Acid Stain (Lonza Rockland Inc., Rockland, ME) diluted in 200 ml of 1 X TBE buffer for one hour. The gel was then de-stained with 200 ml of 1 X TBE for 30 min and the DNA is then visualized using the Molecular Dynamics STORM Phosphor Imager (Model 860-PC, Amersham Biosciences, Piscataway, NJ). Next the DNA was transferred to nitrocellulose and Southern hybridized with [α^{32}P]-dATP labeled HHV-6 cosmids and [γ^{32}P]-ATP labeled mintochondrion oligonucleotides probes (**Tables 3** and **4**) (84, 85, 89).

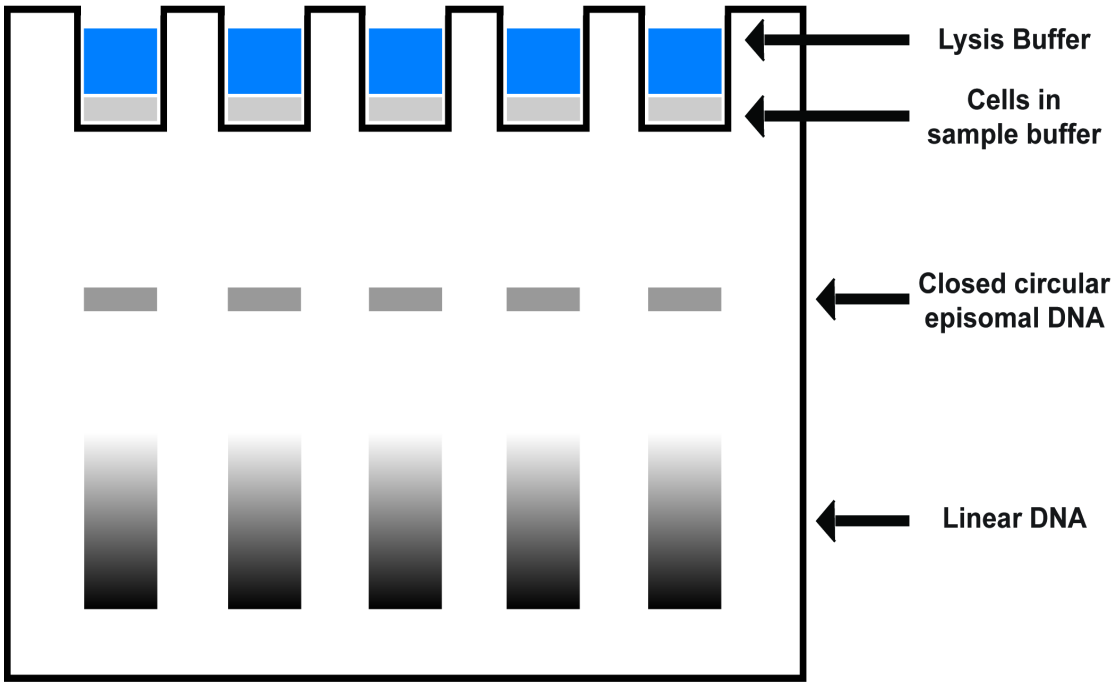

Fig. 4. Diagram of vertical agarose gel of Gardella *et al.* (88). A suspension of 1 x 10^6 cells in sample buffer is loaded into the wells of a vertical agarose gel. Cells were then lysed *in situ* by layering with cell lysis solution followed by the application of an electric current. The high molecular weight cellular DNA is located in the loading well of the gel, while covalently closed circular episomal DNA is in the middle of the gel and linear viral DNA migrates at a faster rate toward the bottom of the gel.

Table 3. HHV-6A cosmids utilized for synthesis of [α^{32}P]-dATP probes (84).

HHV-6A (U1102) Cosmid	Sequence Location
PMF311-12	65 – 75 kbp
PMF335-6	50 – 72 kbp

Table 4. Oligonucleotides for [γ^{32}P]-ATP labeled mitochondrion probes (89).

Oligonucleotide Name	Sequence
2R	5'-TGGACAACCAGCTATCACCA-3'
7F	5'-ACTAATTAATCCCCTGGCCC-3'
7R	5'-CCTGGGGTGGGTTTTGTATG-3'
13F	5'-TTTCCCCCTCTATTGATCCC-3'
13R	5'-GTGGCCTTGGTATGTGCTTT-3'
17F	5'-TCACTCTCACTGCCCAAGAA-3'
17R	5'-GGAGAATGGGGGATAGGTGT-3'
22F	5'-TGAAACTTCGGCTCACTCCT-3'
22R	5'-AGCTTTGGGTGCTAATGGTG-3'

Fluorescent *in situ* Hybridization

Patient PBMCs were stimulated for 72 hrs with PHA followed by the preparation of metaphase chromosomes according to standard cytogenic protocol (90). Viral integration was observed by HHV-6A (U1102 strain) pMF311-12 and PMF335-6 cosmid (84) probes labeled with Fluorescein (**Table 3**). Subsequently, HHV-6 chromosomal integration sites were hybridized with probes for the centromere of chromosome 17 (Vysis), BCL2 gene on chromosome 18 (Vysis), EWSR1 gene on chromosome 22 (Vysis), and telomere-PNA probe (DakoCytomation). DAPI was then used to visualize metaphase chromosomes with Axiophot microscope (Zeiss, Austria). At least 11 metaphase spreads were examined per a sample.

FISH experiments were performed in two independent laboratories (University of Minnesota, Minneapolis, MN and the Children's Cancer Research Institute, Vienna, Austria). Each laboratory was blind to knowledge of the individual and family membership from which each specimen had been obtained (**Table 12**).

CsCl/Ethidium Bromide Density Gradient

The CsCl/Ethidium bromide density gradient enables the segregation of covalently closed circular DNA (cccDNA) from linear DNA. Cesium chloride (CsCl) (1.55 g/ml) and ethidium bromide (EtBr) (1 µg/ml final concentration) was added to DNA (50 µg) isolated from HEK-293 (**Table 2**) and family member T-cells with integrated iHHV-6 (**Table 12**). The volume and density of the gradient was adjusted with the addition of TE and Cs/Cl to a final density of 1.55 g/ml as determined with the use of analytical balance (Mettler, AE50). The samples were then centrifuged in a Beckman L7-75 (VTi65 rotor) for 72 hrs at 45,000 rpm, 20°C. Following centrifugation, 200 µl fractions from the gradient were collected in a 96-well plate. Aliquots from each fraction were then analyzed by electrophoresis in a 0.8 % agarose gel running at 1.2 V/cm in TBE buffer. The high density fractions of cccDNA and the lower density fraction of linear DNA were combined in separate aliquots.

The linear DNA and cccDNA fractions were purified of ethidium bromide by repeated extractions with 1 volume of isopropanol saturated with 5 M NaCl and centrifugation for 3 min at 1500 x g, RT. The DNA from the lower aqueous phase was then precipitated by mixing 1 volume of H_2O and 2.5 volumes of 95 % ethanol, incubated for 30 min at -80°C, and centrifuged for 30 min at 20,000 x g, 4°C. Remaining salts were removed by washing with 70 % ethanol and the DNA pellet was then air dried to remove trace amounts of ethanol followed by resuspension in 1 X TE buffer.

To confirm the independent isolation of cccDNA and linear DNA, PCR with REDTaq® DNA Polymerase (Sigma, St. Louis, MS) was utilized in combination with four primer sets (**Table 5**). Isolation of linear DNA was confirmed with primers to cellular encoded beta actin (91) and cccDNA fraction was confirmed by amplification of the mitochondrion encoded cytochrome-C oxidase (92). The distinction between the integrated genome of iHHV-6 from episome cccDNA fractions was determined through amplification of ORF U94, while the HVS (strain C484) genome was detected using primers to Stp oncogene.

Table 5. Oligonucleotides for CsCl/Ethidium bromide density gradient.

Oligonucleotide Name	Sequence
HVS C484 Stp-F	5'-CTCAGAACGCGGCAACAAACTTGA-3'
HVS C484 Stp-R	5'-TTTCGGCATACCTGGATCCCATGA-3'
Cytochrome-C oxidase-F [ref. (92)]	5'-TTCGCCGACCGTTGACTATT-3'
Cytochrome-C oxidase-R [ref. (92)]	5'-AAGATTATTACAAATGCATGGGC-3'
Beta actin-F [ref. (91)]	5'-CTGGAACGGTGAAGGTGACA-3'
Beta actin-R [ref. (91)]	5'-AAGGGACTTCCTGTAACAATGCA-3'
HHV-6 ORF U94-F	5'-ACAGCCATTCGATGGTTCCCAGAA-3'
HHV-6 ORF U94-R	5'-AACGAACTGGGAGACGTATGCGAT-3'

Agarose Gel Electrophoresis and Southern Blot Analysis

Agarose gel electrophoresis of DNA was carried out in 1 X TBE buffer (20 X stock: 890 mM tris base, 890 mM boric acid, pH 8.0 HCl), staining with ethidium bromide, and visualized with Gel Doc™ XR+ system equipped with a CCD camera (Universal Hood II, Bio-Rad, Hercules, CA) . In preparation of Southern blotting (85), the agarose gel was incubated and gently rocked twice for 15 min in the following solutions:

1) 0.25 M HCl solution for DNA depurination; 2) 1 M NaCl, 0.5 M NaOH solution for DNA denaturation; and 3) 1.5 M NaCl, 0.5 M Tris-HCl (pH 7.0) solution to neutralize.

The DNA from buffered agarose gels were transferred to supported nitrocellulose or positively charged nylon membranes (Amersham Biosciences) through vacuum-blotting (93). A solution of 1 X SSC (Saline-sodium citrate) diluted from a 20 X stock buffer (3 M NaCL, 0.3 M sodium citrate, pH 7.0) was continuously applied to the top of the agarose gel during the 30 – 45 min transfer. DNA was then immobilized to the membrane by baking for 1 h in a vacuum oven at 80°C. Membranes were blocked for nonspecific binding of the radiolabeled probes by incubating 10 ml of pre-hybridization buffer [50 % formamide, 5 X SSC, 10 X Denhardt's solution (0.2 % bovine serum albumin, 0.2 % Ficoll 400, and 0.2 % polyvinylpyrrollidone), 0.5 mg/ml sonicated salmon sperm DNA (or total E.*coli* DNA), 0.05 M Na_3P0_4 (pH 6.5), and 0.1 % SDS] that had been previously boiled for 5 min. During the 10 – 30 min incubation of membranes at 42°C with pre-hybridization buffer, [α^{32}P]-dATP labeled vector DNA is added to 10 ml of hybridization buffer [50% formamide, 5 X SSC, 1 X Denhardt's solution, 0.1 mg/ml sonicated salmon sperm DNA (or total E. *coli* DNA), 0.015 M Na_3P0_4 (pH 6.5), and 0.1 % SDS] and boiled for 5 min to denature the probe. Alternatively, [γ^{32}P]-ATP labeled oligonucleotide probes are added to room temperature hybridization buffer. Once pre-hybridization buffer is removed from the membrane, hybridization buffer with radiolabeled probe is incubated for 16 – 18 hrs while rocking either at room temperature for [γ^{32}P]-ATP labeled oligonucleotides or 42°C for [α^{32}P]-dATP random primer labeling.

The membrane is then washed with 3 – 4 times in a solution containing 0.1 X SSC and 0.1 % SDS. The wash solution is either room temperature for [γ^{32}P]-ATP or 55 – 60°C for [α^{32}P]-dATP. Membranes were sealed in plastic wrap and exposed to a Storage Phosphor Screen (Molecular Dynamics, Sunnyvale, CA) for 8 hrs – 14 days and

analyzed using a Molecular Dynamics STORM Phosphor Imager (Model 860-PC, Amersham Biosciences, Piscataway, NJ).

Synthesis of ^{32}P-Radiolabeled DNA Probes

Oligonucleotide probes were first diluted to a final concentration of 10 ng/µl. Next, oligonucleotides were then end-labeled with [γ^{32}P]-ATP by adding 1.0 µl of 10 X T4 polynucleotide kinase buffer, 1.0 µl (10 U) of T4 kinase (Promega, Madison, WI), 7.0 µl of [γ^{32}P]-ATP isotope (PerkinElmer, Boston, MA), and 1.0 µl (10 ng/µl) oligonucleotide that serves as the probe. The kinase reaction then proceeded for 30 min at 37°C. Then, 50 µl stop buffer consisting of 50 mM EDTA, 20 mM Tris-HCl (pH 7.5), 20 mM NaCl, 0.25 % dextran blue, and 1 % SDS was added. The radiolabeled oligonucleotide probes were incubated at room temperature for 16 -18 hours with the DNA vacuum-blotted membrane or stored at 4°C until use.

Synthesis of random primer [α^{32}P]-dATP-radiolabeling of plasmid probes begins by mixing 3 µl (20 - 100 ng) of plasmid and 3 µl of random primers (500 ng/µl) and denatured for 3 min at 100°C. The microfuge tube is then immediately placed on ice for 5 – 10 min to allow annealing of random primers to the plasmid sequence. Incorporation of [α^{32}P]-ATP into plasmid sequence is achieved by adding 1.5 µl of 10 X DNA polymerase buffer, 1.0 µl DNA polymerase I large fragment-Klenow (5 U) (Promega, Madison, WI), 1.5 µl of 500 µM dNTP-ATP, 5.0 µl [α^{32}P]-dATP isotope (PerkinElmer, Boston, MA), and incubated at room temperature for 4 hrs. Then, 45 µl stop buffer is added to the probe and unincorporated [α^{32}P]-ATP is then removed by applying the probe to a DNA cellulose column. The radiolabeled probe is either incubated at 42°C for 16 -18 hours with the DNA vacuum-blotted membrane or stored at 4°C.

Quantitative Real-Time PCR (qPCR)

Patient T-cells positive for iHHV-6 and HHV-6A *in vitro* integrated HEK-293 cells were treated for three days with TPA (20 ng/ml) and TSA (80 ng/ml) to see if reactivation of the chromosome integrated virus leads to an increase in viral copies. To investigate this, DNA was isolated from treated and untreated (control) cells and subjected to quantitative real time PCR (qPCR) for HHV-6 encoded ORF U94 and normalized to the house keeping gene beta actin. DNA samples were analyzed in triplicate and 10 fold serial dilutions of U94-pZeoSV plasmid was used to generate a standard curve. For negative controls, a no template control and genomic DNA from a HHV-6 negative cell line was analyzed with every set. The master mix for each reaction contained: 100 ng template DNA, 12.5 µl of Syber® Green JumpStart™ Taq ReadyMix™ for Quanitative PCR (Sigma-Aldrich, St. Loius, MO), 0.25 µ internal reference dye, 1 µl of 5 µm stock of forward and reverse primers for ORF U94 and beta actin (**Table 6**), and the volume was increased to 25 µl with H_2O.

Table 6. Oligonucleotides for quantitative real-time PCR.

Oligonucleotide Name	Sequence
Beta actin-F [ref. (91)]	5'-CTGGAACGGTGAAGGTGACA-3'
Beta actin-R [ref. (91)]	5'-AAGGGACTTCCTGTAACAATGCA-3'
HHV-6 ORF U94-F	5'-ACAGCCATTCGATGGTTCCCAGAA-3'
HHV-6 ORF U94-R	5'-AACGAACTGGGAGACGTATGCGAT-3'

The samples were then analyzed with Chromo4 Real-Time PCR Detector (BIO RAD, DNAEngine) using the following thermocycling parameters: 94°C for 2 min, which is the followed by 40 cycles of 94°C for 15 sec, 60°C for 1 min, and 72°C for 30 sec. Next, a melt-curve ranging from 45°C to 90°C with 0.2 ºC increase every 2 sec was

completed to ensure that fluorescence signal recorded by Syber® Green was the result of the specific amplification of beta actin and ORF U94. Data was then analyzed with DNA Engine Software. Fold change ratios of Ct values normalized to beta actin were relative to untreated control. Statistical analysis was completed with the student T-test and $p < 0.05$ was considered significant.

Cloning the Chromosome Integration Site of Human Herpesvirus 6

Inverse PCR

Inverse PCR (IPCR) amplification of the HHV-6 integration site was adapted from Ochman *et al*. (94) (**Fig. 5**). Briefly, 2 µg of patient genomic DNA was restriction digested with 10 U of *MboI* (Promega) for 14 hrs at 37°C. To allow monomeric circularization and prevent ligation of several fragments, *MboI*-digested DNA was diluted to 2 µg/ml, and ligated with 0.045 U/µl T4 DNA ligase (Promega) for 14 hrs at 15°C. Amplification of 100 ng of ligated DNA was performed with primers IPCR-1 and IPCR-2 (**Table 7**) along with Expand 20 kb^{PLUS} PCR System (Roche Diagnostics, Mannheim, Germany). Identification of HHV-6 integration site was then achieved by agarose gel electrophoresis and Southern hybridization with IPCR-probe to HHV-6 and telomere repeat [γ^{32}P]-ATP-radiolabeled oligonucleotides.

Table 7. Oligonucleotides for IPCR amplification and probe.

Oligonucleotide Name	Sequence
IPCR-1	5-'GCACAACCCACCCATGTGGTAGTCGCGG-3'
IPCR-2	5'-CGTGTGTACGCGTCCGTGGTAGAAACGCG-3'
IPCR-probe	5'-CTTACACTTGCCATGCTAGC-3'
Telomere repeat-probe	5'-TTAGGGTTAGGGTTAGGGTTAGGG-3'

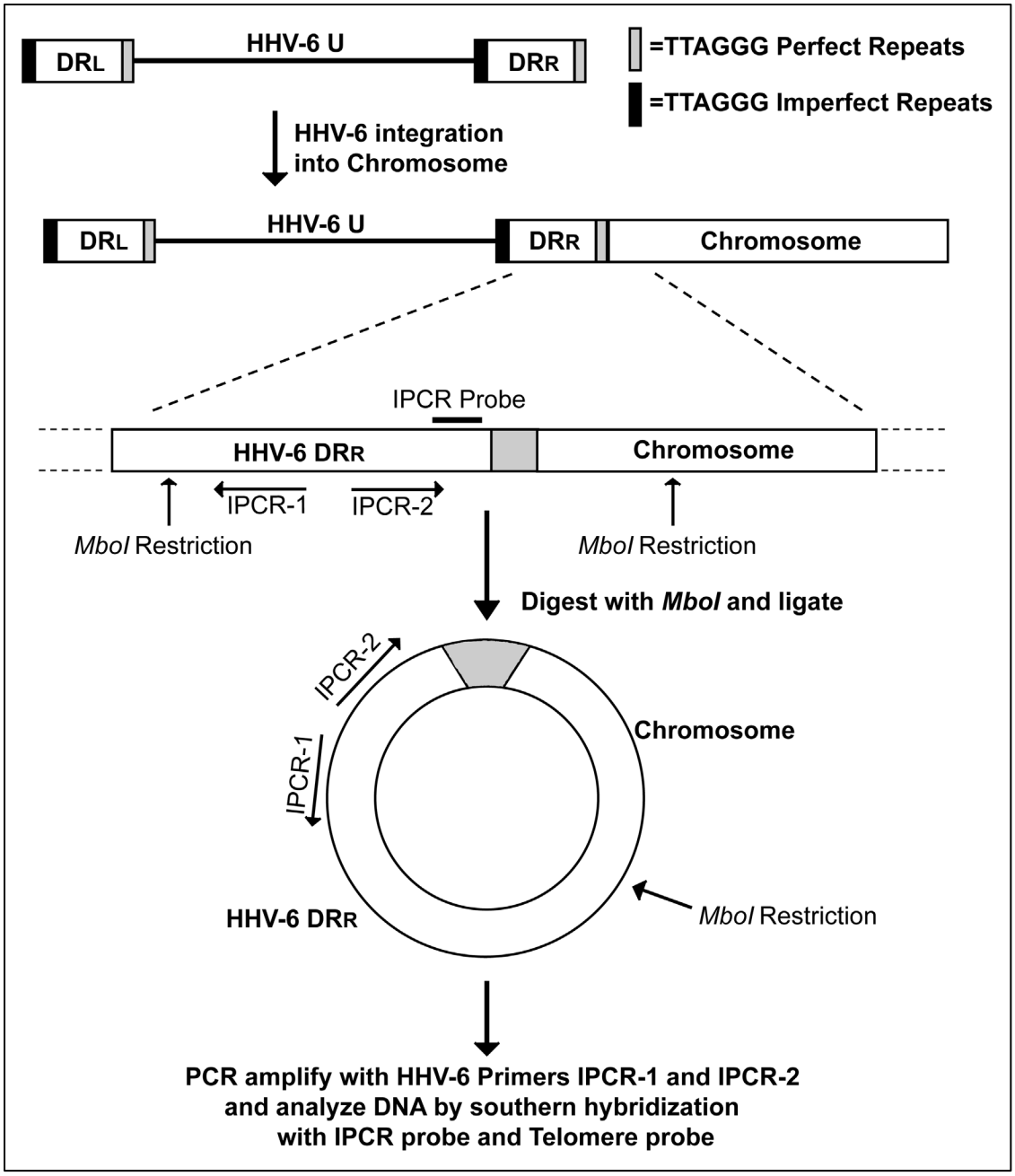

Fig. 5. Diagram illustrating the amplification of HHV-6-chromosome junction by inverse-PCR (IPCR). Hypothesis: integration of HHV-6 occurs within the telomere of a human chromosome via homologous recombination with the TTAGGG perfect repeats within direct repeat right (DR_R) (**Fig. 1**). IPCR involves digestion of genomic DNA with *MboI* followed by self-circularization of HHV-6 DR_R and adjacent chromosomal fragment. PCR amplification of HHV-6-chromosome fragment is achieved through HHV-6 primers IPCR-1 and IPCR-2. Co-hybridization with IPCR-probe and telomere probe via Southern hybridization identified the HHV6-telomere-chromosome junction. DR_L, direct repeat left; U, unique.

Chromosome-Specific PCR for iHHV-6 Integration

Both copies of the HHV-6 DR are bounded on their left by an imperfect TTAGGG repeats and on their right by perfect arrays of the TTAGGG sequence. Thus, the right end of the viral genome has a perfect TTAGGG array that derives from DR_R and the left end of the genome has an imperfect array that derives from DR_L (3, 4). To amplify and sequence the putative viral-chromosomal DNA junction, we created a primer pair homologous to the DR_L and DR_R of the viral genome, as well as a primer to the subtelomere of a specific chromosome (**Fig. 6**). The chromosome subtelomere primer was selected based upon results from FISH of iHHV-6 (**Fig.15**).

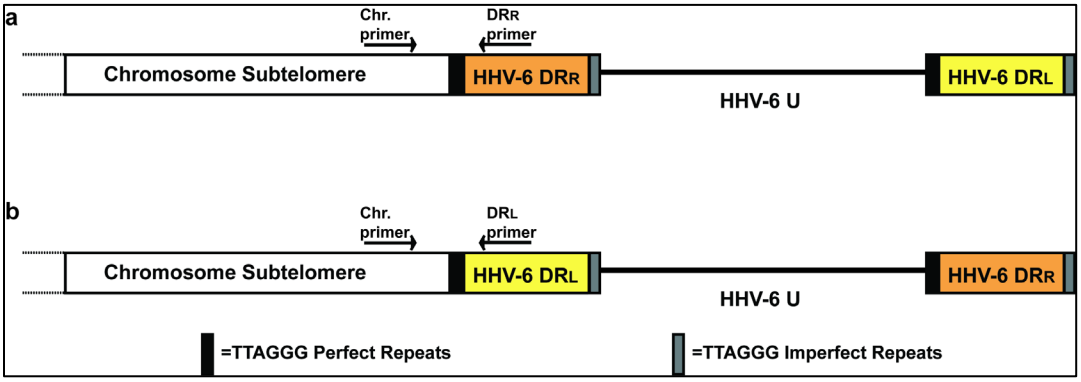

Fig. 6. Strategy of chromosome-specific PCR for iHHV-6 integration. The putative HHV-6-chromosome junction was amplified with a primer to the specific end of chromosome subtelomere and the second primer derived from the (**a**) HHV-6 right direct repeat (DR_R) or (**b**) the left direct repeat (DR_L). Both primers to DR_R and DR_L were utilized since we were unaware whether iHHV-6 integration occurs via the left or right telomere encoded repeats. Arrows indicate position of primers. Unique = U.

The PCR master mix for amplification of iHHV-6 integration site included: 400 ng genomic DNA, HHV-6 DR_R/DR_L and chromosome specific primers (50 µM) (**Table 8**), 500 µM dNTPs, Expand 20 kb^{PLUS} PCR system (Roche Diagnostics, Indianapolis, IN), 10 X taq buffer, and final volume was increased to 25 µl with H_2O. Samples were placed in a Peltier Thermal Cycler PCR (PTC-220, MJ Research Inc, Waltham, Ma) and subjected

to the following PCR conditions: 94°C for 2 min, which is the followed by 35 cycles of 94°C for 10 sec, 64°C for 30 sec, and 68°C for 10 min, and finished with a final extension of 68°C for 7 min.

Agarose gel electrophoresis and Southern blot hybridization with telomere, HHV-6, and chromosome specific [γ^{32}P]-ATP-radiolabeled oligonucleotide probes was utilized for identifying DNA bands representing the putative viral-chromosomal DNA junction. Specific bands were gel extracted with Perfectprep® Gel Cleanup Kit (Eppendorf, Westbury, NY) and cloned with pCR®4-TOPO® (TOPO TA Cloning® Kit for Sequencing, Invitrogen, Carlsbad, CA). A minimum of three clones from each sample was sequenced by the Molecular Biology core facility at H. Lee Moffitt Cancer Center and Research Institute.

Table 8. Oligonucleotides for chromosome-specific PCR and probe.

Oligonucleotide Name	Sequence
HHV-6 DR_R	5'-CATAGATCGGGACTGCTTGAAAGCGC-3'
HHV-6 DR_L	5'-CTTTCTCGCTGTGCCTCACGCTGTC-3'
Chromosome 11q primer (95)	5'-CAGACCTTGGAGGCACGGCCTTCG-3'
Chromosome 17p primer (95)	5'-AACATCGAATCCACGGATTGCTTTGTGTAC-3'
Chromosome 18q primer	5'-CTCATGTCCTCGGTCTCTTGCCTC-3'
Chromosome 17p probe (95)	5'-CCCAAGCAGGTTGAGAGGCTGAGG-3'

Generation of Recombinant Human Herpesvirus 6A BAC Virus Expressing GFP and Neomycin Resistance

The generation of a recombinant HHV-6A (strain U1102) virus was accomplished through the cloning of GFP expression cassette and neomycin resistance between the two polyadenylation sites of ORF U53 and U54 (**Fig. 7a**). The pBeloBAC11 plasmid (New England BioLabs, Ipswich, MA) with U53, U54, GFP, and neomycin resistance

gene was transfected into HEK-293 cells. Cells were subsequently infected with wild type HHV-6A (wt-HHV-6A) to enable homologous recombination between vector ORF U53/U54 sequences with the genome of wt-HHV-6A (**Fig. 8**).

The method of cloning the targeting pBeloBAC11 vector began by PCR amplification of ORF U53 (primers U53L and U53R) and ORF U54 (primers U54L and U54R) from HHV-6A DNA prepared from infected cells with primers containing restriction sites *BamHI* and *SacII* (**Table 9**). In addition, the GFP expression cassette driven by the CMV immediate early gene promoter was amplified from pEGFP-N2 vector template (BD Biosciences Clontech) with primers GFP-N2-L and GFP-N2-R. Next, the sub-cloning of ORF U53, ORF U54, and GFP was completed in pBluescript SK+ (Invitrogen™ Life Technologies™, Carlsbad, CA) followed by sequencing to confirm the absence of PCR generated mutations.

Table 9. Oligonucleotides for generating Human Herpesvirus 6A BAC/GFP/Neo^r.

Oligonucleotide Name	Sequence
U53L	5'-GGCCCGCGGAGTAGTTCCGCGTCAGAATGC-3'
U53R	5'-GGCGGATCCCATTCGTTTTATTGAACGCG-3'
U54L	5'-GGCAAGCTTGCAATGGTTAAAAGTTGTTTTTTG-3'
U54R	5-'GCGCCGCGGCTGCATACTTGCTACCGGAAC-3'
GFP-N2-L	5'-CGCGGATCCATTAATAGTAATCAATTACGG-3'
GFP-N2-R	5'-CGCGGATCCCGCCTTAAGATACATTGATGAG-3'

The targeting vector was assembled by ligating fragments between the restriction sites *BamHI* and *HindIII* of pBeloBAC11 with T4 DNA ligase (Promega, Madison, WI) (**Fig. 7b**). Ligated products were then transfected into ElectroMAX™ DH10B™ *E. coli* cells (Invitrogen™ Life Technologies™, Carlsbad, CA) through electroporation. The size

and orientation of ORF U53, ORF U54, GFP, and neomycin resistance cloned within pBeloBac11 was confirmed by restriction digestion and agarose gel electrophoresis. Positive clones were selected with 30 µg/ml kanamycin and plasmid was purified through QIAGEN® Plasmid Maxi Kit (QIAGEN Sciences, Germantown, MD) according manufactures instructions. To further remove trace amounts of bacterial DNA, RNA, and proteins, U53/U54/GFP/Neo-pBeloBAC11 was subjected to CsCl/ethidium bromide density gradient.

To permit homologous recombination between U53/U54/GFP/Neo-pBeloBAC11 vector with ORF U53 and U54 encoded in the genome of wt-HHV-6A (**Fig. 7b**), the vector was first linearized through digestion with *SacII*. Next, 5 µg of *SacII* digested U53/U54/GFP/Neo-pBeloBAC11 was transfected in a 6-well dish of HEK-293 at 70 % confluency with GenePORTER® Transfection Reagent (Genlantis, San Diego, CA) (**Fig. 8**). After 16 hrs post-transfection, HEK-293 cells were then infected with wt-HHV-6A (U1102) at ~1.0 multiplicity of infection (MOI). Infected cultures were incubated for 5 – 12 days to allow homologous recombination with vector and insertion of GFP and neomycin resistance gene into the HHV-6A genome (HHV-6A^{GFP}). Since infected HEK-293 cells contain both wt-HHV-6A and HHV-6A^{GFP}, cells were lysed through sonication or repeated freeze defrost cycles. HHV-6A^{GFP} virus was then titrated out by infecting Jjahn T-cell cultures with ~1 infectious unit per well in a 96 well plate. HHV-6A^{GFP} was expanded and progress of infection was monitored through GFP expression with Nikon TE300 inverted microscope equipped with SPOT RT-SE6 1.4MP Slider camera (Diagnostic Instrument. Inc.) and flow cytometric analysis.

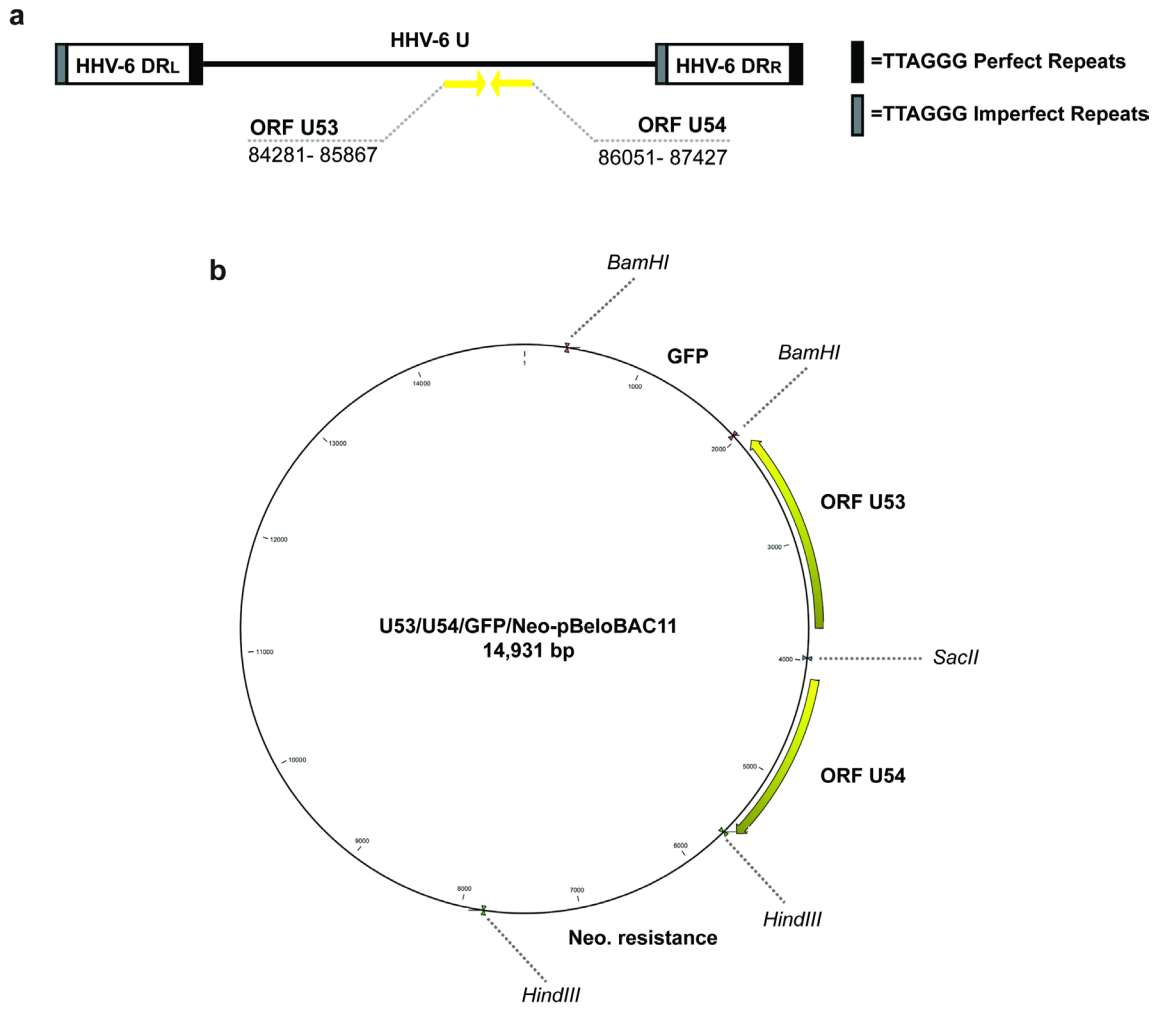

Fig. 7. Cloning of HHV-6A ORF U53 and U54 into pBeloBAC11 for generation of recombinant HHV6A^{GFP}. (**a**) Diagram of the HHV-6A genome with the location of ORF U53 and U54 highlighted. The insertion of GFP/Neo^r/pBeloBAC11 occurs between the polyadenylation sites of ORF U53/U54 to prevent interruption of transcription and/or translation of those viral genes. (**b**) Vector map of U53/U54/GFP/Neo-pBeloBAC11. The targeting vector was assembled by PCR amplify fragments of HHV-6A ORF U53/U54, as well as GFP and Neo^r from pEGFP-N2 vector (BD Biosciences Clontech). Fragments were then ligated between restriction sites *BamHI* and *HindIII* in pBeloBAC11 (New England BioLabs, Ipswich, MA). Restriction enzyme digestion of the *SacII* site between ORF U53 and U54 linearizes the vector in preparation of homologous recombination with HHV-6A genome (**Fig. 8**).

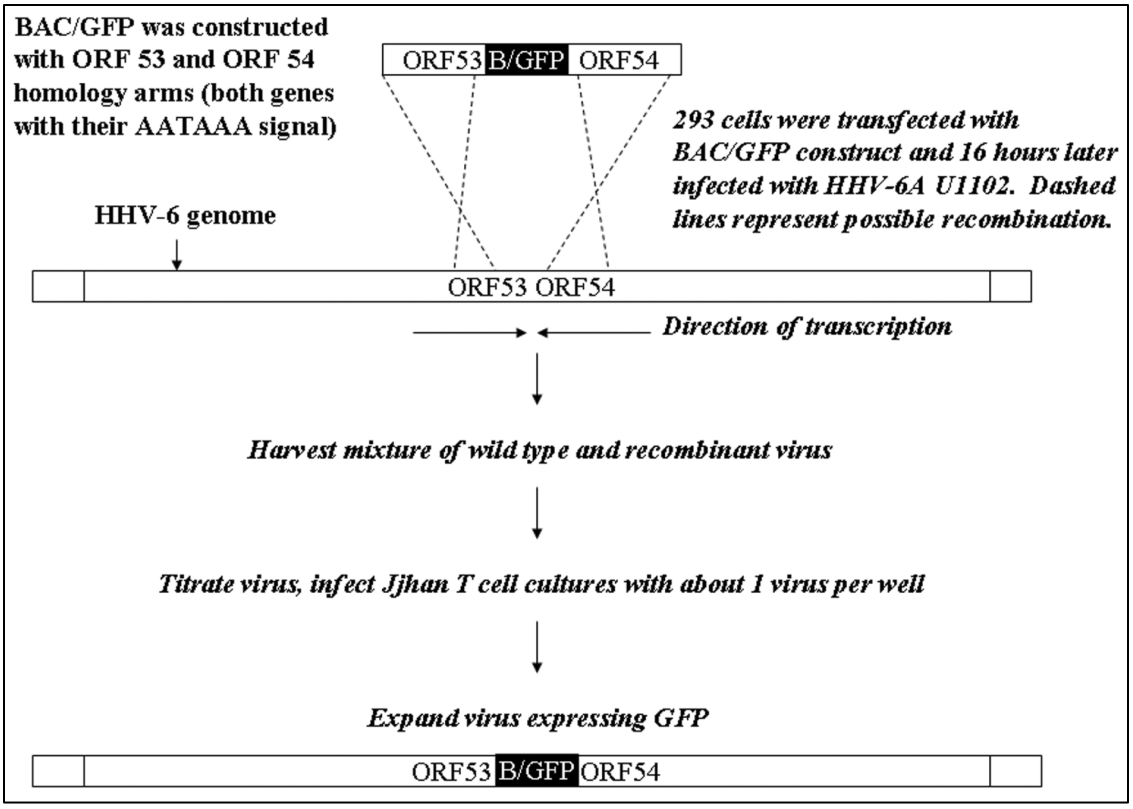

Fig. 8. Strategy for construction of recombinant HHV-6A (U1102) virus expressing GFP (HHV-6A^{GFP}). As outlined in the scheme above, HHV-6A^{GFP} was constructed by homologous recombination between B/GFP vector (U53/U54/GFP/Neo-pBeloBAC11) and the two polyadenylation signals of HHV-6A ORF U53 and U54 (85,981–86,034 bp)

Partial and 454-Deep Sequencing of Germ-Line Integrated Human Herpesvirus 6 Genome

iHHV-6 sequences from PMBCs (**Table 12**) were amplified with primers spanning ORF U94 (fragment 141,267-143,197, primers U94L-1 and U94L-2; U94R-1 and U94R-2) using 300 ng of genomic DNA with REDTaq DNA polymerase (Sigma-Aldrich) (**Table 10**). Cycling conditions were 95°C for 1 min, 66°C for 1 min, and then 72°C for 1.5 min for a total of 24 cycles. Amplification of DR (fragment 421-1474, 151654-152707) with primers DR-1 and DR-2 and cycling 95°C for 1 min, 53°C for 1 min, and 72°C 1.5 min for a total of 24 cycles. DNA bands were isolated from 0.8 % agarose gel and cloned into pCR®4-Topo® vector using the TOPO TA Cloning® Kit for Sequencing (Invitrogen,

Carlsbad, CA). Clones (n=4) were then sequenced by the Molecular Biology core facility at the H. Lee Moffitt Cancer Center and Research Institute.

454-sequencing of the iHHV-6A genome from Family-1/Sibling-2 was completed in collaboration with Rolf Renne and the University of Florida Interdisciplinary Center for Biotechnology Research.

Table 10. Oligonucleotides for amplifying and sequencing DR and ORF U94. Direct Repeat (DR) (U1102 421-1474, 151654-152707) and ORF U94 (U1102 141267-143197).

Oligonucleotide Name	Sequence
DR-1	5'-TGCCGCTTCAACTTCACCTT-3'
DR-2	5'-AGATGTGGAGAGAAACGCGA-3'
U94L-1	5'-TGTTCTTCTGCTAACTCGGACGCA-3'
U94L-2	5'-CAGTTCCAATGGGCGTGGACAAAT-3'
U94R-1	5'-ATCCACGCGTCTTCCGTGACTATT-3'
U94R-2	5'-TGTTCATGTCTTCCGGCGAAAGGT3-'

Single Telomere Length Analysis of iHHV-6

Various methods have quantified the overall length of a population of telomeres (96). However, Baird *et al.* has established a protocol to calculate the length of a telomere from a specific chromosome end (95, 97). The single telomere length analysis (STELA) assay has successfully determined the length of telomeres from chromosomes XpYp, 2p, 11q, 12q, 17p, and 18q with use of primers specific to individual chromosome end. Therefore, we have adapted the STELA assay to determine whether the telomere is extended beyond the left direct repeat (DR_L) of iHHV-6A and iHHV-6B as well as quantify the overall telomere length of the integrated chromosome (**Fig. 9**).

To begin, genomic DNA was isolated from iHHV-6A and iHHV-6B patients PBMCs (**Table 12**) and HHV-6A *in vitro* integrated HEK-293 cells (**Table 2**) with Wizard®

Genomic Purification Kit (Promega) or through proteinase-K digestion and chloroform/isoamyl alcohol (24:1) purification. Next, the linker (Tellorette-2) containing a single TTAGGG repeat was ligated to the end of the telomere by incubating 60 – 150 ng of genomic DNA, 60 - 100 µM of oligonucleotide Telorette-2, and 4.5 U of T4 DNA ligase for 13 hrs at 35°C. The ligation reaction was then purified through phenol chloroform/isoamyl alcohol (24:1) and resuspended in 15 µl TE. Serial dilution of DNA was amplified with a high fidelity taq polymerase (Expand 20 kb^{PLUS} PCR System, Roche), 25 µM linker annealing primer (Teltail-P1), 25 µM iHHV-6 primer (iHHV-6 STELA-P2) (**Table 11**). Cycling conditions were 92°C for 2 min, 27 cycles of 92°C for 15 sec, 59°C for 30 sec, 68°C 13.5min or 18 min, and a final extension of 68°C for 7 min. Amplification products were separated through electrophoresis on a 0.8 % DNA agarose gel and Southern hybridized with [γ^{32}P]-ATP-radiolabeled telomere oligonucleotide probe and PCR amplified (primers P3 + P4) HHV-6 DR_L random primer [α^{32}P]-dATP-radiolabeled probe.

Telomere length of iHHV-6 integrated chromosome was then calculated based upon the mean molecular weight of all bands co-hybridizing with telomere and HHV-6 DR_L probes.

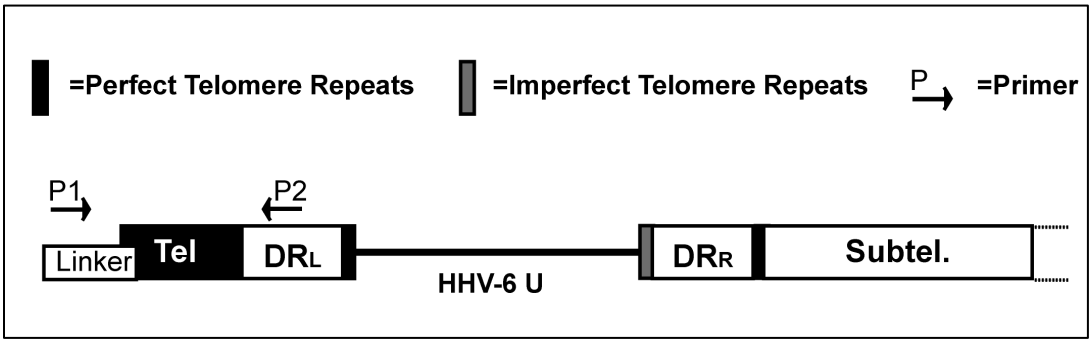

Fig. 9. Diagram illustrates the strategy of single telomere length analysis (STELA) of iHHV-6. To amplify the specific chromosome telomere (Tel) extended beyond the DR_L of iHHV-6; a linker (Telorette-2) oligonucleotide is ligated to the end of the telomere. Amplification of the telomere is then preceded with primers P1 and P2.

Table 11. Oligonucleotides for single telomere length analysis PCR and probe.

Oligonucleotide Name	Sequence
Tellorette-2 (Linker) (97)	5'-TGCTCCGTGCATCTGGCATCTAACCCT-3'
Teltail-P1 (97)	5'-TGCTCCGTGCATCTGGCATC-3'
iHHV-6 STELA-P2	5’-AAGGATGGTAGGGTTTAGGGTCGAACC-3'
iHHV-6 STELA-P3	5’-CCCTAACACTAATCCTCGCATCCGC-3’
iHHV-6 STELA-P4	5’-AAGGATGGTAGGGTTTAGGGTCGAACC-3’

RESULTS

AIM I. To Determine whether the Human Herpesvirus 6A and 6B Genome Integrates into Chromosomes of *in vitro* Infected Cell Lines

Two Novel *in vitro* Models Demonstrate HHV-6A Chromosome Integration

Primary infection of HHV-6 leads to an increase in viral copies present in peripheral blood of children and subsequent decrease in viral copies during latency (5, 13). However, in a select number of patients including adults and children, there are high copies of HHV-6A and HHV-6B consistently detected in peripheral blood measuring greater than 1 million per ml or 1 copy of HHV-6 per cell (31, 33, 64, 65). Through further evaluation of these patients with FISH analysis, it has been suggested that the genome of HHV-6 is integrated into the chromosome (28-32, 34, 98, 99). However, the frequency of HHV-6 integration and whether integration is a product of infection remains unknown. Therefore, in AIM I we developed two novel *in vitro* models of HHV-6A integration to determine the frequency with which new infection of naïve cell lines with HHV-6 leads to chromosomal integration, and whether this is the sole means by which HHV-6 achieves latency.

Single Cell Clones of Chromosome Integrated HHV-6A Human Embryonic Kidney-293 Cell Lines

In our first model we set to determine if HHV-6A *in vitro* infection results in chromosome integration. Since our preliminary experiments indicated that HEK-293 cells do not produce any appreciable amount of virus in cultures reaching full confluency, we therefore expected this cell line to be a candidate to evaluate the *in vitro* integration of HHV-6A (**Table 2**). We infected HEK-293 cells at 50 % confluency with HHV-6A (U1102) at 0.1 multiplicity of infection (MOI). The cultures were incubated for five days. Then the infected HEK-293 cells were washed to remove extracellular virus, and single cells were introduced in each well of a 96 well plate. The single cells in each well were then expanded and amongst these single cell clones, there were three populations. The first population of single cell clones includes those that had reached cell senescence and stopped dividing most likely due to virus infection. The second population of single cells included those that expanded at normal rate as uninfected controls. However, the third population of cells appeared to have ceased cell division, but then proceeded to divide at a much slower rate than uninfected controls. DNA was then extracted from these single cell clones and subjected to PCR for presence of the viral genome using ORF U94-specific primers (**Table 6**) followed by agarose gel electrophoresis. As show in **Figure 10a**, 10 of the 22 HEK-293 cell clones were positive for ORF U94. This indicates the successful infection and the presence of the HHV-6A genome within the HEK-293 single cell clones.

To characterize the HEK-293 single cell clones for the presence of HHV-6A integrated into chromosomes, FISH was completed at the University of Minnesota (**Fig. 10b**). Three PCR-positive clones (clone 1, 2, and 3) and one PCR-negative clone (clone 6) were studied for chromosome integration of HHV-6A by FISH. Metaphase

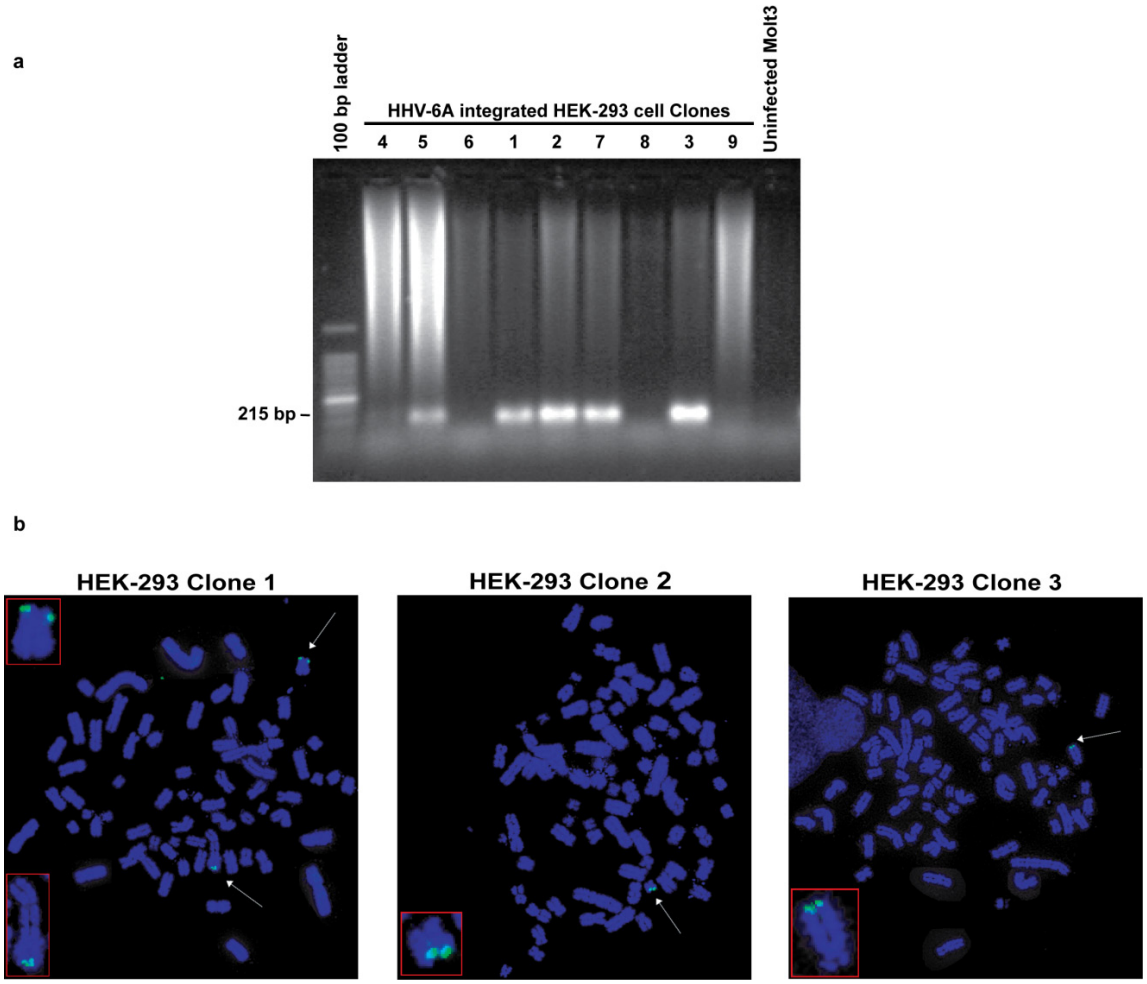

Fig. 10. Detection of the viral genome by PCR and fluorescent *in situ* hybridization (FISH) of HEK-293 cell clones latently infected with HHV-6A (U1102). (**a**) Genomic DNA was isolated from HHV-6A infected HEK-293 cell clones. Amplification of a 215 bp fragment representing ORF U94 was observed in five HHV-6A infected HEK-293 single cell clones. (**b**) Representative FISH from three independent HEK-293 cell clones. Hybridization was performed with HHV-6 cosmids pMF311-12 and pMF335-631 labeled with fluorescein (green) (84). HEK-293/clone-1 had two independent chromosome-associated HHV-6A signals, while HEK-293/clone-2 and HEK-293/clone-3 only had one. The HHV-6A-hybridizing chromosomes are labeled with white arrows and a higher magnification of the chromosomes are shown in red box. Metaphase chromosomes were stained with DAPI. Total of 11 cells were observed for each clone.

chromosomes were obtained through culturing of the HEK-293 clones with colcemid which effectively inhibits the formation of the spindle apparatus through interruption of microtubules (90, 100). HHV-6A *in vitro* chromosome integration was observed by fluorescein labeled HHV-6A (U1102 strain) pMF311-12 and PMF335-6 cosmid probes and metaphase chromosomes were counterstained with DAPI (84). Analysis of HEK-293/clone-2 and HEK-293/clone-3 identified one chromosome-associated HHV-6A signal, while HEK-293/clone-1 had two independent chromosomes associated with the HHV-6A genome (**Fig. 10b**). Furthermore, association of the HHV-6A genome with chromosomes was identified at the termini of the long and short arm of chromosomes, which is in proximity of the telomere

We could not identify the specific chromosomes into which HHV-6A had integrated in the HEK-293 cells using standard cytogenetic methods. This was due to the aneuploidy and chromosomal rearrangements present in these cells. Furthermore, the FISH assay cannot distinguish the non-covalent linkage of ccc episomes from chromosome integrated herpesviruses. Therefore, we studied the *in vitro* integration of HHV-6A into HEK-293 single cell clones using inverse PCR (IPCR) (94). Genomic DNA was first digested with the frequent cutter *Mbo*I, which cleaves methylated DNA. After digestion and heat inactivation, we diluted the *Mbo*I digested DNA to 2 µg/ml, and ligated with 0.045 U/µl T4 DNA ligase for 14 hrs at 15°C. The purpose of diluting digested DNA was to prevent ligation of unrelated fragments and select for self-circularization of the HHV-6A sequence with the adjacent chromosomal fragment. We next amplified the ligated DNA using primers designed from the extreme right end (DR_R) of the genome (**Table 8**), which enabled amplification of the unknown chromosome sequence that is fused with the viral genome (**Fig. 30**). Southern blotting identified IPCR products that hybridized with a human telomere probe as well as an HHV-6 probe from the HHV-6A *in*

vitro integrated HEK-293 single cell clones (**Fig. 11**). No hybridization was observed without ligation of the *Mbo*I fragments. In summary, these experiments reveal that HHV-6A can efficiently integrate into the telomeres of *in vitro* infected HEK-293 cells.

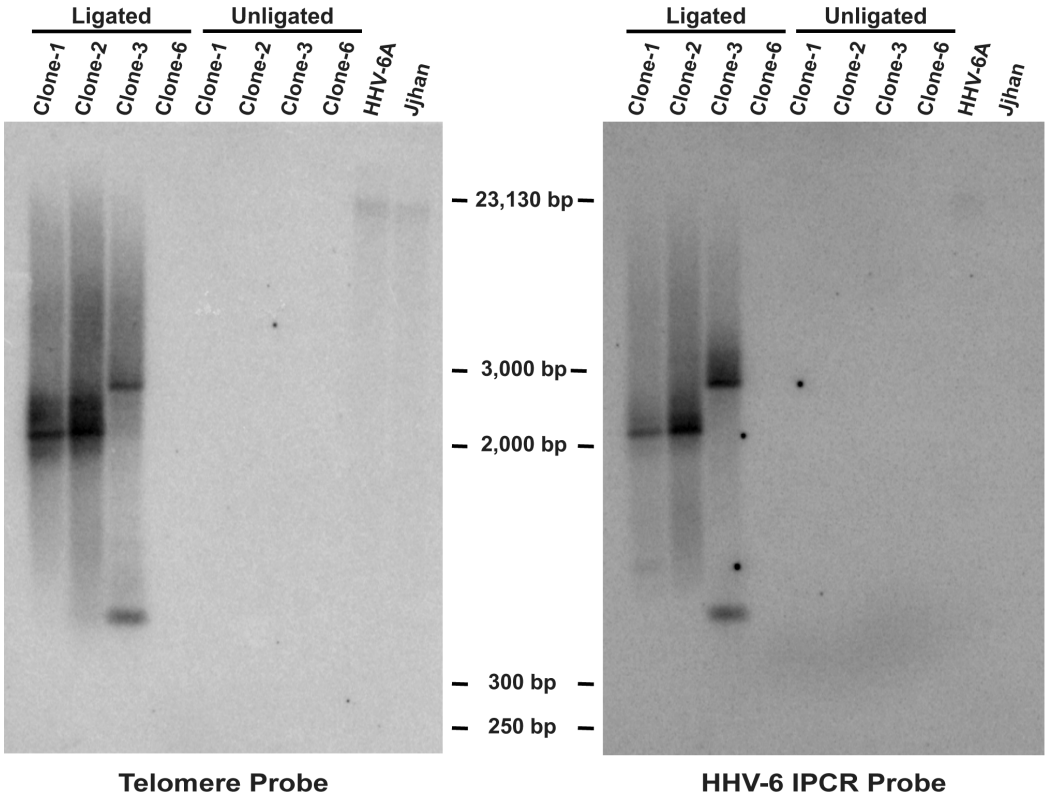

Fig. 11. Inverse PCR (IPCR) (94) analysis of DNA from HHV-6A *in vitro* infected HEK-293 clones. Hypothesis: integration of HHV-6 occurs within the telomere of a human chromosome via homologous recombination with the TTAGGG perfect repeats within right direct repeat (DR_R). Genomic DNA from HEK-293 clones 1, 2, 3, and 6 were digested with *Mbo*I, diluted to prevent ligation of unrelated fragments, followed by self-circularization of HHV-6 DR_R with the adjacent chromosomal fragment. IPCR products were analyzed by Southern blot hybridization with telomere oligonucleotide probe (left panel), and with HHV-6 IPCR probe (right panel). Control IPCR was performed using DNA without ligation (unligated) and hybridization controls HHV-6A infected Jjhan as well as Jjhan (negative control).

Recombinant HHV-6A BAC Virus Expressing GFP and Neomycin Resistance

The use of bacterial artificial chromosomes (BAC) vectors to clone the entire genome of herpesviruses has been instrumental in understanding the means by which viruses replicate, while knockout-mutants have characterized viral proteins. To monitor HHV-6A infection, we constructed an HHV-6A recombinant virus (HHV-6A^{GFP}) carrying the green fluorescent protein (GFP) and neomycin resistance (construction described in **Figs. 5** and **6)**. To accomplish this, we constructed a plasmid in which the GFP expression cassette is flanked by 2 kbp fragments of ORF U53 and ORF U54 cloned from HHV-6A strain U1102. Then we infected several human monolayer cell lines and screened for those that supported lytic replication and in which transfection of the plasmid was efficient. The most promising cell line was HEK-293 cells (101). Preliminary experiments indicated that HEK-293 cells produce infectious virus at low cell density/confluency. To generate HHV-6A^{GFP} recombinants, a HEK-293 monolayer was transfected with the ORF U53-GFP-ORF U54 BAC plasmid. The following day, cells were seeded at about 10 % confluency and infected with 10^3 infectious units of HHV-6A (U1102). After 6 days, we observed the characteristic cytopathic effect (ballooning, refractile giant cells). The virus titer was determined to be 10^3 infectious units.

Since infected HEK-293 cells contain both wt-HHV-6A and HHV-6A^{GFP}, the potential recombinant virus was titrated out by infecting Jjhan T-cell cultures with about one infectious unit per a well in a 96-well plate. In one culture, fluorescence microscopy showed a dramatic increase in the number of green fluorescent Jjhan cells from 7 to 37 days post-infection (**Fig. 12a**). We observed only a few very bright fluorescent large multinucleated cells, which were presumably producing infectious virus. However, the majority of cells in the well displayed dimmer GFP expression.

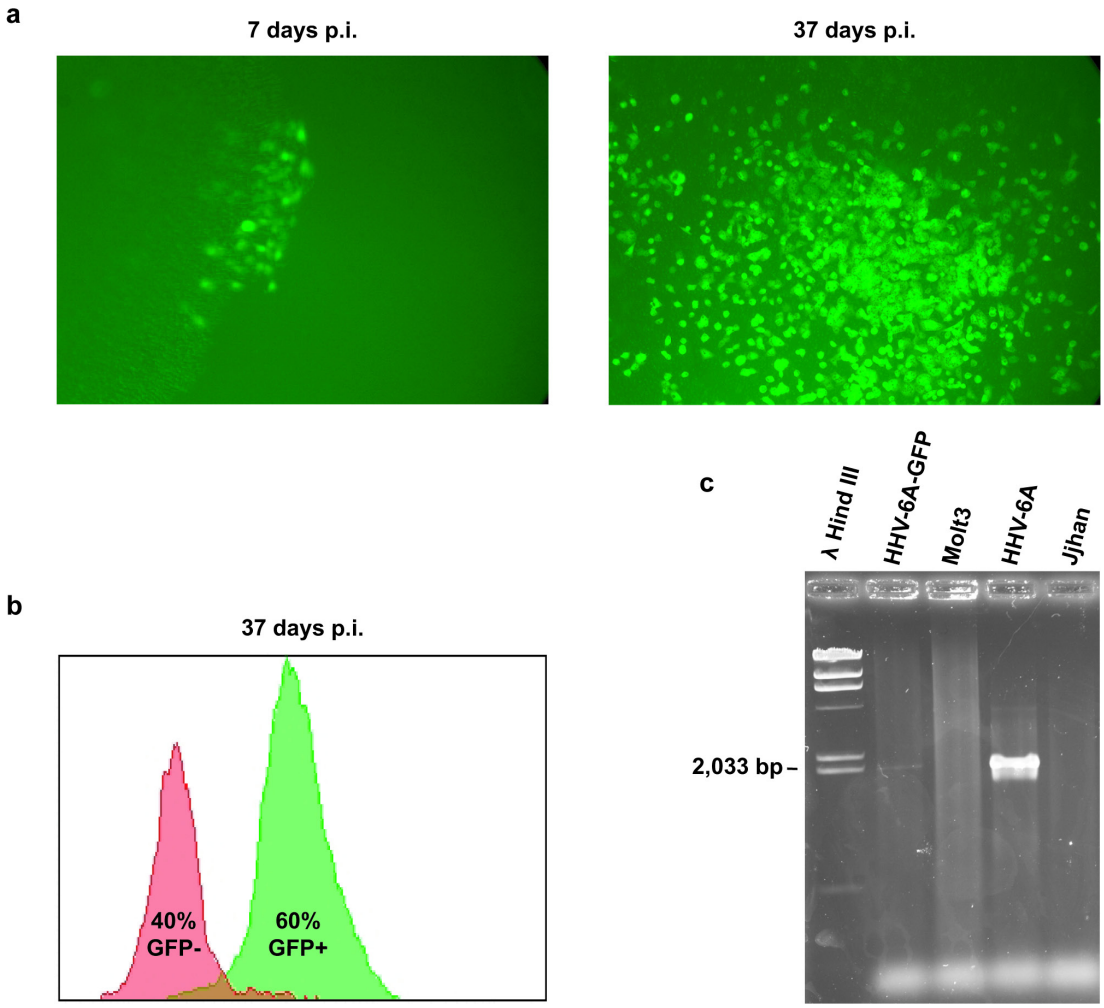

Fig. 12. Microscopic images and flow cytometry analysis of Jjhan cells infected with recombinant GFP expressing HHV-6A (HHV-6A^{GFP}). (**a**) Infection of Jjhan cells resulted in an increase number of green fluorescent cells from 7 to 37 days post-infection as shown by fluorescent microscopy (100 X magnification). (**b**) Flow cytometry analysis indicated that 60 % of Jjhan cells express GFP after 37 days post-infection with HHV-6A^{GFP}. (**c**) DNA from HHV-6A^{GFP} and HHV-6A infected Jjhan cells as well as uninfected Jjhan and Molt3 cells were isolated. PCR amplified ORF U53 with primers U53L and U53R produced a 2033 bp amplicon in HHV-6A and HHV-6A^{GFP} infected cells.

To analyze the distribution of infected Jjhan cells, flow cytometry was used to examine the expression of GFP. Overall GFP expression in HHV-6A^{GFP} infected Jjhan cells was 60 % (**Fig. 12b**). To next evaluate whether GFP fluorescence corresponded to production of HHV-6A^{GFP} virions, we examined two hundred cells of the culture by transmission electron microscopy (TEM) in the Fred Hutchinson Cancer Center EM core laboratory for virus production. Even after examining two hundred cells, no virions were observed. The viral DNA was reproducibly detected by PCR, indicating the presence of the viral genome (**Fig. 12c**). However, despite several attempts, we detected no free circular or linear viral genomes by the method of Gardella *et al.* (88). Therefore, the data are consistent with the hypothesis that HHV-6A^{GFP} established primarily latent infection in Jjhan cells cultured for over one month, and that latency did not involve the formation of viral episomes (Further evaluated in **AIM 2** and **AIM 3**).

Previous attempts by other laboratories to generate an infectious HHV-6 BAC cloned virus were unsuccessful (46, 102). However, we were the first laboratory to successfully produce an infectious HHV-6A virus that expresses GFP and a selectable marker (33). The reproducible cloning system was verified by Tang *et al*. in which they utilized *E. coli* mutagenous techniques to investigate the replication dependence of glycoprotein Q1 (103). The knowledge gained from the adaptation of recombinant HHV-6 viruses focuses future studies to comprehend the clinical balance of viral infection, latency/integration, and reactivation.

The *in vitro* Infection of Human T-cell Lines with HHV-6A and HHV-6B Results in Telomere Integration

Since we have demonstrated the *in vitro* integration of HHV-6A into HEK-293, we next wanted to determine if chromosome integration occurs in multiple cell types during

infection. Specifically, we evaluated whether HHV-6A strain U1102 and HHV-6B strain Z29 can integrate into the telomeres of the T-cell lines Jjhan and Molt3. These cells are routinely used to propagate HHV-6A and HHV-6B, yet we observed that despite supporting lytic infection, Jjhan and Molt3 cells often were not lysed and that many cells survived after the peak of productive infection.

We hypothesized that in some of the infected cells, rather than productive infection leading to cell lysis, the virus had achieved latency through telomere integration. To examine this hypothesis, we prepared DNA from cells at the peak of CPE, containing 10^3 infectious units/ml of virus. We then amplified the putative viral genome-chromosome telomere junction using subtelomere based primers (2p, 11q, 17p, and 18q) and a primer derived near the right end of HHV-6 DR_R (95, 97). The primer to DR_R and not DR_L was utilized because preliminary results determined that HHV-6A *in vivo* integration occurs through the linkage of DR_R with the telomere sequence directly adjacent to the end of the chromosome, while the remaining telomere is fused with DR_L (Results further discussed in **AIM 2**, **Figs. 19** and **23**). Furthermore, the human genome project has yet to fully sequence the ends of chromosomes due to their repetitive sequence and homology shared with other subtelomeres. However, Baird *et al.* has successfully sequenced the ends of chromosomes (subtelomere) and has utilized primers 2p, 11q, and 17p to measure the length of telomeres of specific chromosomes through PCR (95, 97). Consequently, **Fig. 13** shows Southern hybridization of PCR amplified viral genome-chromosome telomere junction from HHV-6B infected Molt3 cells.

To sequence the viral genome-telomere junction of HHV-6B/HHV-6A integrated T-cell lines, we first cloned the PCR amplified fragments through pCR®4-TOPO® cloning system (TOPO TA Cloning® Kit for Sequencing, Invitrogen, Carlsbad, CA). Following

electrical transformation of E. *coli* One Shot® TOP10 (Invitrogen, Carlsbad, CA), positive clones were identified by colony hybridization with [γ^{32}P]-ATP-radiolabeled HHV-6 and telomere oligonucleotide probes. Sequencing of clones confirmed the *in vitro* infection of Jjhan cells results in the HHV-6A genome covalently linked with the telomere of chromosomes 18q, 17p, and 11q (GenBank accession nos. GU784871 and GU784873) (**Fig. 14**). Also, HHV-6B *in vitro* infection of Molt3 cells was found to integrate into telomere of chromosomes 18q, 11q, and 2p. Therefore, the result of these experiments are consistent with the possibility that shortly after *in vitro* infection of Jjahn, Molt3, and HEK-293 cell lines, HHV-6A and HHV-6B can frequently integrate into the telomere region of chromosomes.

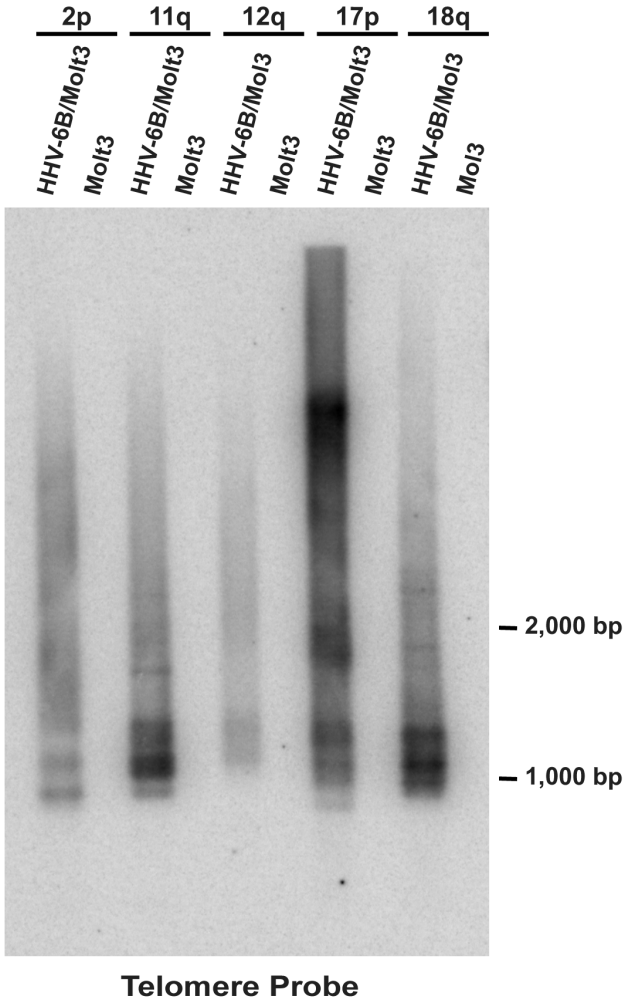

Fig. 13. PCR amplification of virus-chromosome telomere junction from HHV-6B *in vitro*-infected Molt3 cells. DNA from HHV-6B (Z29) infected Molt3 cells were subjected to amplification by PCR primers derived from HHV-6A DR_R and subtelomere primers 2p, 11q, 12q, and 17p published by Baird *et al* (95, 97). Subtelomere primer 18q was designed based upon GenBank sequence information. PCR products from virus-chromosome telomere junction were separated by electrophoresis and analyzed by Southern blot hybridization utilizing a ^{32}P-labeled telomere oligonucleotide probe. Multiple band sizes are due to the variable number of telomere repeats between the DR_R of HHV-6B and the chromosome (**Fig. 14**).

>HHV-6A/Jjhan chromosome 11q integration

CAGACCTTGGAGGCACGGCCTTCGTTTGGGACAATTCGGGGCCGCATCGACGGTGAATAAAATCCTTCCTCTTTGCAGC
CCTGAATAATCAGGGTCAGAGATCAG**TTAGGGTTAGGGTTAGGGTTAGGGTTGGGGTTGGGGTTGGGGTTGGGGTTGGG**
GTTAGGGTTAGGGTTAGGGTTAGGGTTAGGGTTAGGGTTAGGGTTAGGGTTAGGGTTAGGGTTAGGG
TTAGGGTTAGGGTTAGCCGGTGGTTTCCTTTGGCACCGTGCCAGGCGACCGTGGGTCCCAGACGGTGGCACGTCGCGCG
CGATGTCGTTTTGAATTGTCTTCACGTCTCACCCCGGTATGCCCCATCTACGTACCCACCCGCGACTACCACATGGGTG
GGTTGTGCGTGTCTGTGTGTCTGCGTGTGTACGCGTCCGTGGTAGAAACGCGGTGACAACGGATTACGGAGGTGAATGT
TGCGGTGGTTGGGACGGGGAGGGAGTGAAGAGATGTTTCCCGTATAGGTGTTTTTGGAACGTGGTTTTTTTTCTTACA
CTTGCCATGCTAGCGATCGCCCTCTGTCTTCGGTCCGCGTTACCGTGTCGTGTGTACTTCCGCATACTTTTGTCTCTGC
GCCTCGATACACCCCGTTGATTGGATGATCGCCACATGTGTATTGGACGTCACAGTCTGCTATTTTTTTCACTGTCTAT
TTTTAAACCTGTTGTCGTCTTCCCGCCAAGGCTATGTGTCTCCGCCTTTTCTTATATTTTTCTGACGCTGTTCGTTTTC
TACGTTCGCCTCCAATCCCGGACGCACCTCCTTTGTATGTTCACTCCTCCCACCCCCCGGGGTGCCTATATAAGAAGCG
AACGCGACGCGCTTTCAAGCAGTCCCGATCATG

>HHV-6A/Jjhan chromosome 17p integration

TAACATCGAATCCACGGAATGCTTGTGTACTTGGAAACTTAACAATGTGGTCTACAAATCCACAAATAAGATACATTTT
TACATTTACTGGAAGTTTAATTCCTAAGTAATGTCTTATAATTTCCCTCATCTAAGTCTGTCGTTTCATTCCATTTATT
CGTAAGTATAATATTGCTATTGGTATTGTTTAAGGTAGAATTTTCATAATTTGGTGTAGAGATTATTCATTCCTAGCAT
ATACATATAAAATGGAATGTTTGGCCAGGCACCCGGGCTCATACCTGTAACCCAAGCAGGTTGAGAGGCTGAGGAAGGG
TTAGGGTTAGGGTTAGGGTTAGGGTTAGGGTTAGGGTTAGCCGGTGGTTTCCTTTGGCACCGTGCCAGGCGACCGTGGG
TCCCAGACGGTGGCACGTCGCGCGCGATGTCGTTTTGAATTGTCTTCACGTCTCACCCCGGTATGCCCCATCTACGTAC
CCACCCGCGACTACCACATGGGTGGGTTGTGCGTGTCTGTGTGTCTGCGTGTGTACGCGTCCGTGGTAGAAACGCGGTG
ACAACGGATTACGGAGGTGAATGTTGCGGTGGTTGGGACGGGGAGGGAGTGAAGAGATGTTTCCCGTATAGGTGTTTTG
GAACGTGGTTTTTTTTTTCTTACACTGCCATGCTAGCGATCGCCCTCTGTCTTCGGTCCGCGTTACCGTGTCGTGTGTA
CTTCCGCATACTTTTGTCTTGCGCCTCGATACACCCCGTTGATTAGATGATCGCCACATGTGTATTGGACGTCACAGTC
TGCTATTTTTTTCACTGTCTATTTTTAAACCTGTTGTCGTCTTCCCGCCAAGGCTATGTGTCTCCGCCTTTTCTATATT
TTTCTGACGCTGTTCGTTTTCTACGTTCGCCTCCAATCCCGGACGCACCTCCTTTGTATGTTCACTCCTCCCACCCCCC
GGGGTGCCTATATAAGAAGCGAACGCGACGCGCTTTCAAGCAGTCCCGATC

>HHV-6A/Jjhan chromosome 18q integration

CTCATGTCCTCGGTCTCTTGCCTCGGCAAAGATTAGATTAGGGTTAGGGTTTGGGTTCGGGTCAGGGTTAGGGTTAGGG
GTTGGGGTTAGGGTTCGGGTTAGGGTCAGGGTTTGGG**TTAGGGTTAGGGTTA----------**
GGGTTAGGGTTAGGGGTTGGGGTTAGGGTTCGGGTTAGGGTCAGGGTTTGGGTTAGGGTTAGGGTTAGGGTTA
GGGTTAGGGTTAGGGTTAGCCGGTGGTTTCCTTTGGCACCGTGCCAGGCGACCGTGGGTCCCAGACGGTGGCACGTCGC
GCGCGATGTCGTTTTGAATTGTCTTCACGTCTCACCCCGGTATGCCCCATCTACGTACCCACCCGCGACTACCACATGG
GTGGGTTGTGCGTGTCTGTGTGTCTGCGTGTGTACGCGTCCGTGGTAGAAACGCGGTGACAACGGATTACGGAGGTGAA
TGTTGCGGTGGTTGGGACGGGGAGGGAGTGAAGAGATGTTTCCCGTATAGGTGTTTTTGGAACGTGGTTTTTTTTTCTT
ACACTTGCCATGCTAGCGATCGCCCTCTGTCTTCGGTCCGCGTTACCGTGTCGTGTGTACTTCCGCATACTTTTGTCTC
TGCGCCTCGATACACCCCGTTGATTGGATGATCGCCACATGTGTATTGGACGTCACAGTCTGCTATTTTTTTCACTGTC
TATTTTTAAACCTGTTGTCGTCTTCCCGCCAAGGCTATGTGTCTCCGCCTTTTCTTATATTTTTCTGACGCTGTTCGTT
TTCTACGTTCGCCTCCAATCCCGGACGCACCTCCTTTGTATGTTCACTCCTCCCACCCCCCGGGGTGCCTATATAAGAA
GCGAACGCGACGCGCTTTCAAGCAGTCCCGATCTATG

>HHV-6B/Jjhan chromosome 2p integration

GAGCTGCGTTTTGCTGAGCACAGACCTGGGGGTCACCGTAAAGGTGGAGCAGCATTCCCCTAAGCACAGACGTTGGGGC
CACTGCCTGGCTTTGGGACAACTCGGGGCGCATCAACGGTGAATAAAATCTTTCCCGGTTGCAGCCGTGAATAATCAAG
GTCAGAGACCAGTTAGAGCGGTTCAGTGCGGAAAACGGGAAAGCAAAAGCCCCTCTGAATCCTGGGCAGCGAGATTCTC
CCAAGCTAAGGCGAGGGGCTGCATTAAAGGGTCCAGTTGCAGCATCGGAACGCAAATGCAGCATTCCTAATGCACACAT
GATACCCAAAATATAACACCCACGTTGCTCATGTGG**TTAGGGTTAGGGTCAGGGTCGGGGTCGGGGTCGGGGTCAGGGT**
CACGGTTAGGGGTTAAGTGTTAAGGGTTAGGGGTTAAGGGTTAGGGTTAGGGTAGGGTTAGG----------
AGGGTTAGGGTTAGGGTAGGGTTAGGGTTTAGGGTTAGGGTTAGGGTTAGGGTTAGGGTTAGGGTTAGGGTTA
GGGTTAGGGTTAGGGTTAGGGTTAGGGTTAGGGTTAGGGTTAGGGTTAGGGTTAGGGTTAGGGTTAGGGTTAG
GGTTAGGGTTAGGGTTAGGGTTAGATTGCGCCAGCGGTTTCCCTTGGCGTCGTGCCAGGATAGCATGGGTCCGAGACGG
CGGCACGTCGCGCCCGATGCCGTTCCTCATTGTCTTCACATCTGCCCCCCGTATGCTCCCCGCCTGCCCACCCGCGACC
GCCATAGAGGTGGTGTGTGCGTGTCTGCGTGTCTGCGTGTGCACGCGTCTGTGGGAGAAACGCGGAGAAAAGGGATTAC
GGAGGGGGGTGTTGTGGTAGATGGGGTAGGGAGGGATGAAGGGATGTTTCCTTTGTTAGTATATTTCAGCGTTGTTTAT
TTTTTTTTCCTAGCTGCCATGCTAGGGGTCGGCCTTTGTCGTCGGTCCGCGTGACTGTCTGTCGCATGCACTTCCGTAT
ACTTTTTTTTTTTTGCGCGCCGGCACGTCACGTCGATTGGATTGCTGCCACACGTGTATTCGATGGCATGGTCTCCTCTT
TTTTTTTTTCACTGTCTATCTCTGAACCTGTTATCGTCTTCCCGCCAAGGCTATGTGTCTCCGCCTTTCTTATTTTTTT
TACGCCGTTGATTTTCCGCGTTCGTCTCCAACCTCAGACCGACCTCGTGTGTATGTTGGCTCCTCCCACTCCCCGGGGC
GTCTATATAAAAGACGAATGTGGCGCGCTTTCAAGCAGTCCCGATCTATG

>HHV-6B/Jjhan chromosome 11q integration

CAGACCTTGGAGGCACGGCCTTCGTTTGGGACAATTCGGGGCCGCATCGACGGTGAATAAAATCCTTCCTCTTTGCAGC
CCTGAATAATCAGGGTCAGAGATCAG**TTAGGGTTAGGGTTGGGGTTGGGGTTGGGG----------**
AGGGTTTGGGTTGGGGTTGGGGTTGGGGTTGGGGTTGGGGTTAGGGTTAGGGTTAGGTTAGGGTTAGG
GTTAGGGTTAGGGGTTAGGGGTTAGGGTTAGGGTTAGGGTTAGGGTTAGGGTTAGGGTTAGGGTTAG
GGTTAGGGTTAGGGTTAGGGTTAGGGTTAGGGTTAGGGTTAGGGTTAGATTGCGCCAGCGGTTTCCCTTGGCGTCGTGC
CAGGATAGCATGGGTCCGAGACGGCGGCACGTCGCGCCCGATGCCGTTCCTCATTGTCTTCACATCTGCCCCCCGTATG
CTCCCCGCCTGCCCACCCGCGACTGCCATAGAGGTGGTGTGTGCGTGTCTGCGTGTCTGCGTGTGCACGCGTCTGTGGG
AGAAACGCGGAGAAAAGGGATTACGGAGGGGGGTGTTGTGGTAGATGGGGTAGGGAGGGATGAAGGGATGTTTCCTTTG
TTAGTATATTTCAGCGTTGTTTATTTTTTTTTCCTAGCTGCCATGCTAGGGGTCGGCCTTTGTCGTCGGTCCGCGTGAC
TGTCTGTCGCATGCACTTCCGTATACTTTTTTTTTTGCGCGCCGGCACGTCACGTCGATTGGATTGCTGCCACACGTGT
ATTCGATGGCATGGTCTCCTCTTTTTTTTTTTCACTGTCTATCTCTGAACCTGTTATCGTCTTCCCGCCAAGGCTATGT
GTCTCCGCCTTTCTTATTTTTTTTACGCCGTTGATTTTCCGCGTTCGTCTCCAACCTCAGACCGACCTCGTGTGTATGT
TGGCTCCTCCCACTCCCCGGGGTGTCTATATAAAAGACGAATGTGGCGCGCTTTCAAGCAGTCCCGATCTATG

>HHV-6B/Jjhan chromosome 18q integration

CTCATGTCCTCGGTCTCTTGCCTCGGCAAAGATTAGA**TTAGGGTTAGGGTTTGGGTTCGGGTCAGGGTTAGGGTTAGGG**
TTAGGGTTAGGGTTAGGGTTAGGGTTAGGGTTCGGGTTCGGGTCAGGGTTAGGGTCAGGGTTAGGGTTAGGGTT
TAGGGTT----------
AGGGTTAGGGTTAGGGTTAGGGTTAGGGTTAGGGTTAGGGTTAGGGTTCGGGTTCGGGTCAGGGTTAGGGTCAGGGTTA
GGGTTAGGGTTAGGGTTAGGGTTAGGGTTAGGGTTAGGGTTAGGGTTAGGGTTAGGGTTAGGGTTAGGGTTGGGTTAGG
GTTAGGGTTAGGGTTAGGGTTAGGGTTAGGGTTAGGGTTAGGGTTAGGGTTAGGGTTAGGGTTAGGGTTAGGG
TTAGGGTTAGGGTTAGGGTTAGGGTTAGGGTTAGGGTTAGGGTTAGATTGCGCCAGCGGTTTCCCTTGGCGTCGTGCCA
GGATAGCATGGGTCCGAGACGGCGGCACGTCGCGCCCGATGCCGTTCCTCATTGTCTTCACATCTGCCCCCCGTATGCT
CCCCGCCTGCCCACCCGCGACTGCCATAGAGGTGGTGTGTGCGTGTCTGCGTGTCTGCGTGTGCACGCGTCTGTGGGAG
AAACGCGGGGAAAAGGGATTACGGAGGGGGGTGTTGTGGTAGATGGGGTAGGGAGGGATGAAGGGATGTTTCCTTTGTT
AGTATATTTCAGCGTTGTTTATTTTTTTTTCCTAGCTGCCATGCTAGGGGTCGGCCTTTGTCGTCGGTCCGCGTGACTG
TCTGTCGCATGCACTTCCGTATACTTTTTTTTTTTGCGCGCCGGCACGTCACGTCGATTGGATTGCTGCCACACGTGTA
TTCGATGGCATGGTCTCCTCTTTTTTTTTTTTCACTGTCTATCTCTGAACCTGTTATCGTCTTCCCGCCAAGGCTATGT
GTCTCCGCCTTTCTTATTTTTTTTACGCCGTTGATTTTCCGCGTTCGTCTCCAACCTCAGACCGACCTCGTGTGTATGT
TGGCTCCTCCCACTCCCCGGGGTGTCTATATAAAAGACGAATGTGGCGCGCTTTCAAGCAGTCCCGATCTATG

Fig. 14. Sequencing of virus-chromosome telomere junction from HHV-6A infected Jjhan cells and HHV-6B infected Molt3 cells. DNA from HHV-6A (U1102) infected Jjhan cells and HHV-6B (Z29) infected Molt3 cells were subjected to amplification by PCR primers derived from HHV-6A DR_R and subtelomere primers 2p, 11q, and 17p published by Baird *et al.* (95, 97). Subtelomere primer 18q was designed based upon GenBank sequence information. After cloning and sequencing of PCR products data was subjected to GenBank nucleotide sequence analysis. Virus-chromosome telomere junction is indicated: telomere TTAGGG repeats underlined and bold, HHV-6 DR_R text is red, and chromosome subtelomere text is blue.

AIM II. To Determine that Human Herpesvirus 6A and 6B Genome Integrates into the Telomeres of Patients through Germ-Line Transmission

The HHV-6A and HHV-6B Genome Integrates into Telomeres of *in vivo* Infected T-cells during Latency

Results from **AIM 1** illustrate the *in vitro* infection of human T-cell lines as well as HEK-293 cells with HHV-6A and HHV-6B results in the integration of the viral genome into the telomere of chromosomes. Studies have also suggested that individuals can harbor the HHV-6A or HHV-6B genome integrated into their chromosomes (28-31, 34, 98, 99) and may be vertically transmitted in the germ line (32). However, evidence of *in vivo* integration is based primarily on fluorescent labeling of chromosomes with HHV-6 probes through FISH. This assay cannot distinguish non-covalent linkage of viral episomes from chromosome integration and nor can establish the specific site of viral integration. Therefore we sought to determine whether the *in vivo* integration of HHV-6A and HHV-6B actually occurs and define the specific site of viral integration.

Several individuals were identified with neurological symptoms including CNS dysfunction, ataxia, and chronic fatigue (**Table 12**). Family members of those individuals also shared the same symptoms or were asymptomatic. A total of 13 patients from 4 different families living in various regions around the world were enrolled in this study. Peripheral blood was isolated from each family member and quantitative real time PCR identified more than one family member, including a parent and at least one child, had an unusually high copy numbers of HHV-6 DNA. The copy numbers from individuals

from 4 different families were at least one million copies of HHV-6 per ml of peripheral blood (**Table 12**). However, Kondo *et al.* determined the copy number during the peak of primary infection was only 637 ± 273 in 10^4 monocytes/macrophages and 115 ± 42 in 10^4 CD4+ T-cells (10). Therefore, the elevated copy numbers consistently detected in patients of this study suggests chromosome integration of the viral genome.

To investigate the possibility that HHV-6A/HHV-6B had integrated into the family members' chromosomes, we first performed fluorescence *in situ* hybridization (FISH) on T-cell cultures derived from peripheral blood. The experiments were performed in two independent laboratories (University of Minnesota, Minneapolis, MN and Children's Cancer Research Institute, Vienna, Austria). Each laboratory was blind to knowledge of the individual and family membership from which each specimen had been obtained. In each experiment, HHV-6-specific fluorescence was detected in association with the telomeric regions of chromosomes (**Table 12** and **Fig. 15**). The specific chromosome was identified by co-hybridization with viral and chromosome specific probes. HHV-6-specific FISH signal was detected in chromosomes *17p13.3*, *18q23*, and *22q13.3*, in the three families studied with FISH. In each of these family members with integrated HHV-6, the chromosome of integration was identical between both parent and children, suggesting vertical transmission through the germ-line [inherited HHV-6 (iHHV-6)]. Furthermore, iHHV-6 and telomere FISH signals overlapped which signifies chromosome integration occurs specifically at the telomere.

TABLE 12. Patients from four independent families with chromosome integrated iHHV-6

Family Number	Age, Sex	Subject	Disease Stage	HHV-6 Q-PCR[a] (copies/ml)	HHV-6 Subtype[b]	Chromosome HHV-6 FISH	Percent Sequence Identity to HHV-6A (U1102)	
							U94	Direct Repeat
1	58, M	Father	Asymptomatic	629,000	A	18q23	98%	98%
1	54, F	Mother	PCR Negative	Negative	Negative	n/a	n/a	n/a
1	24, M	Sibling-1	Asymptomatic	1,400,000	A	18q23	98%	Not done
1	22, F	Sibling-2	CNS Dysfunction, hypersomnia	1,700,000	A	18q23	98%	Not done
1	12, M	Sibling-3	CNS Dysfunction, ataxia	1,600,000	A	18q23	Not done	Not done
2	80, F	Mother	Mild dementia	625,000	A	17p13.3	98%	Not done
2	45, F	Sibling-1	CNS Dysfunction, fatigue	4,100,000	A	17p13.3	98%	98%
3	76, M	Father	Asymptomatic	2,000,000	B	22q13.3	Not done	Not done
3	61, F	Mother	PCR Negative	Negative	Negative	n/a	n/a	n/a
3	34, M	Sibling-1	CNS Dysfunction, fatigue	2,000,000	B	22q13.3	Not done	Not done
4	62, F	Mother	Asymptomatic	4,000,000	B	Not Done	Not done	Not done
4	36, M	Sibling-1	Asymptomatic	4,500,000	B	Not Done	Not done	Not done
4	29, F	Sibling-2	CNS Dysfunction, fatigue, ataxia	4,200,000	B	Not Done	Not done	Not done

[a]Q-PCR on whole blood completed by ViraCor Laboratories, Lee's Summit MO
[b]Subtypes were determined using PCR with subtype-specific primers

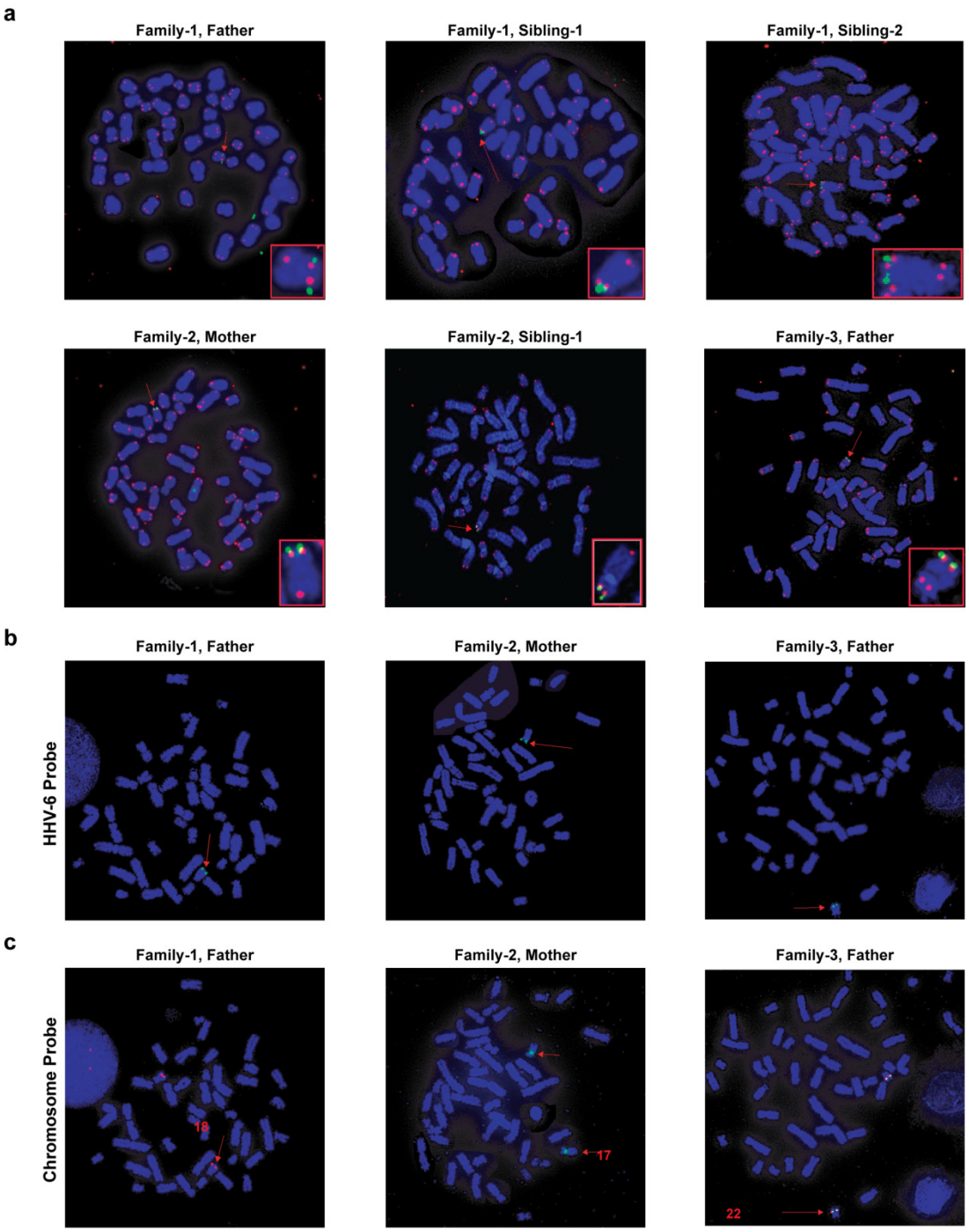

Fig. 15. Fluorescent *in situ* hybridization (FISH) of metaphase chromosomes from T-lymphocytes of family members. PBMCs were stimulated for 72 hrs with 20 ng/ml PHA then cultured in RPMI 1640 medium containing 50 U/ml IL-2 and 10 % FCS. Metaphase chromosomes were generated according to standard cytogenic protocol (90), stained with DAPI and hybridized with various probes as follows; (**a**) FITC-conjugated HHV-6A (U1102 strain) cosmid probes pMF311-2 and pMF335-6 (green)

(84) and cy5-conjugated telomere peptide nucleic acid (PNA) probe (red) (DakoCytomation). The viral genome was present in the same chromosome of the corresponding parents and siblings suggesting germ line transmission (32, 33): Family-1 chromosome *18q23*; Family-2 chromosome *17p13.3*; and Family-3 chromosome *22q13.3*. Lower right hand corner of each figure contains magnification of the chromosome with integrated iHHV-6l DNA. (**b**) Representative FISH from members of Families 1-3. Hybridization with FITC-conjugated HHV-6A (U1102 strain) cosmid probes pMF311-2 and pMF335-6 (84). (**c**) cy5-conjugated BCL2 probe (Chromosome 18) (red), FITC-conjugated chromosome 17 centromere probe (green), and cy5 and FITC-conjugated EWSR1 probe (Chromosome 22) (dual labeled-red and green bottom row) (Vysis).

To investigate whether the FISH method truly detects integration of iHHV-6 into the chromosome of human telomeres rather than an association of the telomere with episomal viral DNA, we analyzed T-cells from members of Family-1 with the method of Gardella *et al.* (88). This method utilizes a vertical agarose gel capable of distinguishing cellular genomic DNA from covalently closed circular DNA (episomes), and replicating linear viral DNA (**Fig. 4**). This occurs through the gently release of the DNA by *in situ* lysis of 1×10^6 PBMCs or T-cells within the loading well of the vertical agarose gel followed by the application of an electric current. Southern hybridization with an HHV-6A cosmid probe (84) confirmed the association of the viral genome with cellular DNA located in the loading well of these gels (**Fig. 16**). No circular episomal and unit length linear viral DNA was detected in these experiments which indicates that chromosome integration is potentially a novel method in which a human herpesvirus can establish latency. As a control, the blot was stripped and hybridized with a mitochondrion oligonucleotide probe to illustrate successful cell lysis and separation of high molecular weight mitochondrion DNA still remaining in the loading well from the circular and linear forms.

To further validate the Gardella gel results, T-cells from member of Families 1, 2, and 3 were immortalized using *Herpesvirus saimiri* (HVS) strain C484 and then applied

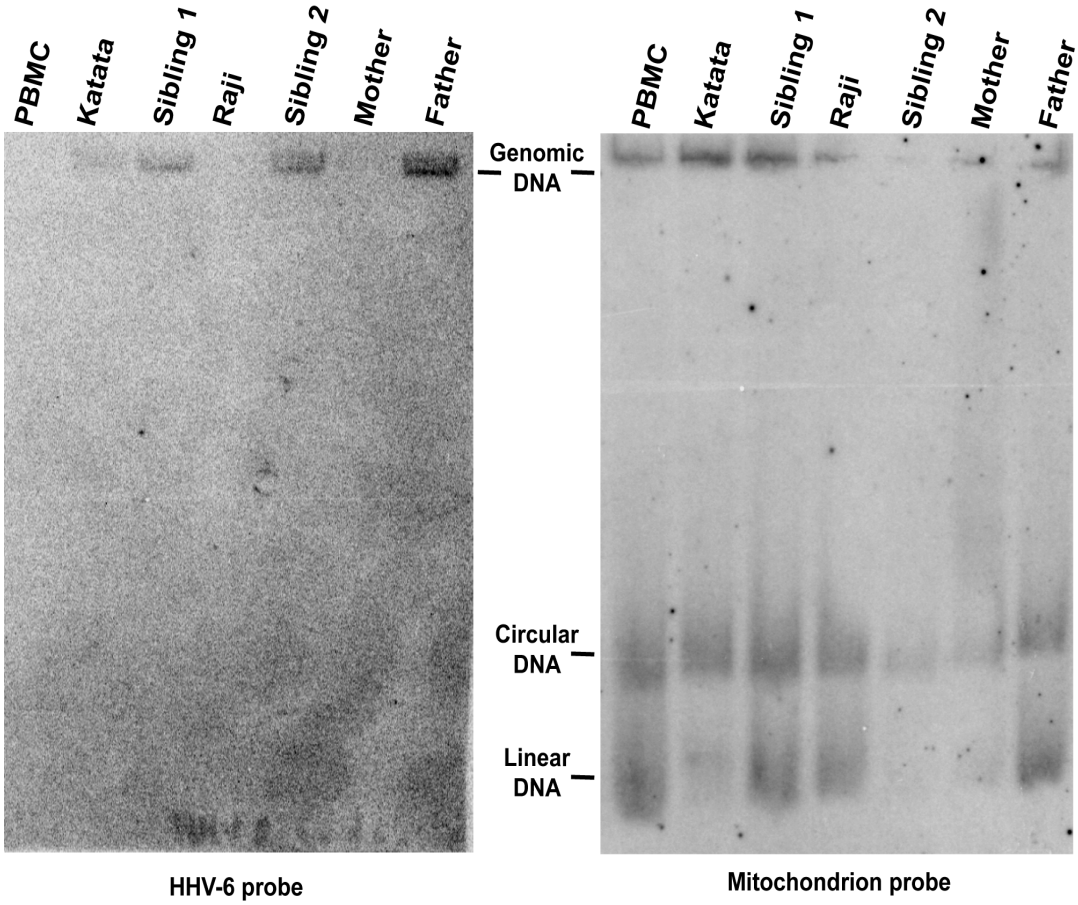

Fig. 16. The vertical agarose gel technique identifies HHV-6 present in the host genomic fraction of Family-1 T-cells. One million T-cells isolated from Family-1 members, control uninfected PBMCs, and HHV-6 positive Katata cell line (HHV-6B integrated Burkitt's lymphoma cell line) (83). Cells were loaded on a vertical agarose gel and analyzed for episomal, linear, or integrated DNA by the method of Gardella *et al.* (88). Southern hybridization with HHV-6A cosmid probe (Left panel) (84). Blot was stripped and hybridized with mitochondrion oligonucleotide probe (Right panel) (89).

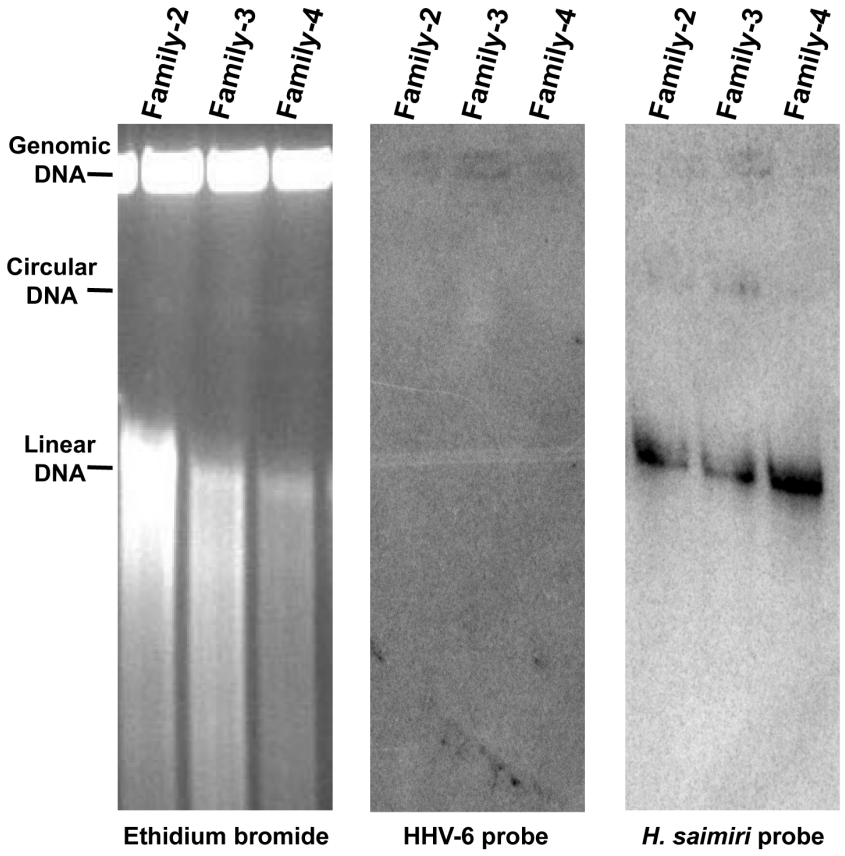

Fig. 17. Analysis of HVS immortalized T-cells from iHHV-6 family members with the vertical agarose gel technique. T-cells isolated from family members immortalized with *H. saimiri* (HVS) strain C484 were subjected to vertical agarose gel technique of Gardella *et al.* (88). Agarose gel was stained with ethidum bromide (left panel) and southern hybridization with HHV-6A cosmid probe (middle panel) (84) illustrates viral integration into the genome. Proper cell lysis and separation of linear and circular fractions was evaluated by striping blot and hybridized with *H. saimiri* cosmid probe (right panel) (86).

to the Gardella gel. Southern hybridization with HHV-6A cosmid (84) probe detected viral signal only within the genomic fraction (loading well) of the Gardella gel (**Fig. 17**), which is consistent with results in **Fig. 16**. Hybridization of the same Southern blot with HVS probe detected both circular episomal and replicating linear HVS DNA, confirming proper release of herpesvirus DNA in the gel as well as the sensitivity of this assay (**Fig. 17**). Therefore, integration of iHHV-6 genome into the chromosome of Family-1, 2, and 3 members occurs during latency, while episome and replicating linear viral DNA was not detected.

In **Aim 1**, we utilized Southern hybridization coupled with IPCR to establish that HHV-6A *in vitro* integration of HEK-293 cells occurs at the telomeres (**Fig. 11**). Likewise, IPCR experiments were also performed using DNA samples isolated from PBMCs from members of Family-1. Briefly, genomic DNA was digested with the frequent cutter *Mbo*I, which cleaves methylated DNA (**Fig. 5**). After digestion and heat inactivation, we diluted the DNA to 2 µg/ml and incubated with T4-ligase for 16 hrs at 15°C. The purpose of diluting digested DNA was to prevent ligation of unrelated fragments and select for self-circularization of the iHHV-6 sequence with the adjacent chromosomal fragment. We next amplified the ligated DNA using primers designed from the extreme right end (DR_R) of the genome (**Table 8**), which enabled amplification of the unknown chromosome sequence that is fused with the viral genome. Southern hybridization of IPCR products were shown to hybridize with the HHV-6 and telomere specific probe (**Fig. 18**). It is noteworthy that the IPCR products were identical in size from iHHV-6A positive Family-1 members.

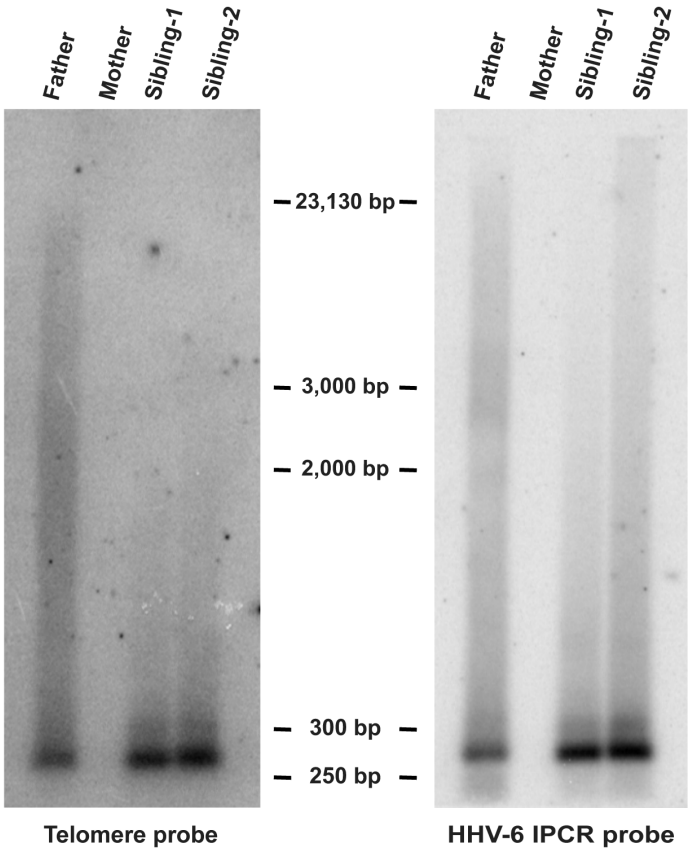

Fig. 18. Inverse PCR (IPCR) analysis of iHHV-6A infected T-cells from Family-1. Genomic DNA isolated from Family-1 T-cells were digested with *Mbo*I and diluted to select for ligation of unrelated fragments. PCR amplification of HHV-6-chromosome telomere fragments were then achieved through HHV-6 primers IPCR-1 and IPCR-2 (**Table 7**). Co-hybridization of HHV-6 IPCR (right panel) and telomere (left panel) oligonucleotide probe via Southern hybridization detects viral integration into human telomeres. Mother's genome was negative control for IPCR (**Table 12**).

Covalent Linkage of the HHV-6 Genome with the Subtelomere of Chromosomes is Mediated through the Viral Telomere Repeats Encoded in DR_R

To build upon the experiments in the previous section, we next wanted to definitely illustrate the *in vivo* integration of HHV-6A and HHV-6B into the telomeres of chromosomes by directly amplifying and sequencing the site of integration. The HHV-6A and HHV-6B genomes encode a perfect TTAGGG telomere repeat array at the right end direct repeat (DR_R) and an imperfect TTAGGG repeat at the end of left end direct repeat

(DR_L) (**Fig. 1**) (3, 4, 104). We established a working hypothesis that HHV-6A and HHV-6B integrates into telomeres via homologous recombination.

To amplify the putative viral-chromosomal DNA junction, we created a primer pair homologous to the DR_L and DR_R of the viral genome, as well as a primer to the subtelomere of chromosome 17p (**Figs. 6** and **19a**). The subtelomere is the chromosomal region immediately adjacent to the TTAGGG telomere repeat array. T-cell DNA isolated from Family-2 members were analyzed in these experiments since FISH had identified the integration of HHV-6A into chromosome *17p13.3* (**Fig. 15**), and the sequence of telomere-subtelomere junction of chromosome 17p is known (95). Amplification with the primer pair designed from DR_R and 17p subtelomere successfully amplified the viral-cellular junction as determined by co-Southern hybridization with HHV-6 DR_R, telomere, and chromosome 17p oligonucleotide probes (**Fig. 19b**). Furthermore, the absence of amplification with a primer derived from DR_L confirmed the integration of HHV-6A into human subtelomere is mediated through the perfect TTAGGG found at the end of DR_R.

To conclusively illustrate the HHV-6A DR_R-subtelomere-chromosome junction, the predominant 1.5 kbp amplicon was excised from the gel and cloned into pCR®4-Topo® vector using the TOPO TA Cloning® Kit for Sequencing (Invitrogen, Carlsbad, CA). E. *coli* One Shot® TOP10 (Invitrogen, Carlsbad, CA) was transformed through electroporation and cultured with LB plates (30 µgl/ml kanamycin). Clones containing the HHV-6A DR_R-subtelomere-chromosome junction were determined through colony hybridization with radiolabeled telomere, HHV-6, and chromosome 17p oligonucleotide probes (**Table 8**). Plasmid DNA from positive clones was isolated with QIAprep® Spin Miniprep Kit (Qiagen, MD) and Sanger sequencing was completed by the Molecular

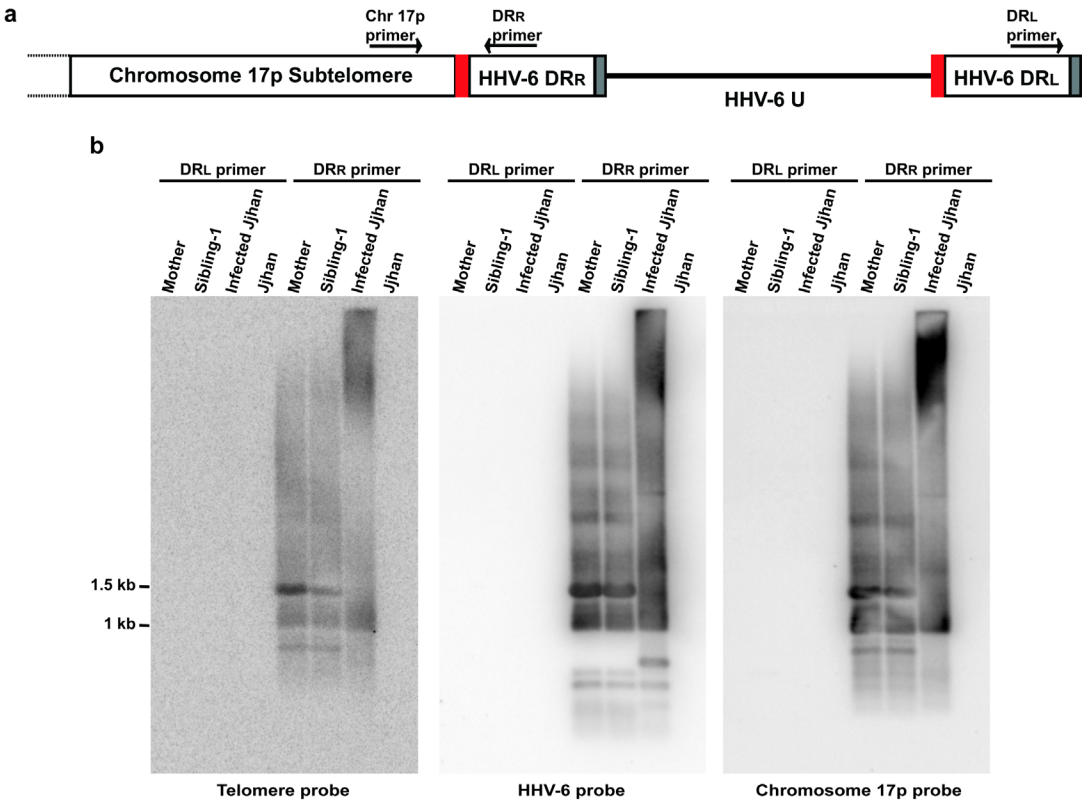

Fig. 19. Chromosome 17p subtelomere-specific PCR analysis of Family-2 members. (**a**) The putative HHV-6A-chromosome 17p junction. Arrows indicate position of primers derived from the direct repeat left (DR_L) and right (DR_R) of the viral genome (Unique = U) and to chromosome 17p subtelomere (95). (**b**) Genomic DNA subjected to amplification: Family-2 Mother and Sibling, HHV-6A infected, and uninfected Jjhan cells. PCR amplicons were separated by electrophoresis and analyzed by Southern blotting using ^{32}P-labelled oligonucleotide probes as indicated at the bottom of each panel. Co-hybridization of a 1.5 kbp fragment with all three probes illustrates the chromosome telomere joining with HHV-6A DR_R. (**c**) The predominant 1.5 kbp amplicon from Family-2/Mother was cloned (n=3) and sequenced. Genbank homology search confirmed the presence of chromosome subtelomere 17p sequence (top) joined with TTAGGG telomere repeats (red and underlined), and HHV-6A DR_R sequence (bottom). GenBank accession no. GU784872.

Biology core facility at H. Lee Moffitt Cancer Center and Research Institute using T3 and T7 primers. Sequencing results indentified the HHV-6A DR_R covalently linked with the subtelomere sequence of chromosome 17p from members of Family-2 (**Fig. 19c**). The integration site contained 5 TTAGGG repeats, and integration resulted in the loss of 79 nucleotides from the far right end (DR_R) the iHHV-6A genome (GenBank accession no. GU784872). This observation is in agreement with other publications that have found variability in the number of telomere repeats at the end of HHV-6 DR_R and DR_L (45, 99).

The Chromosome Telomere is Covalently Linked to the DR_L of iHHV-6 Genome

Results in the previous section illustrate the telomere integration of iHHV-6 occurs through recombination with the perfect telomere repeats encoded in the DR_R (**Fig. 19**). Therefore, we sought to further characterize the genomic structure of iHHV-6. Specifically, we wanted to determine if the DR_L of iHHV-6 was conserved with the integrated genome and whether the tandem array of telomere repeats [$(TTAGGG)_n$] at the end of the chromosomes was extend beyond the DR_L (**Fig. 20**).

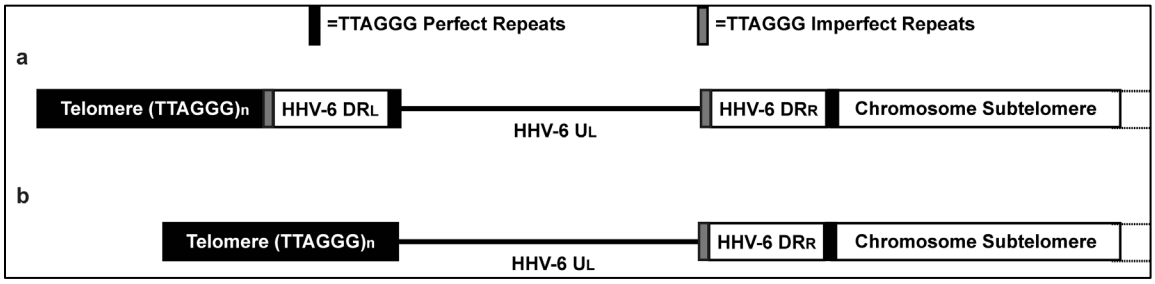

Fig. 20. Analysis of the genome conformation of chromosome integrated iHHV-6. Results in **Fig. 19** illustrate the DR_R of iHHV-6 fused with the chromosome subtelomere. However, it's unknown whether homologous recombination occurs with the DR_L (**a**) perfect or (**b**) imperfect telomere repeats. Therefore there is a possibility the DR_L could be lost from the integrated genome during the process of integration.

Experiments by Frenkel *et al.* has demonstrated the deletion of DR1 through the first exon of DR6 from a laboratory strain of HHV-6A (U1102) was dispensable for *in vitro* replication (47, 102). The deletion of DR was found during the process of cloning the linear concatemer form of the virus during lytic replication. Therefore, we have developed two PCR based assays to determine if the DR_L of iHHV-6 was conserved with the integrated genome of patients in this study (**Table 12**).

In the first experiment, the DR_L was successfully amplified from Family-1 members' genomic DNA (**Fig. 21**). Following Southern hybridization with telomere specific oligonucleotide probe, we identified variability in the predicted molecular weight of the amplified fragments. The variable number of telomere repeats between DR and U has been previously characterized in clinical HHV-6 isolates (33, 45).

To confirm the results in the previous experiment, we evaluated the DR_L in a second group of patients with iHHV-6 and utilized a second primer set in combination with restriction enzyme digestion (**Fig. 22a**). The PCR amplified DR_L fragment has two *DraI* restriction sites that lead to the expected fragment sizes of 1027, 217, 186 bp according to the HHV-6A genome (strain U1102) (4). Similar to the results in **Fig. 21**, the DR_L was present in the iHHV-6 genome of all patients evaluated with PCR amplification and *DraI* digestion (**Fig. 22b**).

Since we have illustrated the conservation of the DR_L from iHHV-6, we next wanted to determine whether the tandem array of telomere repeats $[(TTAGGG)_n]$ at the end of the chromosome was extend beyond the DR_L. Various methods have quantified the overall length of a population of telomeres (96). However, Baird *et al.* has established a protocol to calculate the length of a telomere from a specific chromosome end (95, 97). The single telomere length analysis (STELA) assay has successfully determined the length of telomeres from chromosomes XpYp, 2p, 11q, 12q, 17p, and

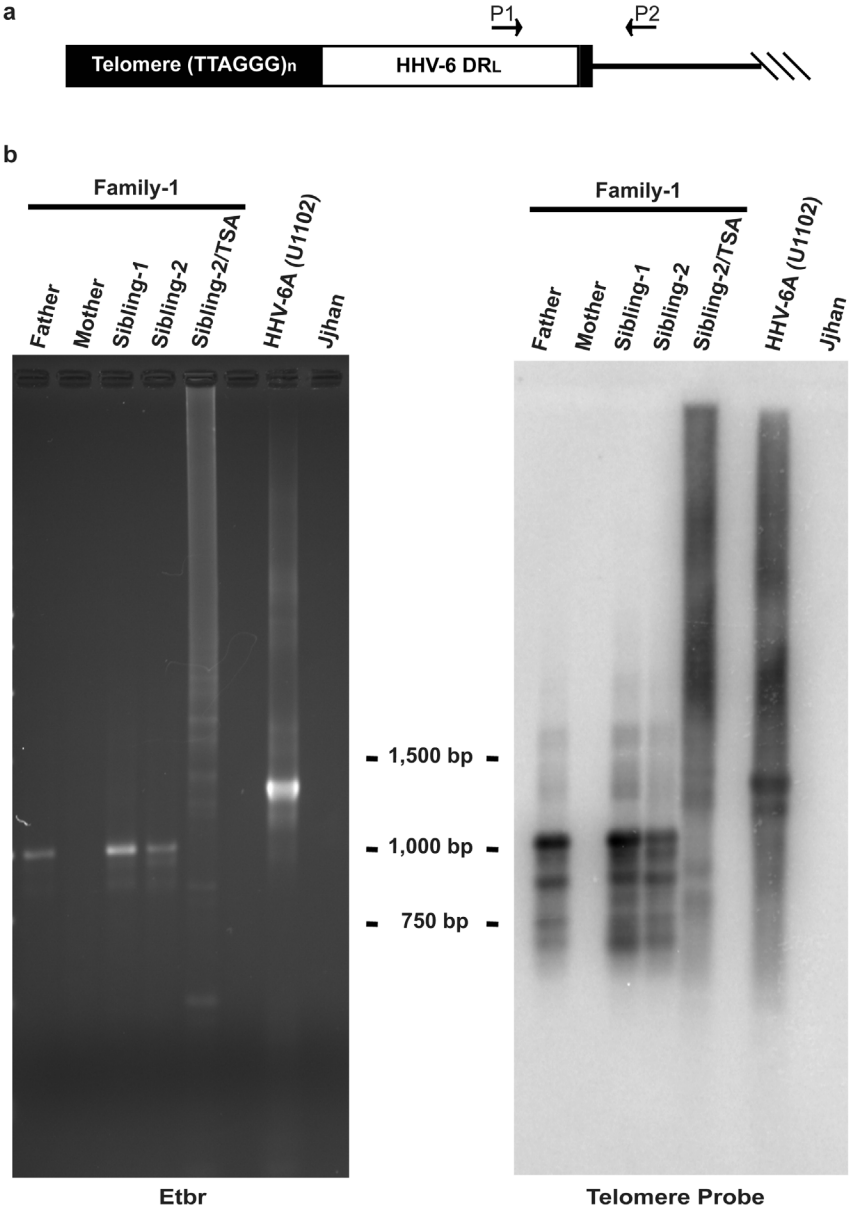

Fig. 21. Amplification of the DR_L from chromosome integrated iHHV-6. (**a**) Diagram for the amplification of DR_L in which primer 1 (P1) binds to region inside of DR_L and primer 2 (P2) binds within the U region of iHHV-6. (**b**) Amplification of DR_L from members of Family-1 results in the predicted size of 1,198 bp (HHV-6A U1102) as shown in the ethidium bromide (Etbr) staining (left panel). Southern hybridization with telomere oligonucleotide probe (right panel). Controls: HHV-6A (U1102) positive control while Family-1/Mother and Jjhan were negative controls.

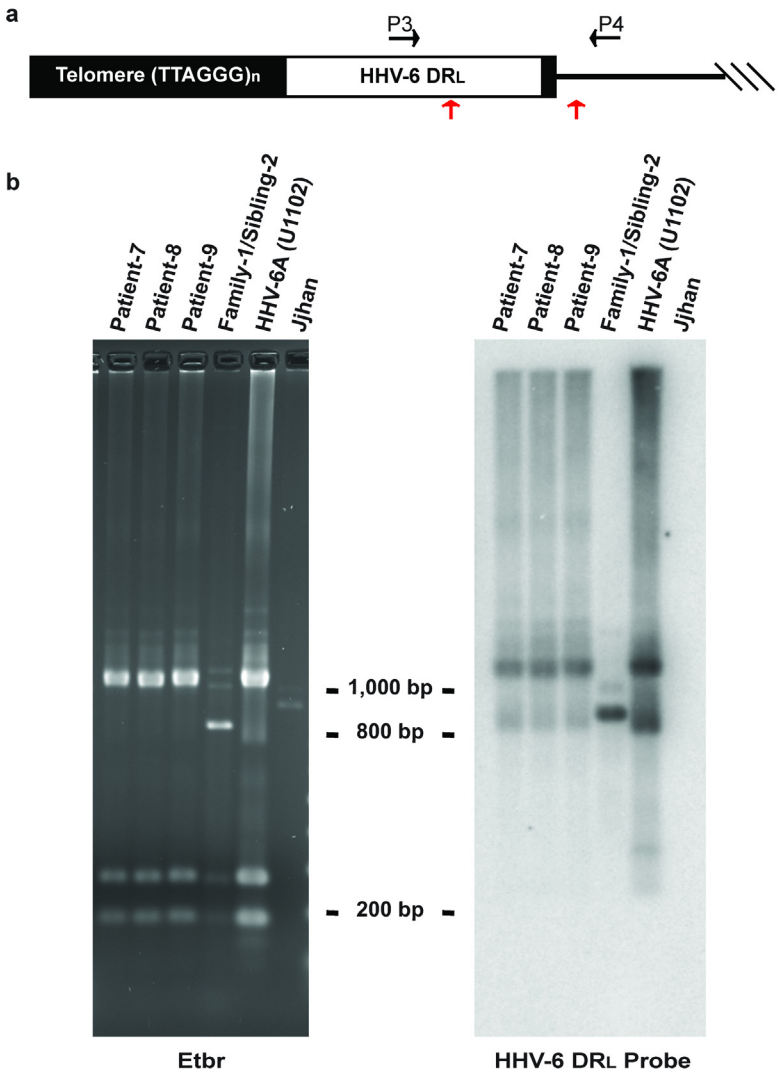

Fig. 22. Amplification and restriction digestion of the DR_L from chromosome integrated iHHV-6. (**a**) Diagram for the amplification of DR_L in which primer 3 (P3) binds to region inside of DR_L and primer 4 (P4) binds within the U_L of iHHV-6. *DraI* restriction sites are indicated by red arrows. (**b**) Amplification and restriction digestion with *DraI* results in the predicted 1027, 217, 186 bp (HHV-6A U1102) as shown in the ethidium bromide (Etbr) staining (left panel). Southern hybridization with HHV-6 DR_L oligonucleotide probe hybridizes with DR_L 1027 bp band (right panel). Controls: HHV-6A (U1102) positive control and Jjhan negtaive control.

18q with use of primers specific to individual chromosome ends. Therefore, we have adapted the STELA assay to determine whether the telomere is extended beyond the left direct repeat (DR_L) of iHHV-6A and iHHV-6B as well as quantify the overall telomere length of the integrated chromosome (**Fig. 20**).

To begin, genomic DNA was isolated from iHHV-6A and iHHV-6B patients (**Table 12**) with Wizard® Genomic Purification Kit (Promega). Next, the linker (Tellorette-2) containing a single TTAGGG repeat was ligated to the end of the telomere by incubating 60 – 150 ng of genomic DNA with T4 ligase for 13 hrs at 35□C (**Fig. 23a**). The reaction was then purified through phenonl chloroform/isoamyl alcohol (24:1) and resuspended in TE. Serial dilution of linker-DNA was amplified with a high fidelity taq polymerase (Expand 20 kb^{PLUS} PCR System, Roche), linker annealing primer (Teltail-P1), and iHHV-6 primer (P2) (**Fig. 23a**). The specific amplification of telomere sequences at the end of DR_L was indentified through southern hybridization with [γ^{32}P]-ATP-radiolabeled telomere oligonucleotide probe (**Fig. 23bc**).

To confirm the specific amplification of telomere sequences extended beyond DR_L of iHHV-6, the nitrocellulose blot was stripped and re-hybridized with PCR amplified iHHV-6A DR_L random primer [α^{32}P]-dATP-radiolabeled probe. Co-hybridization of telomere and DR_L probes confirmed amplification of adjoining chromosome telomere with the DR_L of iHHV-6 (**Fig. 20a**). The heterogeneity of amplified telomere fragments has also been previously observed in non-iHHV-6 integrated human somatic cells (95, 97). Furthermore, the specific telomere length of iHHV-6A integrated chromosome 17p of Family-1/Sibling-2 PBMCs was 5,158 bp. This was calculated by determining the mean molecular weight of all bands co-hybridizing with telomere and iHHV-6A DR_L radiolabeled probes from eight different PCR reactions.

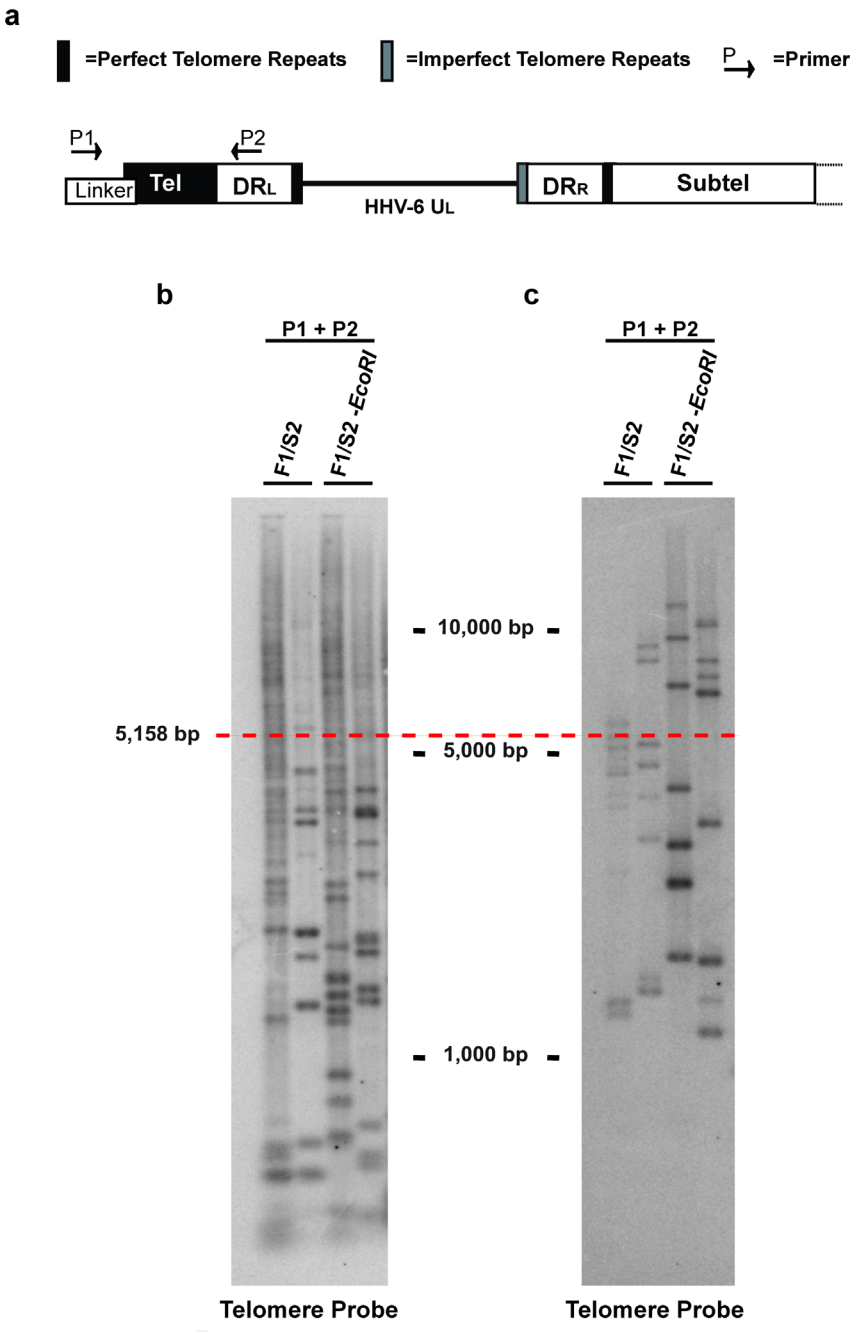

Fig. 23. Single telomere length analysis of iHHV-6 integrated PBMCs. (**a**) Diagram illustrating the strategy of single telomere length analysis (STELA) of iHHV-6. To amplify the specific chromosome telomere (Tel) extended beyond the DR_L of iHHV-6; a linker (Telorette-2) oligonucleotide is ligated to the end of the telomere. Amplification of the telomere is then preceded with primers P1 and P2. Serial dilution of (**b**) 150 ng and (**c**) 60 ng of DNA (*EcoRI* digested +/- for DNA solubilization) isolated from Family-1/Sibling-2 (F1/S2) PBMCs was amplified with STELA primers. The specific telomere length of iHHV-6A integrated chromosome 17p of Family-1/Sibling-2 PBMCs was 5,158 bp, while the amplified range was 12,307 bp to 1,300 bp.

HHV-6 Maintains its Latent Genome through Integration into Telomeres of Chromosomes in the Absence of Covalently Closed Viral Episomes

Following infection, the genome of herpesviruses circularizes and the genome replicates through rolling-circle replication facilitated by the viral DNA polymerase (26, 27). Replication leads to the formation of concatemers of linear viral genomes linked in a head-to-tail conformation. The viral concatemer is subsequently cleaved to give rise to single copies of the full length viral genome. However during latency, the genome of herpesviruses remains as a nuclear circular episome, while the cellular DNA polymerase and latency-associated viral genes promote replication of the viral genome without formation of infectious virus (1, 26, 27). Moreover, the viral latency genes EBNA1 and LANA promote the association of EBV and KSHV episomes with chromosomes via protein-protein interactions (35, 36). This ensures each infected cell obtains multiple copies of the viral episome during cell division. Therefore, the central dogma of herpesvirus replication is that the viral genome establishes latency as a nuclear circular episome and reactivation occurs through rolling-circle DNA replication (1, 26, 27).

We previously utilized the Gardella gel assay (88) to demonstrate the *in vivo* integration of iHHV-6A into the chromosomes of members from Family-1 during latency (**Fig. 16**). Furthermore, even after utilizing P^{32} radiolabeled HHV-6A cosmid probes (84), the Gardella gel assay did not detect the presences of HHV-6 episomes. Therefore, we looked for small numbers of episomes that might not have been detectable by the Gardella gel assay (88).

Genomic DNA was isolated from HHV-6A integrated HEK-293 cells (**Table 2**), and HVS immortalized iHHV-6A integrated T-cells from a member of Family-1 and 2 (**Fig. 17**). We next subjected these cells to CsCl/ethidium bromide gradient ultracentrifugation to isolate the viral episome from the cccDNA fraction and the

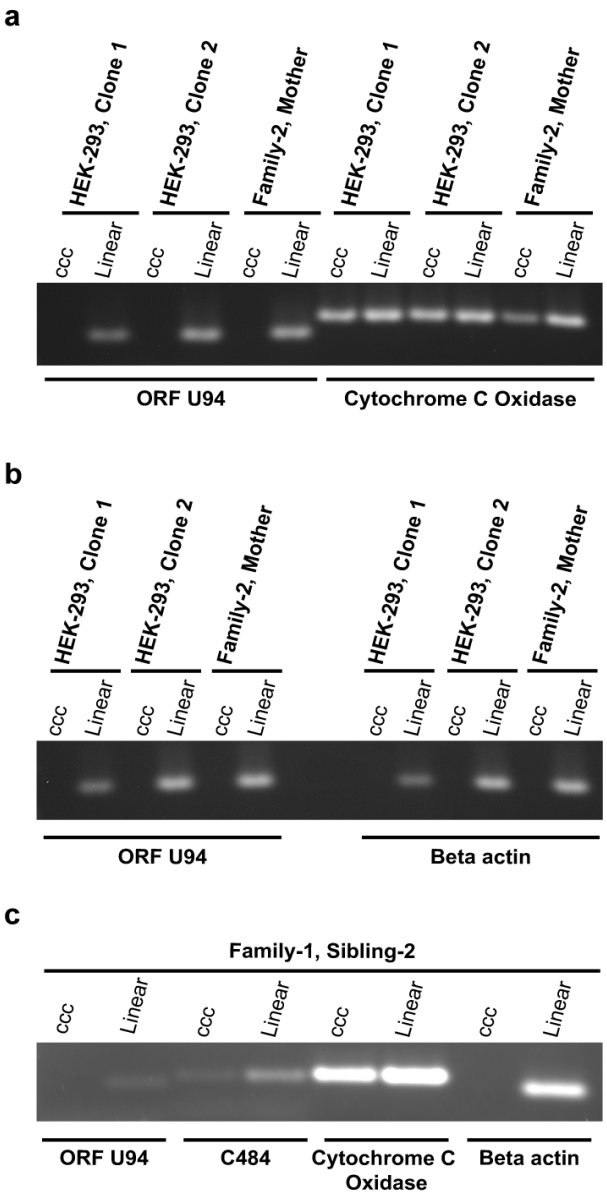

Fig. 24. PCR amplification fails to detect HHV-6 DNA in episomal fractions of CsCl/ethidium bromide (EtBr) gradients. To search for covalently linked circular viral episomes by a method more sensitive than the method of Gardella (88), 50 µg DNA from two latently infected HEK-293 clones, T-cells from Family-2/Mother, and T-cells from Family-1/Sibling-2 immortalized with HVS strain C484 were subjected to CsCl/EtBr gradient ultracentrifugation for two days (CsCl density 1.55 g/ml, 10 µg/ml EtBr, VTI 65 rotor 40K rpm). After centrifugation fractions were collected, linear and episomal (ccc) DNA identified by agarose electrophoresis. Salt and EtBr were removed from combined linear and episomal ccc fractions and were subjected to PCR based amplification using primers to (**a**) HHV-6 ORF-U94 and mitochondrial cytochrome c oxidase (positive episomal control), (**b**) ORF U94 (HHV-6 genome) and beta actin (positive chromosome control), and (**c**) HHV-6 ORF-U94, C484 (Stp), and cytochrome c oxidase (positive episomal control). ccc stands for covalently closed circular episomal fraction.

chromosome integrated iHHV-6A from the linear fraction. Fractions were subjected to PCR amplification with primers to beta actin and cytochrome C oxidase (mitochondrion genome) to identify the linear DNA and cccDNA fractions respectively (91, 92). PCR amplification of ORF U94 (HHV-6) was then utilized to determine if the viral genome was integrated or a circular episome during latency. Following CsCl/ethidium bromide gradient and PCR amplification, iHHV-6 DNA was detected only in the linear fraction, and was completely absent from the episomal (ccc) DNA fraction in both patient T-cells and HEK-293 cells (**Fig. 24ab**).

Since our PCR assay can detect as few as 1-5 molecules, the CsCl/ethidium bromide gradient ultracentrifugation experiment confirmed that the HHV-6 episome cannot be detected even by a highly sensitive method. The amplification of mitochondrial sequence in the linear fraction is expected since replicating and relaxed mitochondrial episomes band together. Furthermore, the detection of HVS episomes in immortalized iHHV-6A integrated T-cells demonstrate the sensitivity of this assay (**Fig. 24c**).

The Genome Sequence of Germ-Line Integrated HHV-6 from Patient T-cells is Divergent from HHV-6A (strain U1102) and HHV-6B (strain Z29)

To investigate whether the iHHV-6 genome integrated in chromosomes of Family-1 is the same among family members and to determine the degree of similarity to HHV-6A (strain U1102) and HHV-6B (strain Z29), Southern hybridization of *Eco*RI digested genomic DNA was performed (**Fig. 25**). Hybridization using a mixture of HHV-6A (U1102 strain) cosmids (84) representing about 80% of the viral genome, revealed that the banding pattern was indistinguishable among iHHV-6 positive members of

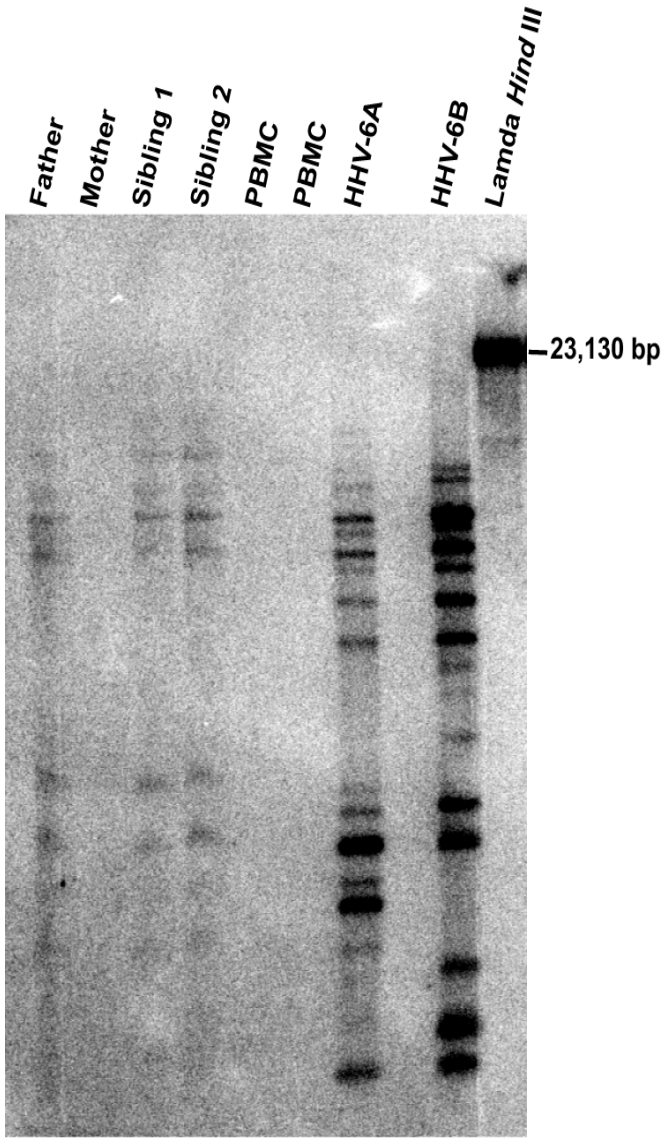

Fig. 25. *EcoRI* restriction site analysis of integrated iHHV-6A in Family-1 T-cells. Total genomic DNA was isolated from iHHV-6 integrated Family-1 members' PBMCs, HHV-6A (U1102 strain) infected Jjhan cells, HHV-6B (Z29 strain) infected Molt3 cells, and uninfected PBMCs with Wizard Genomic DNA Purification Kit (Promega) according to manufacturer's protocol. 5 µg of genomic DNA was digested with 24 U of *EcoRI* (Promega) and separated on 0.8% horizontal agarose gel. Southern hybridization was completed with HHV-6A (U1102) cosmid (84) probe mixture.

Family-1. However the pattern of the integrated viral DNA was significantly different from prototype HHV-6A (U1102) or HHV-6B (Z29).

To evaluate the degree of variation between Family-1 and Family-2 integrated iHHV-6 from the prototypical HHV-6A and HHV-6B strains, ORF U94 (141267-143197 bp) and DR (421-1474 bp, 151654-152707 bp) were amplified by PCR and cloned into the pCR®4-TOPO® vector (Invitrogen). Sequencing was completed with primers T7 and T3 by the Molecular Biology core facility at the H. Lee Moffitt Cancer Center and Research Institute. The viral sequences from various family members were identical as illustrated by the multiple sequence alignment (**Fig. A1**). However, the sequence DR shared 96% identity with HHV-6A and 89% identity with HHV-6B (**Table 12**). DNA sequences of the rep gene ORF U94 were more conserved; 98% identity with HHV-6A and 95% identity with HHV-6B. It is noteworthy that chromosomal integrated iHHV-6 sequences obtained from Family-1 and Family-2 were more closely related to each other than to HHV-6A and HHV-6B alone. Therefore, the similar viral sequences (**Fig. A1** and **Table 12**) and identical sites of chromosome integration (**Fig. 15** and **Table 12**) between family members confirms vertical transmission of the iHHV-6 genome through the germ-line.

In a study completed by Rapp *et al.*(105), sequences of the ORF U94 gene shared remarkable conservation among isolates of HHV-6A (U1102 strain-99.4% identity) and HHV-6B (Z29 strain-99.7% identity) among 17 isolates from three different geographical locations. In contrast, our work has found only 98% sequence identity between ORF U94 from the integrated iHHV-6 genome in two families (**Table 12**).

Since we have completed partial sequencing of the iHHV-6 genome (ORF U94 and DR), we now sought to determine the complete genome sequence of the reactivated iHHV-6 (**AIM 3**) and compare the sequence to HHV-6A (strain U1102) and HHV-6B

(strain Z29). To begin, genomic DNA was isolated from Family-1/Sibling-2 PBMCs and 454-Sequencing was completed in collaboration with the University of Florida Interdisciplinary Center for Biotechnology Research. 454-Sequencing analyzed 156,609 bp of the iHHV-6 genome, which correlates to a genome coverage of 98.3%. Sequence identity between the genome of iHHV-6 and HHV-6A (strain U1102) was 97.2%, while only 88.3% sequence identity was shared with HHV-6B (strain Z29).

AIM III. To Determine if the Chromosome Integrated Human Herpesvirus 6A Genome can Reactivate from Latency and Produce Infectious Virus

TSA and TPA/Hydrocortisone can Induce Lytic Replication of Chromosome Integrated HHV-6A

Experiments from **AIM 1** and **2** provided substantial evidence that HHV-6A and HHV-6B achieves latency via integration into the telomeres of human PBMCs *in vivo* and following infection of T-cell lines and HEK-293 cells *in vitro*. It appears that in cell lines capable of supporting productive, lytic infection, some of the cells also become latently infected through chromosomal integration, and remain viable. Moreover, in neither the *in vivo* or *in vitro* studies did we find HHV-6 DNA in episomal form—the strategy by which other human herpesviruses achieve latency (**Figs. 16, 17,** and **24**). Therefore, it remained unknown whether iHHV-6 can reactivate from its integrated state to produce infectious virions, making integration a molecular strategy for viral latency.

To determine if chromosomally-integrated HHV-6A and HHV-6B can reactivate, we collected HHV-6A integrated HEK-293 cells and T-cells from five patients with iHHV-6 (**Table 2** and **12**). These cells were cultured either in the presence trichostatin A (TSA)—a histone deacetylase inhibitor known to reactivate latent herpesviruses—or with 12-O-Tetradecanoyl-13 acetate (TPA) and hydrocortisone for three days (106-110). Genomic DNA was then isolated from these cells and the increase in viral copies was determined by amplification of HHV-6 ORF U94 through quantitative real time PCR (qPCR). TSA induced a 3.7 fold increase in viral copies for HEK-293 cells with

integrated HHV-6A and 1.4 fold increase in viral copies from patient T-cells with iHHV-6 as compared to untreated control (**Fig. 26**). TPA and hydrocortisone produced similar though milder effects.

To determine if the increase in viral DNA copies resulted in the production of infectious virus, we cultured PBMCs from six members of Family-1 and Family-2 with TPA and hydrocortisone. We then co-cultured these cells with Molt3 T-cell line in the presence of TPA and hydrocortisone. After 2 weeks, lytic reactivation of iHHV-6 was evident by observing syncytia in the infected Molt3 cells (**Fig. 27**).

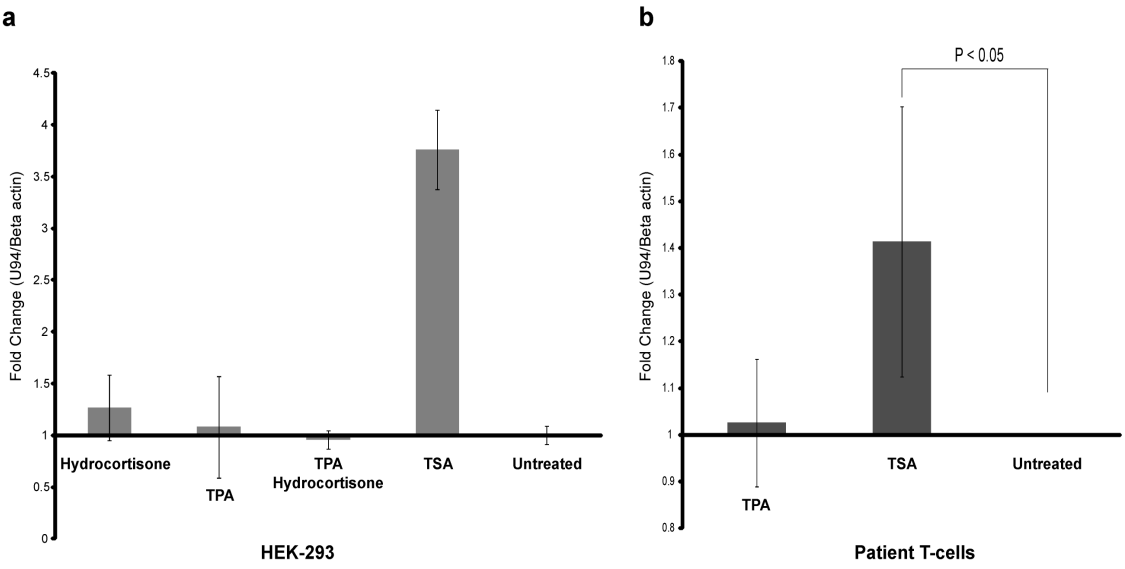

Fig. 26. HHV-6 DNA qPCR analysis of patient T-cells and *in vitro* latently infected HEK-293 cell lines induced by TPA and TSA. T-cell cultures from five family members and three latently infected HEK-293/HHV-6A cell lines were cultured in AIM-V or DMEM medium supplemented with 10% FCS and treated with 20 ng/ml TPA, $1x10^{-6}$ M hydrocortisone, and 80 ng/ml TSA for three days. DNA isolated from cells (in triplicate) were subjected to quantitative real time PCR (qPCR) for ORF U94 and fold change ratios of Ct values normalized to beta actin were relative to untreated control. (**a**) HEK-293 (n=3) and (**b**) T-cells (n=5). TSA promoted significant increase in viral DNA replication, while the stimulation with TPA and hydrocortisone had a milder effect. Statistical analysis was based upon the student T-test and $p < 0.05$ was considered significant.

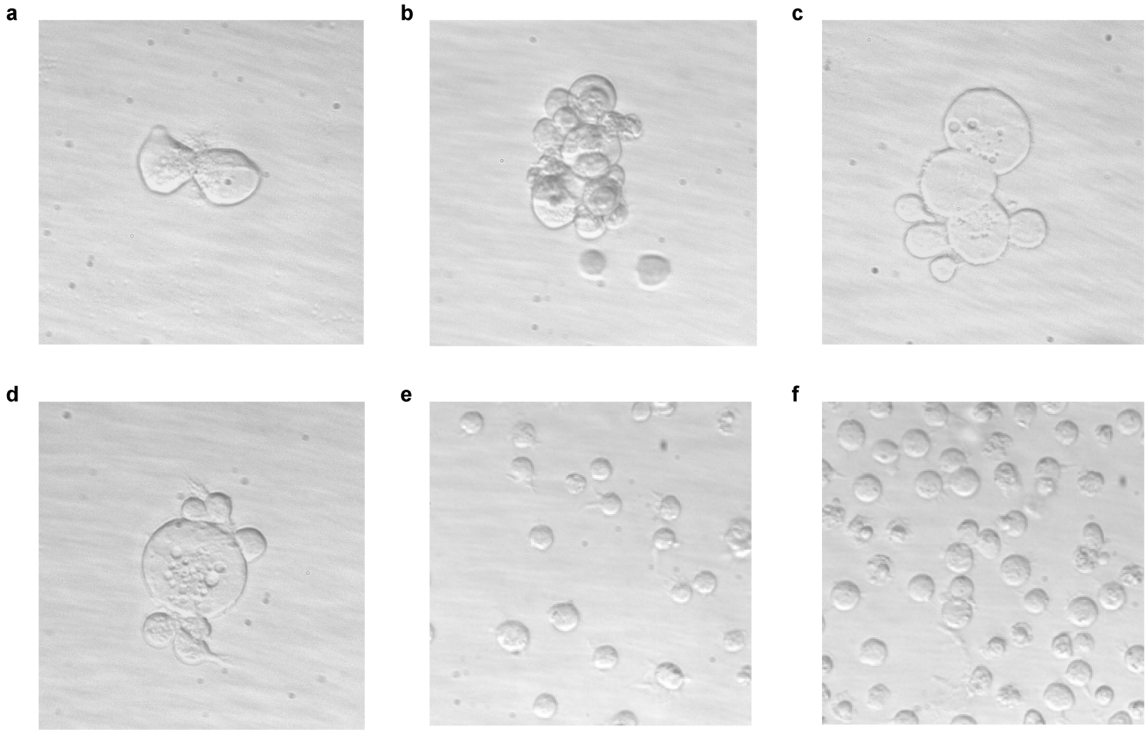

Fig. 27. Reactivation of iHHV-6A induces syncytium formation in a naïve T-cell line. (**a-d**) Freshly isolated PBMC from Family-1/Sibling-2 stimulated with 20 ng/ml TPA and $1x10^{-6}$ M hydrocortisone. PBMC were co-cultured with Molt3 cells for 2 weeks. Syncytium formation (400X magnification) was documented. (**e**) Molt3 cells treated with TPA and hydrocortisone and (**f**) Molt3 cells untreated.

To determine the stage of viral replication of iHHV-6A, we analyzed the reactivated virus isolated from Family-1/Sibling-2 PBMCs through the Gardella gel (88). Southern hybridization with HHV-6A cosmid probes demonstrated the lytic replication as shown by the presence of replicating iHHV-6A linear DNA and RNA (**Fig. 28**). Furthermore, sequencing of the DR region from latent chromosome-integrated iHHV-6A (Family-1/Sibling-2) PBMCs was identical to the reactivated virus cultured in the Molt3 cells (**Fig. A1**). This confirms the successful reactivation of integrated iHHV-6 from patient cells.

Taken together, the data suggest that HHV-6A and HHV-6B are unique among human herpesviruses: they specifically and efficiently integrate into telomeres of

chromosomes during latency rather than forming episomes—the strategy by which other human herpesviruses achieve latency. Moreover, the integrated viral genome is capable of reactivation to produce infectious virions. Thus, the integration of iHHV-6A and iHHV-6B is not an unusual dead-end phenomenon, but a means of achieving latency.

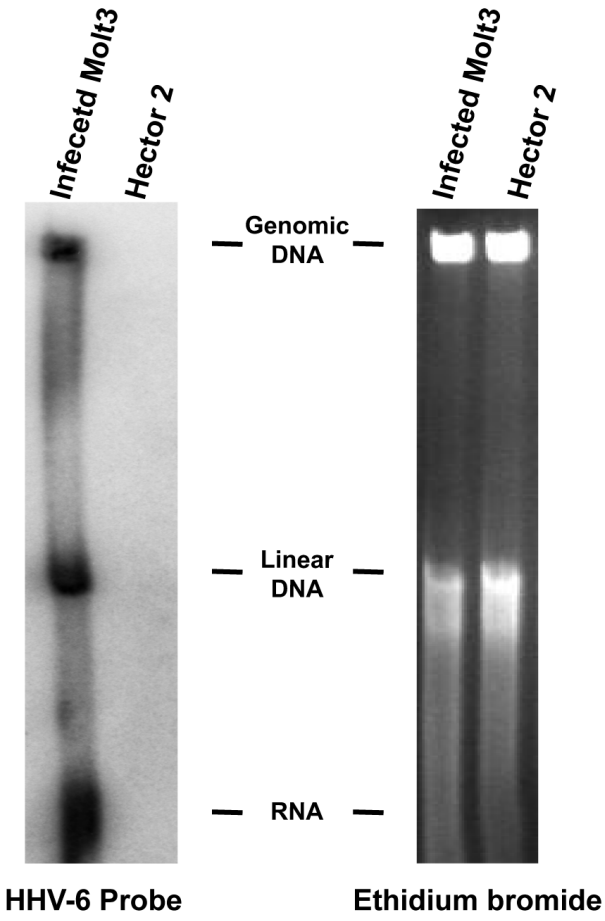

Fig. 28. Analysis of *in vitro* reactivated iHHV-6A patient PBMCs with the vertical agarose gel technique of Gardella *et al.* (88). Gardella gel analysis of infected Molt3 cells two weeks after co-culturing with PBMCs treated with TPA and hydrocortisone from Family-1/Sibling-2. Hector 2 T-cell line carrying one copy of HHV-6A per a cell. Reactivation was shown through linear DNA and RNA detected with HHV-6A cosmid probe (84).

During Reactivation, the Integrated iHHV-6 Genome Replicates via Formation of Concatemers

Reactivation of the integrated iHHV-6A virus from individuals' PBMCs as well as cell lines was inducible after stimulation with TPA and TSA. Co-cultivation studies indicated that the latent, integrated genome was capable of producing fully competent virus. Reactivation of the integrated iHHV-6 resulted in the increase in viral copies (**Figs. 26** and **28**) and induction of syncytium (**Fig. 27**). However, we set out to determine whether reactivation of iHHV-6 genome resulted in rolling-circle replication and the formation of concatemers and/or episomes of viral genomes similar to the replication of other herpesviruses (1, 26, 27).

To reactivate HHV-6A (strain U1102) from latent integration, HEK-293 cells (**Table 2**) were cultured with TSA at concentration of 160 ng/ml, 80 ng/ml, 40 ng/ml, 20 ng/ml, and 10 ng/ml for 3 days. Detection of viral episomes and/or concatemers was completed by PCR amplification of the DR by two primers that annealed to either end of the U region of HHV-6A (**Fig. 29a**). Thus amplification of DR would only occur during circularization of the viral genome or concatemers of HHV-6A genomes linked in a head-to-tail conformation (26, 27, 47, 102, 111, 112). Following co-hybridization with telomere, DR, and U HHV-6A oligonucleotide probes, hybridization of DR specific fragments was found in HHV-6A integrated HEK-293 cells treated with TSA (**Fig. 29b**). Furthermore, DR specific signal was also detected in control HHV-6A lytic infected Jjahn cells. We also identified variability in the molecular weight of the amplified DR fragments. The amplification of multiple molecular weight bands is possibly due to insertion of variable number of telomere repeats between DR and U during reactivation mediated by homologous recombination. No hybridization was identified in either control HEK-293 and untreated HEK-293/HHV-6A, which illustrates the *in vitro*

reactivation of integrated HHV-6A is dependent on the histone deacetylase inhibitor TSA.

In summary of **AIM 3**, reactivation of iHHV-6 genome after treatment with TSA resulted in rolling-circle replication and the formation of viral concatemers add/or episomes, which is similar to the replication strategy of herpesviruses (1, 26, 27).

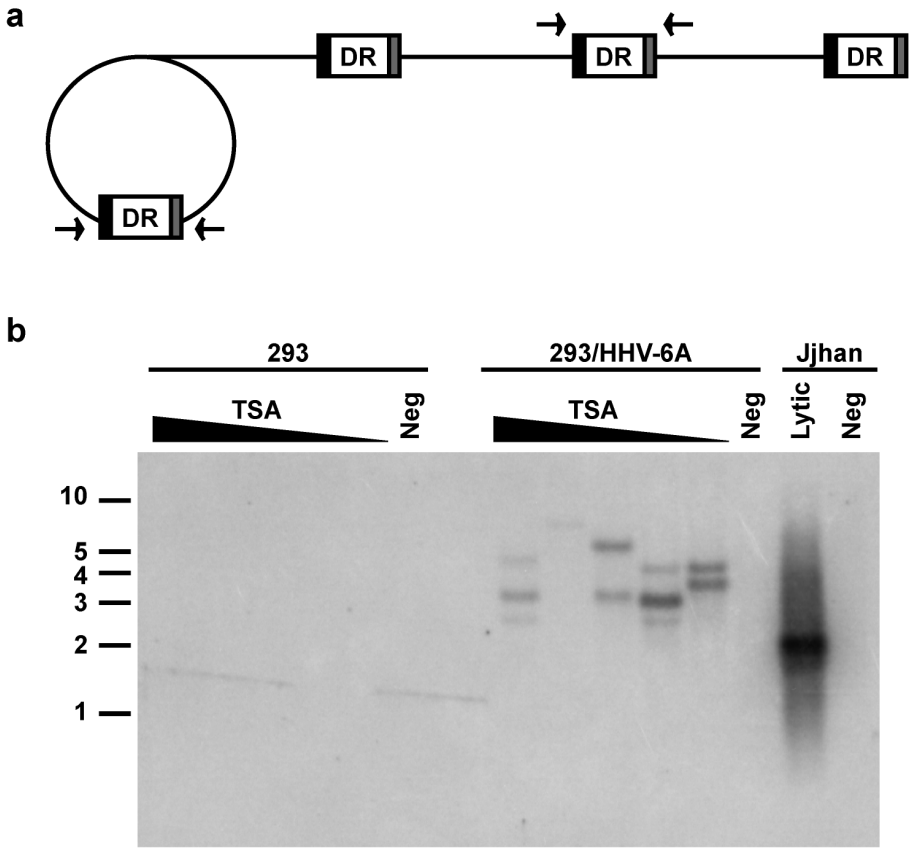

Fig. 29. Reactivation of chromosome integrated HHV-6A from HEK-293 cells induces episome and/or concatemer replication. (**a**) Schematic illustrating rolling-circle replication of herpesviruses results in concatemers of viral genomes (1, 26, 27). Arrows indicate the location of primers utilized in the amplification of DR during lytic infection. (**b**) HEK-293 cells with chromosome integrated HHV-6A (293/HHV-6A) and HEK-293 cells (negative control) were culture with TSA at concentration of 160 ng/ml, 80 ng/ml, 40 ng/ml, 20 ng/ml, and 10 ng/ml for 3 days. DR amplification and Southern hybridization with telomere, U, and DR oligonucleotide probes demonstrate rolling-circle replication following TSA treatment. HHV-6A lytic infection of Jhan cells (Positive control). No amplification was detected in untreated 293/HHV-6A or 293 cells (Negative controls).

DISCUSSION

HHV-6A/HHV-6B Achieves Latency through Chromosomal/Telomere Integration

Overall, this study provides substantial evidence that HHV-6A and HHV-6B establishes latency through an alternative mechanism differing from other human herpesviruses (**Fig. 30**). HHV6-A and HHV-6B integrates into the telomeres of human peripheral mononuclear cells *in vivo* (**Figs. 15**, **16**, **17**, **18**, and **19**), and following infection in Jjhan T-cells, Molt3 T-cells, and HEK-293 cells *in vitro* (**Figs. 10**, **11**, **12**, **13**, and **14**). It appears that in cell lines capable of supporting productive, lytic infection, some of the cells quickly become latently infected through chromosomal integration, and remain viable. Thus, HHV-6A and HHV-6B integration is not an unusual dead-end phenomenon, but an alternative means of achieving latency.

Previous studies have used FISH to suggest that HHV-6 is capable of chromosomal integration (28-32, 98). However, FISH cannot distinguish non-covalent linkage from integration. In this dissertation, evidence that HHV-6A and HHV-6B can integrate comes from multiple complementary methods besides FISH (**Figs. 10** and **15**): chromosome-specific PCR (**Figs. 13** and **19**), sequencing (**Figs. 14, 19,** and **A1**) IPCR (**Figs. 11** and **18**), Gardella gels (**Figs. 16, 17,** and **28**), Cs/Cl Etbr ultracentrifugation (**Fig. 24**), and two novel models (**Figs. 10** and **12**).

The results illustrate that iHHV-6A and iHHV-6B integrate into the host genome via homologous recombination with human telomeres. In particular, telomere integration of iHHV-6A and iHHV-6B occurs through recombination of the perfect telomere repeats

encoded in the DR_R juxtaposed to the end of the chromosome (**Fig. 30c**). Moreover, the tandem array of telomere repeats [$(TTAGGG)_n$] at the end of chromosomes was shown to extend beyond the DR_L of iHHV-6. Therefore, the structure of the iHHV-6 is as follows: chromosome-subtelomere-$(TTAGGG)_{5\text{-}41}$-DR_R-U-DR_L-$(TTAGGG)_n$.

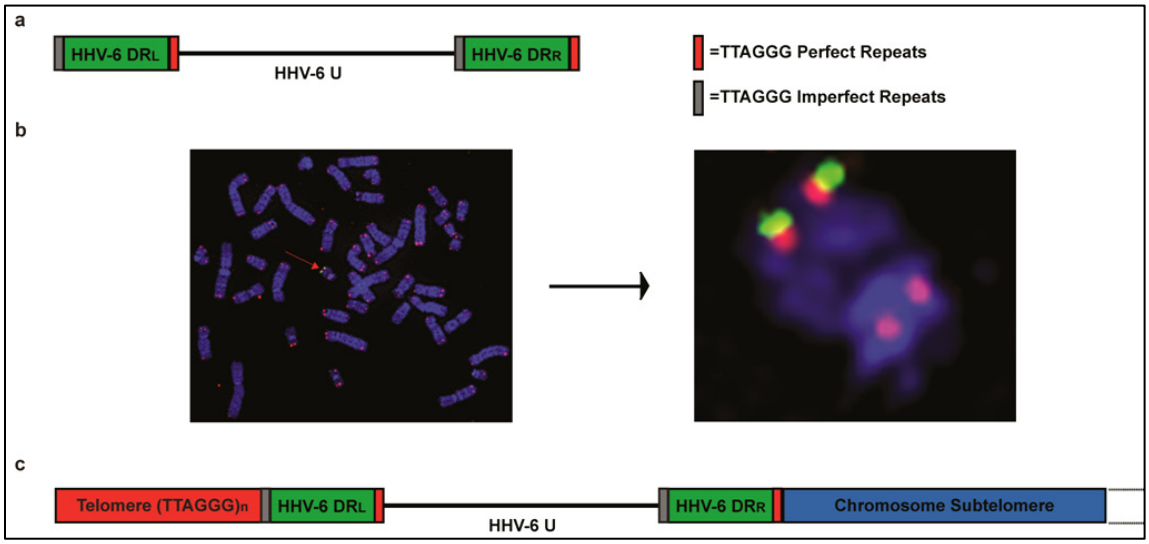

Fig. 30. Schematic comparing the genome structure of HHV-6 to germ-line inherited HHV-6 (iHHV-6). (**a**) The linear HHV-6 genome contains a unique (U) region of ~143 kbp with left and right direct repeats (DR) of ~8 kbp at the termini. Perfect and imperfect telomere sequence (TTAGGG) positioned at end of DR play role HHV-6 chromosome integration into the telomere. (**b**) Fluorescence in situ hybridization (FISH) of PBMCs from a patient with iHHV-6A integrated into the telomere of chromosome 22q. Metaphase chromosomes counterstained with DAPI (blue), cy5-PNA telomere probe (red), and FITC-conjugated HHV-6 cosmid probe (green). (**c**) Genome structure of iHHV-6 in which HHV-6 DR_R is fused with the telomere repeats near the chromosome subtelomere and the DR_L fused with the remaining telomere repeat array $(TTAGGG)_n$ (33).

We also found that the latent integrated genome of iHHV-6A was inducible after stimulation with TPA and TSA, and co-cultivation studies indicated that the latent, integrated genome was capable of producing fully competent virus (**Figs. 26**, **27**, and **28**). During reactivation, iHHV-6 is excised from the integrated genome via homologous recombination between flanking telomere sequences and generation of the DR_R-DR_L

junction signifies circularization and concatemer formation through rolling-circle replication (**Fig. 29**). Moreover, in neither the *in vivo* or *in vitro* studies did we find HHV-6 DNA in episomal form—the strategy by which other Human Herpesviruses achieve latency. Taken together, the data suggest that HHV-6A and HHV-6B are unique among Human Herpesviruses: they have the potential to specifically and efficiently integrate into telomeres of chromosomes during latency in the absence of circular episomes.

Reactivation of Chromosome Integrated HHV-6A/HHV-6B

The current understanding of HHV-6A and HHV-6B chromosome integration and direct clinical link to disease is in its initial stages of development. Nevertheless, over the last 20 years significant progress has been made. Considering the clinical implications that iHHV-6 has when manifested into a patients' DNA, it's crucial to determine whether reactivation of virus occurs from its latent integrated state. The first experiment conducted by Daibata *et al.* induced lytic genes and capsid mRNA expression from chromosomally integrated HHV-6 Burkitt's lymphoma cell line through culturing with the phorbol ester TPA (28).

Furthermore, results from **AIM III** demonstrate reactivation of iHHV-6A from patient T-cells as well as viral integration amongst HEK-293 cells and T-cell lines *in vitro* (33). Reactivation was achieved by means of co-culturing patient T-cells with the HDAC inhibitor TSA or with TPA plus hydrocortisone. Reactivation of the integrated virus induced increase in viral copies, while cytopathic effect was visibly evident by cell lysis and syncytium formation in a naïve T-cell line (**Figs. 26**, **27**, and **28**). Moreover, partial and 454 sequencing of the viral genome confirmed the iHHV-6A reactivation from its latent integrated state (**Fig. A1**). This evidence further demonstrates that chromosome

integration of iHHV-6 into telomeres is an alternative mechanism for a Human Herpesvirus to establish latency, reactivates, and possibly induces disease.

Proposed Model for Latent HHV-6A/HHV-6B Chromosome Integration and Reactivation

As previously discussed, integration of HHV-6A and HHV-6B into the telomeres of chromosomes is unique and alterative means for a human herpesvirus to establish latency (33). Comparable, the chicken hepresvirus MDV also integrates into the telomeres of chromosomes during latency (39-41). However, the mechanism of MDV integration differs from that of HHV-6A/HHV-6B as the genome of MDV integrates as long concatemers. Furthermore iHHV-6A, iHHV-6B, and MDV can reactivate from their latent integrated state to produce a lytic infection of naïve T-cells through chemicals inducers (28, 33, 41). However, the mechanism of iHHV-6A, iHHV-6B, and MDV telomere integration as well as reactivation remains to be fully elucidated.

In this next section, we propose a model (**Fig. 31**) to explain how the integration of HHV-6A/HHV-6B into chromosome telomeres occurs during latency. The process of integration emerges through homologous recombination between the viral and host telomere repeats. During this process, we propose the binding of TRF1 and/or TRF2 proteins to the viral encoded TTAGGG repeats [similar to the binding of EBV Orip TTAGGGTTA repeat (113, 114)]. This enables the linear HHV-6A/HHV-6B genome to sit proximally to the chromosome telomere and permit homologous recombination. Second, during the process of latency, ORF U94 may play a role in transcriptional repression of lytic viral genes expression and aid in the specific integration of HHV-6 into to the telomeres. Similar actions were observed in the rep68/78 mediated integration of AAV-2 into chromosome *19q13.4* (115-117). Third, reactivation of iHHV-6 from its linear

integrated state serves as a template for the replication of a linear dsDNA genome. The induction of iHHV-6A, iHHV-6B, and MDV with HDAC inhibitors supports the notion that reactivation precedes chromatin decondensation (**Fig. 32**) (28, 33, 41). This is followed by circularization via recombination of the telomere sequences flanking the viral genome and subsequent rolling-circle replication leads to concatemer formation of viral genomes linked in a head-to-tail tandem conformation. Finally, cleavage of concatemers to unit-length viral genomes takes place during encapsidation of the viral DNA. Therefore future studies need to determine if telomere proteins (TRF1 and TRF2) and TERRA interact with the HHV-6A/HHV-6B encoded TTAGGG repeat and thus promote viral integration into the telomeres.

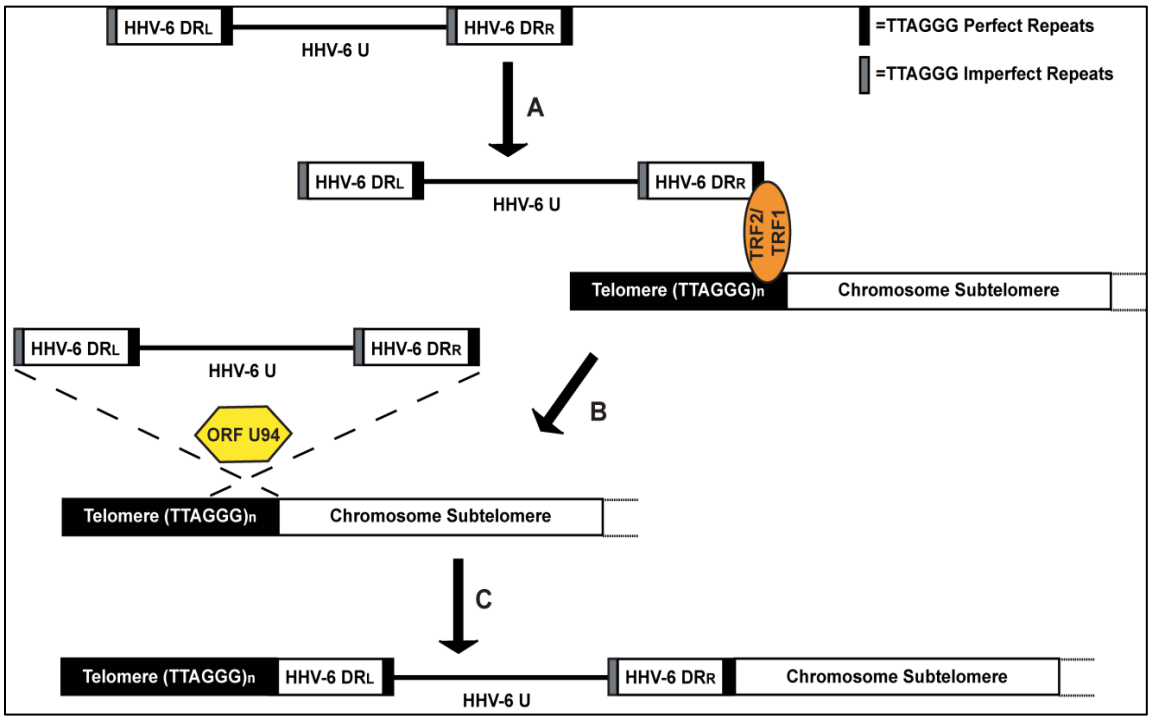

Fig. 31. Proposed model for HHV-6A/HHV-6B integration into chromosome telomeres. (**A**) We hypothesizes that localization of the linear HHV-6A/HHV-6B genome to chromosome telomeres occurs through TRF2 and TRF1 bidding of chromosome and HHV-6 DR encoded telomere repeat. (**B**) The viral rep gene ORF U94 then promotes homologous recombination between viral and chromosome telomere repeats, (**C**) which results in the integration of HHV-6A/HHV-6B into chromosome telomeres. The telomere integration event may also utilize alternative lengthening of telomeres (ALT) for recombination.

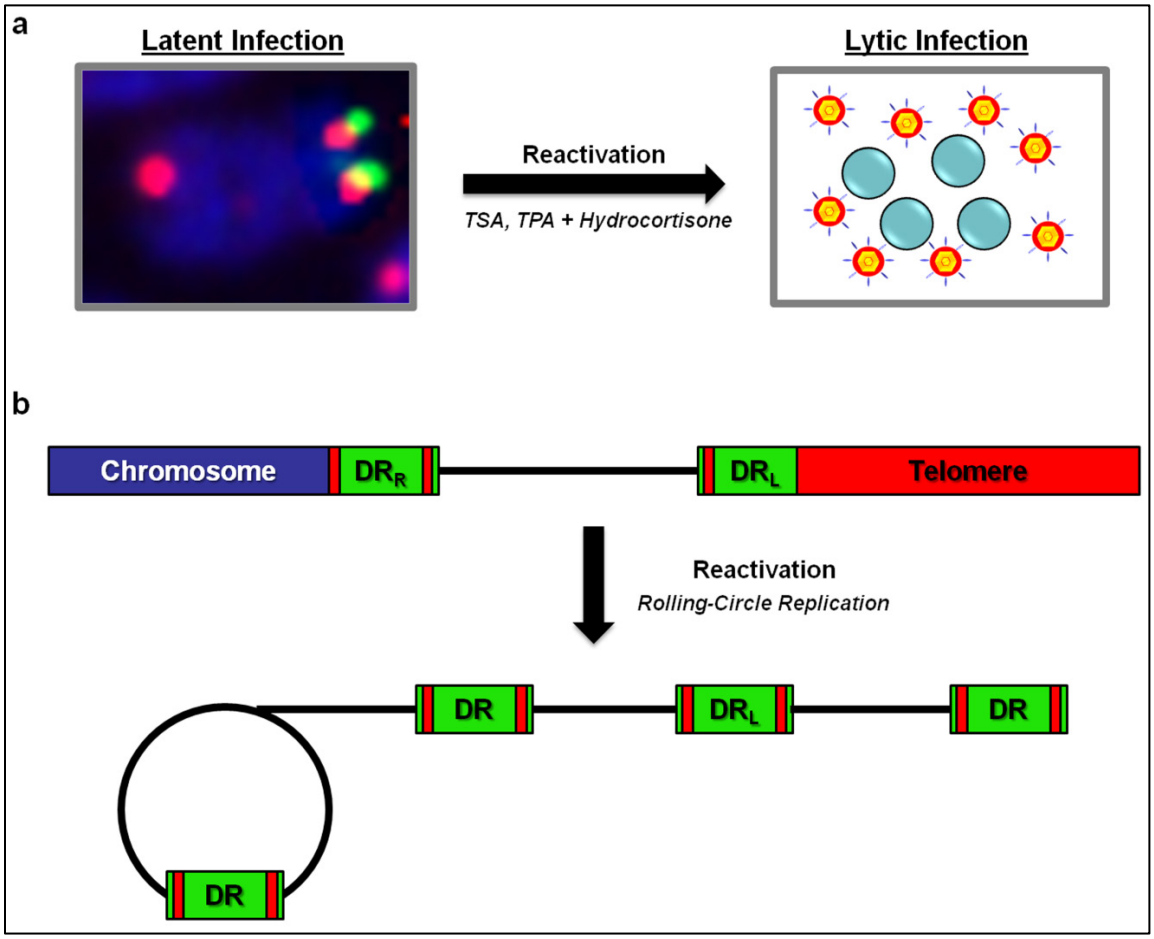

Fig. 32. Proposed model for iHHV-6 *in vitro* reactivation. (**a**) During latency, HHV-6A and HHV-6B can integrate into the telomeres during *in vivo* and *in vitro* infection. However, reactivation of iHHV-6 can be achieved through culturing of latently integrated cells with TSA, or TPA plus hydrocortisone. (**b**) Reactivation of the integrated iHHV-6 results in genome replication through rolling-circle replication.

It has been estimated that 85% of all malignant and transformed cells have telomerase active in order to prevent telomere attrition (74). However, in those remaining cells it is expected that telomere length is maintained through alternative lengthening of telomeres (ALT) (75). The mechanism of ALT has yet to be fully characterized; however one method suggests that circular extrachromosomal telomeric repeats (T-circle) formed from the lost of the telomere-loop (T-loop) at the end of telomeres may serve as a template for telomere lengthening through rolling-circle replication (77-80). Similarly, herpesviruses replicate their genome through rolling-circle replication to form a concatemer of linear viral genomes in a head-to-tail conformation (1, 26, 27). Therefore, the telomere repeats found at the end of DR_L and DR_R of the HHV-6A/HHV-6B genome may serve as an initial template for telomere elongation through rolling-circle replication and thus allow the integration of the viral genome into telomeres similar to the ALT pathway.

The Role of Human Herpesviruses Latency Genes in the Maintenance of the Latent Viral Genome

KSHV: LANA and EBV: EBNA1

Latency genes expressed by Human Herpesviruses promote maintenance and replication of the viral episome while inhibiting the expression of lytic genes (16). Examples of Herpesviruses latency genes include EBV nuclear antigen-1 (EBNA-1) and KSHV latency associated nuclear antigen (LANA) (35, 36). The Epstein-Barr virus latency gene EBNA-1 was shown to bind to the origin of plasmid replication (OriP) of the EBV encoded TTAGGGTTA repeat (imperfect telomere repeat) in cooperation with telomere binding protein TRF2 binding (113, 114). TRF2 and EBNA-1 binding of OriP

stabilizes the EBV episome during latency and enables the attachment of the EBV genome to metaphase chromosomes through protein-protein interaction (36, 114).

Similarly, LANA binds within the KSHV terminal repeats (TR) to stabilize the viral episome (118). Within the TR of KSHV, the transmembrane glycoprotein K1 promoter is responsible for activating the signaling pathways for lytic infection (119). Therefore, the binding of LANA to the TR suppresses both transcription of K1 and lytic replication. A second target for LANA to establish latency is through inhibition of Rta, which is an IE gene responsible for promoting lytic gene replication (120). Lan *et al.* established that LANA has the ability to directly repress Rta's promoter activity, and inhibit the auto-activation of viral transcription. Furthermore, the association of KSHV episome to chromosomes is achieved by binding LANA's C-terminus to the TR of KSHV and the N–terminus to histones H2A-H2B (35, 121).

HHV-6: ORF U94

Currently, there are several lines of evidence suggesting that the unique gene ORF U94 encoded by HHV-6A and HHV-6B may have a role in the establishment and maintenance of latency. First, the expression of ORF U94 transcripts were observed in latently infected PBMCs from healthy donors, while lytic viral transcripts were not expressed (122). Second, lymphoid cell lines stably expressing ORF U94, were permissive to HHV-6A infection, however no cytopathic effect was observed. There was a steady decline in copies of viral DNA and transcripts detected 22 days post-infection. Furthermore, the expression of ORF U94 decreased viral replication of betaherpesviruses CMV and HHV-7 (123). Moreover, the ssDNA binding activity of ORF U94 may have an impact on viral replication through transcriptional regulation (124). This hypothesis is supported by studies that have shown ORF U94 to suppress H-ras

mediated transformation in NIH3T3 cells and inhibit HIV-1 LTR expression at the level of the promoter (125). The transcriptional regulation by ORF U94 was further verified by *in vivo* and *in vitro* immunoprecipitation assay that indentified ORF U94 binding to the human TATA-Binding Protein (hTBP) (126). hTBP functions as a subunit of the TATA box binding transcription factor TFIID. This binding activity is a critical step for the formation of the pre-initiation complex. Therefore, the transcriptional regulation of HHV-6A/HHV-6B lytic genes could possibly occur through the interaction of ORF U94 with hTBP and thus create a mechanism by which HHV-6A/HHV-6B can shift from a lytic to a latent infection.

Interestingly, ORF U94 shares 24% sequence identity with latency gene rep68/78, derived from the human adeno-associated virus type 2 (AAV-2) (127). Rep68/78 regulates viral gene expression and directs the site specific integration of AAV-2 into the *AAVS1* site in chromosome *19q13.4* (115-117, 128). The function of rep68/78 is through DNA binding, endonuclease, and helicase activities. Furthermore, in a rep68/78 deficient AAV-2 model, the virus no longer integrates into the chromosome (129). However, the expression of ORF U94 was able to complement the activity of rep68/78 and rescue the mutant AAV-2 virus to replicate and integrate. Therefore, this suggests that ORF U94 may function as a latency gene and possibly facilitate HHV-6A/HHV-6B specific integration into telomeres similar to its AAV-2 encoded rep68/78 counterpart.

Despite the fact that the 490 amino acids of ORF U94 shares only 24% sequence identity with rep68/78 (127), there are structural features that may exhibit similar biological functions (**Fig. 33**). The ORF U94 C-terminus (residues 229-490 aa) corresponds to the helicase and ATPase domain of rep68/78. Specifically, the sequence codes for Walker A and B motifs that form the core of the class SF3 helicase

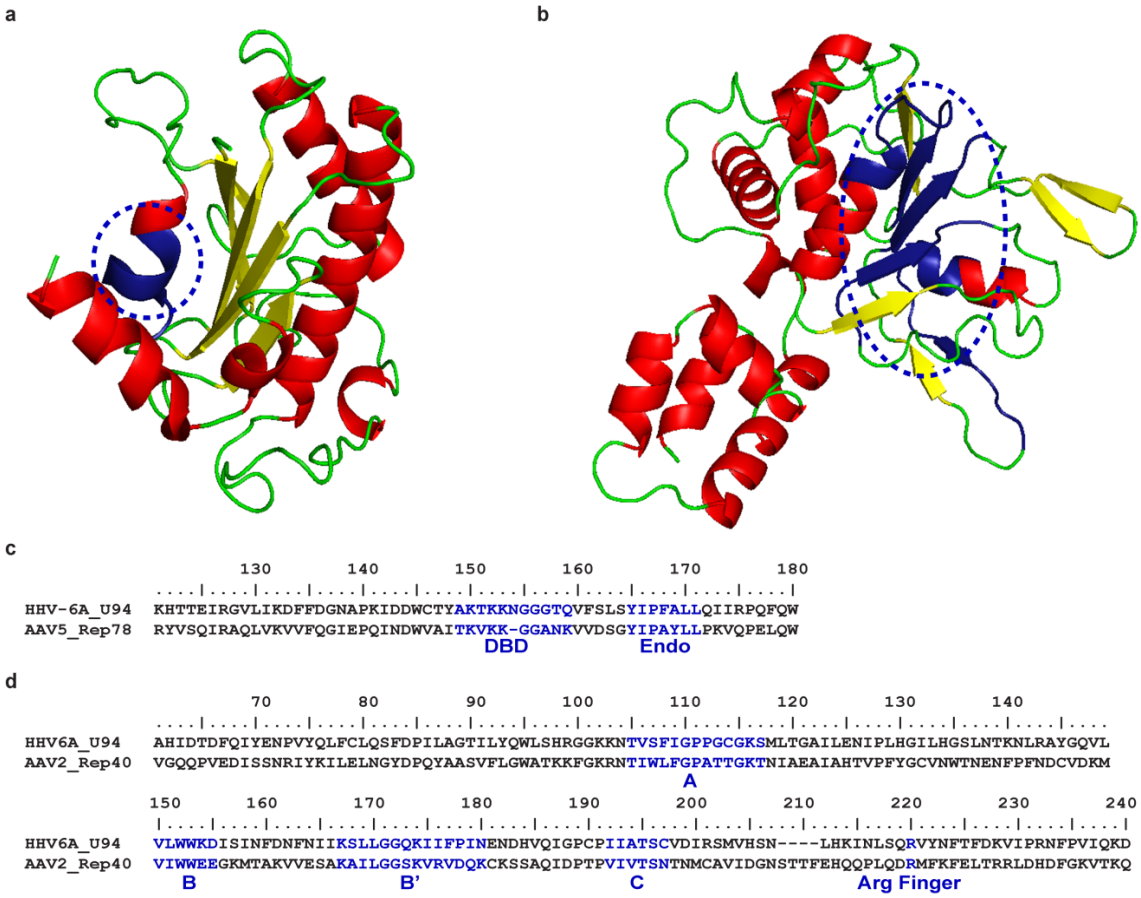

Fig. 33. Structural SWISS-MODEL and consensus sequence of HHV-6A ORF U94 N and C-terminus. (**a**) The predicted ribbon diagrams of the U94 N-terminus (15-206 aa) corresponds to the AAV rep nuclease domain [Protein Data Bank (PDB) accession number 1uut (128)). (**b**) The C-terminus (229-490 aa) of ORF U94 corresponds to the AAV rep helicase domain [PDB accession number 1s9h (130)] circled in blue. (**c**) Consensus protein sequence of AAV-2 Rep78 illustrates the DNA-binding domain (DBD) and endonuclease (Endo) domain for the N-terminus of HHV-6A ORF U94. (**d**) The consensus protein sequence of AAV-2 Rep40 helicase domain and C-terminus of HHV-6A U94. The Walker (A, B, B', and C) motifs form the core of the SF3 helicase and the arginine (Arg) finger catalyzes ATP hydrolysis when the protein forms a hexamer structure.

active site and an arginine finger which is critical player in ATP hydrolysis (130). Furthermore, the N-terminus (15-206 aa) of ORF U94 corresponds to the DNA binding and endonuclease domain of rep68/78 (128). It has been found that the N-terminus of ORF U94 has ssDNA-binding activity (124) and the endonuclease domain of rep68/78 is required for the site specific cleavage of the AAVS1 site which is shared by both the inverted terminal repeats of AAV-2 and chromosome *19q13.4* (128). In conclusion, the structural features shared between ORF U94 and rep68/78 emphasizes the importance of elucidating the function of this protein and implications it may have on viral replication, integration, and latency.

Possible Impact of HHV-6A/HHV-6B Integration on Telomere and Chromosome Stability

Theoretically, the ability of HHV-6A and HHV-6B to integrate into the genome could alter the stability of individual chromosomes and the expression of adjacent subtelomeric genes. Interestingly, subtelomeric rearrangement and deletions of chromosomes has been associated with mental retardation (131). In a review of 1,718 patients with mental retardation from 14 studies, 97 patients (5.8%) had subtelomeric rearrangements or deletions (132). In particular, terminal deletion or subtelomere rearrangements of chromosome *17p13.3* PAFAH1B1 gene results in Miller-Dieker syndrome which is characterized by mental retardation, lissencephaly, growth deficiency, seizures, and facial abnormalities (133, 134). de Grouchy syndrome is characterized by mental retardation, growth deficiencies, and hearing loss due to deletion of chromosome region *18q23* (133). Moreover, genetic mapping of patients with bipolar disorders has identified a deletion at chromosome *18q23*, however the link remains controversial and the specific locus has not been identified (135, 136). In

conclusion, iHHV-6A and iHHV-6B integration into chromosomes *17p13.3*, *18q23*, and *22q13.3* (**Table 12**) warrants direct sequencing and further cytogenetic analysis for chromosome deletions and rearrangements during integration.

Potentially, the integration of iHHV-6A and iHHV-6B into the telomere of chromosomes could alter the expression of adjacent subtelomeric genes through the inhibition of telomere position effect (TPE) (137). TPE is characterized by transcriptional repression of telomere adjacent genes through the recruitment of HDAC and histone H3K9 methylation emanating from the constitutive heterochromatin state of the telomere. The epigenetic regulation of TPE is well characterized in *Saccharomyces cerevisiae* (137-140). The use of reporter systems (GFP, luciferase, URA3) has identified TPE in excess of 20 kbp downstream of the telomere sequence in *S. cerevisiae*. However less established in human cells, Baur *et al.* observed a 10 fold decrease in the expression of telomere adjacent luciferase reporter when compared to reporter that was integrated near the centromere (141). Moreover, the heterochromatin state of TPE was reversible after treatment of human cells with TSA. This resulted in the suppression of HDACs and transcriptional activation of the luciferase reporter, which is similar to the TSA mediated reactivation of iHHV-6A and iHHV-6B from its latent integrated state (**Figs. 26**, **27**, **28**, **29**, and **32**). Therefore, further experiments are needed to determine if TPE plays a role in suppressing iHHV-6A and iHHV-6B lytic genes during latency, and whether the integrated viral genome alters the expression of nearby genes due to interruption of TPE.

These findings might also have relevance for telomerase activity. Mammalian and yeast chromosomes express a telomeric repeat-containing noncoding RNA (TERRA) (142). TERRA is proposed to regulate telomerase and many important telomere functions (142), and TERRA transcription is initiated in the subtelomere (**Fig.**

34a). Therefore, it's possible that telomere integration of HHV-6A/HHV-6B could alter the expression of TERRA leading to dysfunction of telomerase or telomere chromatin decondensation (**Fig. 34bc**).

The integration of HHV-6A and HHV-6B into telomeres is a newly identified form of human herpesvirus latency and the knowledge attained from the virus telomere biology may play a critical role in understanding the process of virus replication and integration. The length of telomeres in somatic cells is 5-15 kbp and after every cell division, 250-300 bp are lost from the end of telomeres due to the challenges encountered with the process of end replication (70). Cells reach the Hayflick limit once their telomeres reach a critical length, and undergo replicative senescence or apoptosis.

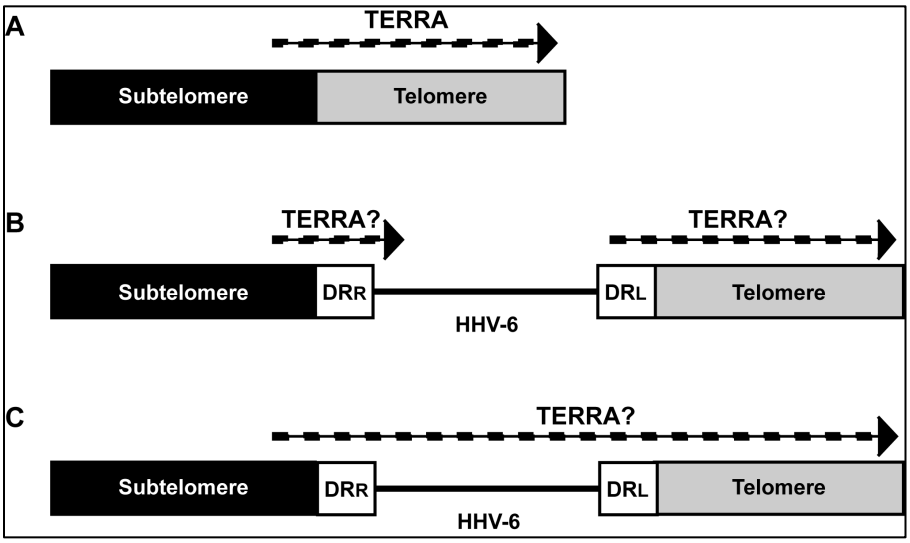

Fig. 34. TERRA expression and the possible impact of HHV-6A/HHV-6B telomere integration. (**a**) The expression of the TERRA transcript is initiated in the chromosome subtelomere. Alternatively, it's unclear if HHV-6 integration alters TERRA expression. (**b**) It possible that TERRA expression could be initiated in the DR_R or DR_L of HHV-6 or (**c**) the transcript is produced across the genome of HHV-6.

Alternatively, telomeres can be lengthened by telomerase reverse transcriptase (TERT) through the addition of the TTAGGG repeat (70). Telomerase mediated telomere lengthening has been detected in germ-line cells, cancer cells, and stem cells.

The repetitive telomere sequence and the complex of six telomere associated proteins protect the ends of chromosomes from double stranded breaks, chromosome fusions, and inhibits telomerase mediated lengthening (68, 69). The complex of telomere associate proteins known as the shelterin complex contains: TRF1 (TTAGGG Repeat Factor 1), TRF2 (TTAGGG Repeat Factor 2), and Pot1 (Protection of Telomeres 1) directly bind to the telomeric TTAGGG repeat. The complex protein interaction of the shelterin complex is maintained through TIN2 (TRF1-Interacting Nuclear Factor 2), TPP1 (TINT1, PIP1, PYOP1), and RAP1 (Repressor Activator Protein 1). In turn, TERRA stabilizes the shelterin complex and facilitates telomere heterochromatin formation through the direct interaction with TRF1 and TRF2 (72).

From the six shelterin proteins, TRF2 was shown to bind to the three nonamer EBV encoded TTAGGGTTA repeat (imperfect TTAGGG repeat) within the origin of plasmid replication (OriP) in cooperation with viral latency gene EBNA-1 (113, 114). TRF2 and EBNA-1 binding of OriP stabilizes the EBV episome during latency and enables the association of the viral genome to metaphase chromosomes (36, 114). This mechanism ensures division of the EBV genome amongst daughter cells during mitosis. Moreover, Lieberman *et al.* also found that EBNA-1 directly interacted with TERRA, however the principle of this interaction has not been fully elucidated (72). Similarly, we hypothesize that the binding of telomere repeats encoded in the DR of HHV-6A and HHV-6B by TRF2/TRF1 plays a role in telomere mediated integration by facilitating the localization of the viral genome to the telomere of chromosomes (**Fig. 31**). This in turn promotes homologous recombination of the viral telomere repeats and that of the chromosome telomere.

The integration of iHHV-6A and iHHV-6B into the same chromosome telomeres of family members lends itself to vertical transmission through the germ-line (**Table 12**)

(32, 33, 143). Moreover, studies have shown that iHHV-6A and iHHV-6B preferentially integrates into telomeres of chromosomes *9q34.4*, *17p13.3*, *18q23*, *19q13.4*, and *22q13.3* (28, 29, 32, 33, 144). These results may be explained by three different mechanisms. First, a number of chromosome ends may be more accessible for homologous recombination between the viral and chromosomal TTAGGG repeats due to heterochromatin structure of the chromosome telomere. Alternatively, HHV-6A/HHV-6B may integrate randomly into all 92 telomere regions at the end of chromosomes, but the integrated genome may be unstable in some telomeres (33). After a series of cell divisions, it's possible that cells with unstable chromosomes would be "negatively" selected over those with stable chromosomes. Finally, telomere integration could have occurred as a single event and thus inheritance of the genome occurs through multiple generations.

Results thus far have shown that between *in vivo* integrated iHHV-6 amongst patients and *in vitro* integrated cell lines, the viral DR_R of the genome is integrated within 5 - 41 telomere repeats from the end of the chromosome (**Figs. 14, 19,** and **30**) (33). The proximity of the ~160 kbp iHHV-6 genome integrated between the end of the chromosome and tandem array of telomere repeats suggests that the virus has a minimal impact on the telomere/shelterin complex. However, if the iHHV-6 genome was to integrate near the end of the telomere, one would expect progressive shortening of the telomere leading to loss of sequences from the viral genome. Subsequently, this loss may lead to chromosome instability as the result of chromosome fusion, replicative senescence, or the inability of the shelterin complex to bind the non-telomere coding sequence of the virus to form the cap at the end of telomere.

Transmission of iHHV-6A/iHHV-6B via the Germ-Line

Following primary infection, HHV-6A/HHV-6B establishes a latent infection primarily within monocytes/macrophages and in the salivary gland (10, 16). It is believed that the predominant means of acquiring HHV-6A/HHV-6B is the result of horizontal transmission through viral shedding from the saliva of infected individuals to uninfected infants and children. However, vertical transmission of inherited HHV-6 (iHHV-6) through the germ-line has proven to be a novel mechanism by which the virus integrates during latency. Daibata *et al.* described the first reported case of iHHV-6 vertical transmission through the germ-line of parent to their child (145). This initial observation was confirmed by several other laboratories (32, 33, 98, 143). In each of these reports, both parents and children with iHHV-6 contained identical sites of chromosome integration (**Table 12** and **Fig. 15**). Furthermore, the same virus strain of iHHV-6 was inherited through the germ-line between parent and child. This was evident because iHHV-6 integrated in each family member contained similar restriction fragment polymorphism profiles and similar sequence of select viral genes (**Fig. 25, Table 12,** and **Fig. A1**) (33).

Additional evidence supporting vertical transmission of the iHHV-6 genome was described in a study showing cases of HHV-6 congenital infection obtained through germ-line transmission or transplacental infection of the fetus (98). It was reported that from a total of 254 infants enrolled in a study, 16.9% (43/254) had acquired a congenital HHV-6 infection and 16.5% (42/254) acquired HHV-6 through primary infection by 36 months. Furthermore, the majority of congenital HHV-6 was acquired through germ-line in which, 14.6% (37/254) infants were positive for iHHV-6 and only 2.4% (6/254) had acquired HHV-6 through transplacental infection. Furthermore, germ-line transmission results in viral integration within the chromosome of every cell that resides in the

individual. This statement coincides with the information previously describing the viral load of patients consistently detected at or above 1 copy per cell (32, 33, 98, 143).

Frequently observed in hematopoietic stem cell transplant patients, HHV-6 may reactivate and induce graft rejection, bone marrow suppression, and encephalitis (1, 16, 22). Moreover, even after ablation of the recipient's bone marrow in preparation for transplantation, it has been shown that the donor stem cells may transfer iHHV-6 to the recipient (144, 146, 147). This results in the subsequent rise of HHV-6 viral copies within the recipient peripheral blood as well as introduction of iHHV-6 positive stem cells. Investigations are also necessary to understand how immunosuppressive agents used to prevent graft rejection affect iHHV-6 infected patients. Will clinicians also have to consider screening for iHHHV-6 during blood donations? The initial studies on the transmission of integrated iHHV-6 into chromosome of hematopoietic stem cells during transplantation has not been studied sufficiently, and additional studies must be performed to understand the long-term effects on those patients who received stem cell transplants with iHHV-6.

Possible Pathologies Associated with Vertically Transmitted iHHV-6A/iHHV-6B

The documentation of integrated iHHV-6 also raises important questions. Is the immune system of patients born with iHHV-6 tolerant of any viral antigens? Given that the viral genome is present in every cell and capable of producing competent virions, are these patients at particular risk for any diseases? Are the patients susceptible to superinfection with another strain of HHV-6A, or to infection with HHV-6B? Answers to these questions await further study.

HHV-6A and HHV-6B infection occurs by means of attachment and entry into cells through the complement regulator receptor CD46 (25). The diverse cell tropism

and multiple disease associations with HHV-6A/HHV-6B are due, in part, to the expression of CD46 present on the surface of all nucleated cells. In particular, HHV-6B primary infection of young children is the etiological agent of exanthema subitum (roseola), which is characterized by high fever, diarrhea, and a mild skin rash along the trunk, neck, and face (5, 12). There is no classic textbook clinical disease caused by HHV-6A at this time. However, HHV-6A has been suggested to act as a co-factor in AIDS progression by contributing to the killing of CD-4 lymphocytes (11, 20, 54) and enhancement of HIV replication through activation of the long terminal repeats (LTR) (21). Following primary infection, reactivation of HHV-6A/HHV-6B in immune compromised patients has led to graft rejection in solid organ and bone marrow transplants, seizures, and encephalitis (6, 16-19, 53).

Patients with iHHV-6 present a wide range of symptoms and various diseases associated with the integrated viral genome, while other patients show no signs of clinical disease (**Table 12**) (28-34, 64, 67, 98, 144). It remains unknown why some patients' manifest neurological symptoms of the disease and others don't. However *in vitro* iHHV-6 reactivation of patient T-cells (28, 33), suggests that the virus may be in a latent integrated state in patients showing no signs of disease, while patients presenting symptoms of disease may have iHHV-6 reactivated from its integrated state.

Furthermore, when considering the transmission of iHHV-6 through the germ-line, in every cell of the patient there is at least one integrated copy of the viral genome (32, 33, 98, 143). Reactivation can occur in any number of tissues within the body of the patient, which can lead to cell death, changes in cell function attributed to viral gene expression, and subsequent spread to neighboring CD46+ cells. Therefore, the ability of HHV-6A/HHV-6B to infect the majority of nucleated cells through CD46 and the

presences of iHHV-6 integrated in every cell sheds light on the various symptoms and diseases associated with this virus.

However pertaining to iHHV-6, the direct clinical link between neurological disease and active viral replication is still underway. It remains uncertain if CNS dysfunction is due to reactivation of iHHV-6 or if the virus is merely an opportunistic infection within the brain. However, antiviral therapy has initially shown some short term success in reducing neurological symptoms associated with iHHV-6 (148).

HHV-6A/HHV-6B and Malignant Diseases

Previous studies have evaluated patients with HHV-6A/HHV-6B presenting neurological symptoms and various lymphomas, which include Hodgkin's lymphoma, Burkitt's lymphoma, acute lympoblastic leukaemia (ALL), chronic myelogenous leukemia (CML), and acute myeloid leukemia (AML) (28, 34, 110, 145, 149, 150). However, the prevalence of HHV-6A/HHV-6B in children with ALL and AML does not differ significantly from the healthy populations (150). Therefore the direct clinical link between cancer and HHV-6A/HHV-6B is not completely conclusive, but reactivation of the virus can be linked to graft rejection in hematopoietic stem cell transplant patients treated with immunosuppressive drugs (16, 53).

HHV-6A/HHV-6B may not play a direct role in cancer development, but these viruses may play a role in cancer progression by complementing oncogenic viruses in an environment that condones cancer development. Similarly, HHV-6A has the ability to increase HIV replication through activation of the long terminal repeats (LTR) and enhance AIDS progression in macaques (20, 21). Also, HHV-6A/HHV-6B can increase RNA expression of human papillomavirus virus (HPV) oncogenes E6 and E7 in cervical epithelial cells (151). HHV-6A/HHV-6B and HPV co-infection of cervical epithelial cells

increased production of E6 and E7 RNA and accelerated tumor growth in mice by 3 weeks as compared to the 6 week time period normally expected with HPV infection alone.

During the course of human evolution, human endogenous retroviruses (HERV) integrated into the germ-line roughly 10 million years ago (152). HERVs no longer produce mature virus due to mutations and deletions in their sequence, however in a study by zur Hausen *et al.*, HHV-6 induced transcription of gag, pol, and env genes from HERV found in normal PBMCs and in cell lines (153). Moreover, HERV env protein has also been found to be expressed in various cancer cells. Duelli *et al.* hypothesized that cell fusions caused by endogenous viruses and syncytium-forming viruses like HHV-6 can lead to aneuploidy and subsequently induce chromosome instability and malignant transformation (154). Therefore the ability of HHV-6 and HERV to induce cell fusion, and increase expression of HERV *env* protein by HHV-6, emphasizes the need of further clinical studies to determine the potential impact of HHV-6 and iHHV-6 on cancer as well as their effect on MS, CFS, DRESS, and bone marrow suppression in transplants.

Prevalence of Chromosome Integrated iHHV-6 in the Healthy Population; Not Yet Identified Diseases?

To appreciate the significance of latent iHHV-6 integration into the telomere of chromosomes, several studies have investigated the prevalence of iHHV-6 integration amongst congenital infection, normal blood donors, and hospitalized patients (64, 65). The prevalence of iHHV-6 chromosome integration with high viral loads (10^6-10^7 copies per ml of blood) has been described in several British cohort studies (**Table 13**) (64, 65). In normal healthy blood donors it was found that 0.8 % (4/500) (64) and 1.0 % (57/5638) (81) had high viral loads most likely attributed to iHHV-6 integration in the germ-line. In

contrast, prevalence of integrated iHHV-6 in hospitalized patient was higher, 2.9 % (13/449) (64) and 3.3 % (6/184) (65). In conclusion, the transmission of iHHV-6 through the germ-line and its prevalence in the population implies the necessity for research to characterize the significance and possible pathologies of iHHV-6 integration. Moreover, it is essential that researchers determine the overall impact the integrated virus may have on hospitalized patients and understand disease progression associated with iHHV-6.

Table 13. Prevalence of chromosome integrated iHHV-6 among patients and blood donors.

Authors	Location	Individuals	Positive
Griffiths (155)	London, UK	Liver transplant pt	3/60 (5 %)
Kidd (156)	London, UK	Renal transplant pt	1/52 (1.9 %)
Ward (65)	London, UK	Encephalitis	6/184 (3.3 %)
Tanaka-Taya (32)	Japan	Hospitalized pt	5/2332 (0.21 %)
Leong (64)	London, UK	Hospitalized pt	13/449 (2.9 %)
Ward (65)	London, UK	Blood donors	10/653 (1.5 %)
Leong (64)	London, UK	Blood donors	4/500 (0.8 %)
Hall (81)	Rochester, NY	Cord blood donors	57/5638 (1.0 %)

Summary and Future Directions

We hypothesized and established by a broad range of experiments that during latency, the Human Herpesvirus 6A and 6B genome integrates into the telomeres of human chromosomes through homologous recombination with the n(TTAGGG) viral repeats, while transmission can occurs through the germ-line. Furthermore, we have demonstrated the induction of the integrated virus to lytic replication. The second objective of this dissertation was also achieved as the data contributes to our

understanding of HHV-6A/HHV-6B latency and pathology as well as presents the current and preceding knowledge of iHHV-6.

Since HHV-6A and HHV-6B are both important pathogens, our studies provide several tools for future clinical investigations. Over 90% (or more likely 100%) of the population has acquired a primary HHV-6 infection by three years of age and the virus remains latent for the life of the host (13, 14). Investigators have established that HHV-6B is the etiological agent of roseolla and HHV-6A is identified as a cofactor in AIDS progression (6, 16-21, 53, 55-57). HHV-6A is perhaps associated with MS, while both HHV-6A and HHV-6B are linked to graft rejection in transplants, and various neurological disorders. Integration of HHV-6A and HHV-6B in telomeres may explain some of the clinical symptoms associated with these diseases.

Future experiments need to determine the overall clinical impact of germ-line integrated iHHV-6A/B. Furthermore, there is a need to determine the relationship between HHV-6A/HHV-6B infection and MS, CFS, cancer, AIDS progression, and various neurological disorders. ***Second***, determine the physiological effect and impact on the stability of iHHV-6 has on telomeres during integration. This questions is of interest to investigators since telomere shortening leads to cell senescence and/or telomerase activation, which is a hallmark of chromosome instability (69). ***Third***, characterize the molecular switches that dictate whether, following new infection in a cell line capable of sustaining productive lytic infection, alternatively, the virus integrates and establishes latency. ***Fourth***, determine the switches that activate transcription of lytic genes leading to reactivation of iHHV-6. ***Fifth***, investigate whether the viral latency gene ORF U94 and telomere binding proteins TRF1 and TRF2 do in fact play a role during the process of telomere integration. ***Sixth***, evaluate the effect of TPE on virus reactivation and disruption of transcriptional repression of telomere adjacent chromosome genes.

Seventh, determine if the TTAGGG repeats encoded in DR of HHV-7 promotes viral telomere integration similar to HHV-6A/B and MDV.

The use of BAC vectors to clone the entire genome of herpesviruses are instrumental in understanding the means by which viruses replicate, while the creation of knockout-mutants characterize viral proteins. To begin to answer some of the questions listed above, initial attempts to generate an infectious HHV-6 BAC cloned virus were unsuccessful (46, 102). However, Arbuckle *et al.* were the first to successfully produce an infectious HHV-6A virus that expresses GFP and a selectable marker (33). This reproducible cloning system was then verified by Tang *et al.* (103). The knowledge obtained from HHV-6A and HHV-6B integration and the adaptation of recombinant HHV-6 viruses should facilitate understanding of the clinical impact viral latency/integration has on the host.

LITERATURE CITED

1. Fields BN, Knipe DM, & Howley PM (2007) *Fields virology* (Wolters Kluwer Health/Lippincott Williams & Wilkins, Philadelphia) 5th Ed pp 2 v. (xix, 3091, 3086 p.).

2. Salahuddin SZ*, et al.* (1986) Isolation of a new virus, HBLV, in patients with lymphoproliferative disorders. (Translated from eng) *Science* 234(4776):596-601.

3. Dominguez G*, et al.* (1999) Human herpesvirus 6B genome sequence: coding content and comparison with human herpesvirus 6A. *Journal of virology* 73(10):8040-8052.

4. Gompels UA*, et al.* (1995) The DNA sequence of human herpesvirus-6: structure, coding content, and genome evolution. *Virology* 209(1):29-51.

5. Yamanishi K*, et al.* (1988) Identification of human herpesvirus-6 as a causal agent for exanthem subitum. *Lancet* 1(8594):1065-1067.

6. Ahlqvist J*, et al.* (2005) Differential tropism of human herpesvirus 6 (HHV-6) variants and induction of latency by HHV-6A in oligodendrocytes. *J Neurovirol* 11(4):384-394.

7. Kondo K, Kondo T, Okuno T, Takahashi M, & Yamanishi K (1991) Latent human herpesvirus 6 infection of human monocytes/macrophages. *The Journal of general virology* 72 (Pt 6):1401-1408.

8. Black JB*, et al.* (1989) Growth properties of human herpesvirus-6 strain Z29. *J Virol Methods* 26(2):133-145.

9. De Bolle L, Van Loon J, De Clercq E, & Naesens L (2005) Quantitative analysis of human herpesvirus 6 cell tropism. *J Med Virol* 75(1):76-85.

10. Kondo K*, et al.* (2002) Strong interaction between human herpesvirus 6 and peripheral blood monocytes/macrophages during acute infection. *J Med Virol* 67(3):364-369.

11. Lusso P*, et al.* (1991) Productive infection of CD4+ and CD8+ mature human T cell populations and clones by human herpesvirus 6. Transcriptional down-regulation of CD3. *J Immunol* 147(2):685-691.

12. Asano Y*, et al.* (1994) Clinical features of infants with primary human herpesvirus 6 infection (exanthem subitum, roseola infantum). *Pediatrics* 93(1):104-108.

13. Okuno T*, et al.* (1989) Seroepidemiology of human herpesvirus 6 infection in normal children and adults. *J Clin Microbiol* 27(4):651-653.

14. Zerr DM*, et al.* (2005) A population-based study of primary human herpesvirus 6 infection. *N Engl J Med* 352(8):768-776.

15. Cameron B*, et al.* (2010) Serological and virological investigation of the role of the herpesviruses EBV, CMV and HHV-6 in post-infective fatigue syndrome. *J Med Virol* 82(10):1684-1688.

16. De Bolle L, Naesens L, & De Clercq E (2005) Update on human herpesvirus 6 biology, clinical features, and therapy. *Clin Microbiol Rev* 18(1):217-245.

17. Donati D*, et al.* (2003) Detection of human herpesvirus-6 in mesial temporal lobe epilepsy surgical brain resections. *Neurology* 61(10):1405-1411.

18. Jones CM, Dunn HG, Thomas EE, Cone RW, & Weber JM (1994) Acute encephalopathy and status epilepticus associated with human herpes virus 6 infection. *Dev Med Child Neurol* 36(7):646-650.

19. Yamashita N & Morishima T (2005) HHV-6 and seizures. *Herpes* 12(2):46-49.

20. Lusso P*, et al.* (2007) Human herpesvirus 6A accelerates AIDS progression in macaques. *Proceedings of the National Academy of Sciences of the United States of America* 104(12):5067-5072.

21. Lusso P*, et al.* (1989) Productive dual infection of human CD4+ T lymphocytes by HIV-1 and HHV-6. *Nature* 337(6205):370-373.

22. Ablashi DV*, et al.* (2010) Review Part 3: Human herpesvirus-6 in multiple non-neurological diseases. *J Med Virol* 82(11):1903-1910.

23. Yao K, Crawford JR, Komaroff AL, Ablashi DV, & Jacobson S (2010) Review part 2: Human herpesvirus-6 in central nervous system diseases. *J Med Virol* 82(10):1669-1678.

24. Santoro F*, et al.* (2003) Interaction of glycoprotein H of human herpesvirus 6 with the cellular receptor CD46. *J Biol Chem* 278(28):25964-25969.

25. Santoro F*, et al.* (1999) CD46 is a cellular receptor for human herpesvirus 6. *Cell* 99(7):817-827.

26. Jacob RJ, Morse LS, & Roizman B (1979) Anatomy of herpes simplex virus DNA. XII. Accumulation of head-to-tail concatemers in nuclei of infected cells and their role in the generation of the four isomeric arrangements of viral DNA. *Journal of virology* 29(2):448-457.

27. Poffenberger KL & Roizman B (1985) A noninverting genome of a viable herpes simplex virus 1: presence of head-to-tail linkages in packaged genomes and requirements for circularization after infection. *Journal of virology* 53(2):587-595.

28. Daibata M, Taguchi T, Taguchi H, & Miyoshi I (1998) Integration of human herpesvirus 6 in a Burkitt's lymphoma cell line. *Br J Haematol* 102(5):1307-1313.

29. Nacheva EP*, et al.* (2008) Human herpesvirus 6 integrates within telomeric regions as evidenced by five different chromosomal sites. *J Med Virol* 80(11):1952-1958.

30. Torelli G*, et al.* (1995) Targeted integration of human herpesvirus 6 in the p arm of chromosome 17 of human peripheral blood mononuclear cells in vivo. *J Med Virol* 46(3):178-188.

31. Ward KN*, et al.* (2006) Human herpesvirus 6 chromosomal integration in immunocompetent patients results in high levels of viral DNA in blood, sera, and hair follicles. *J Clin Microbiol* 44(4):1571-1574.

32. Tanaka-Taya K*, et al.* (2004) Human herpesvirus 6 (HHV-6) is transmitted from parent to child in an integrated form and characterization of cases with chromosomally integrated HHV-6 DNA. *J Med Virol* 73(3):465-473.

33. Arbuckle JH*, et al.* (2010) The latent human herpesvirus-6A genome specifically integrates in telomeres of human chromosomes in vivo and in vitro. *Proceedings of the National Academy of Sciences of the United States of America* 107(12):5563-5568.

34. Luppi M*, et al.* (1993) Three cases of human herpesvirus-6 latent infection: integration of viral genome in peripheral blood mononuclear cell DNA. *J Med Virol* 40(1):44-52.

35. Ballestas ME, Chatis PA, & Kaye KM (1999) Efficient persistence of extrachromosomal KSHV DNA mediated by latency-associated nuclear antigen. *Science* 284(5414):641-644.

36. Marechal V*, et al.* (1999) Mapping EBNA-1 domains involved in binding to metaphase chromosomes. *Journal of virology* 73(5):4385-4392.

37. Hurley EA*, et al.* (1991) When Epstein-Barr virus persistently infects B-cell lines, it frequently integrates. *Journal of virology* 65(3):1245-1254.

38. Gao J, Luo X, Tang K, Li X, & Li G (2006) Epstein-Barr virus integrates frequently into chromosome 4q, 2q, 1q and 7q of Burkitt's lymphoma cell line (Raji). *J Virol Methods* 136(1-2):193-199.

39. Delecluse HJ & Hammerschmidt W (1993) Status of Marek's disease virus in established lymphoma cell lines: herpesvirus integration is common. *Journal of virology* 67(1):82-92.

40. Osterrieder N, Kamil JP, Schumacher D, Tischer BK, & Trapp S (2006) Marek's disease virus: from miasma to model. *Nat Rev Microbiol* 4(4):283-294.

41. Delecluse HJ, Schuller S, & Hammerschmidt W (1993) Latent Marek's disease virus can be activated from its chromosomally integrated state in herpesvirus-transformed lymphoma cells. *EMBO J* 12(8):3277-3286.

42. Okazaki S, Ishikawa H, & Fujiwara H (1995) Structural analysis of TRAS1, a novel family of telomeric repeat-associated retrotransposons in the silkworm, Bombyx mori. *Mol Cell Biol* 15(8):4545-4552.

43. Anzai T, Takahashi H, & Fujiwara H (2001) Sequence-specific recognition and cleavage of telomeric repeat (TTAGG)(n) by endonuclease of non-long terminal repeat retrotransposon TRAS1. *Mol Cell Biol* 21(1):100-108.

44. Secchiero P*, et al.* (1995) Identification of human telomeric repeat motifs at the genome termini of human herpesvirus 7: structural analysis and heterogeneity. *Journal of virology* 69(12):8041-8045.

45. Achour A*, et al.* (2009) Length variability of telomeric repeat sequences of human herpesvirus 6 DNA. *J Virol Methods* 159(1):127-130.

46. Kondo K, Nozaki H, Shimada K, & Yamanishi K (2003) Detection of a gene cluster that is dispensable for human herpesvirus 6 replication and latency. *Journal of virology* 77(19):10719-10724.

47. Borenstein R, Zeigerman H, & Frenkel N (2010) The DR1 and DR6 first exons of human herpesvirus 6A are not required for virus replication in culture and are deleted in virus stocks that replicate well in T-cell lines. *Journal of virology* 84(6):2648-2656.

48. Ablashi D (1993) Human herpesvirus-6 strain groups: a nomenclature. *Arch Virol* 129(1-4):363-366.

49. Miller CS, Avdiushko SA, Kryscio RJ, Danaher RJ, & Jacob RJ (2005) Effect of prophylactic valacyclovir on the presence of human herpesvirus DNA in saliva of healthy individuals after dental treatment. *J Clin Microbiol* 43(5):2173-2180.

50. Tajiri H*, et al.* (1997) Chronic hepatitis in an infant, in association with human herpesvirus-6 infection. *J Pediatr* 131(3):473-475.

51. Hashimoto H*, et al.* (2002) Hematologic findings associated with thrombocytopenia during the acute phase of exanthem subitum confirmed by primary human herpesvirus-6 infection. *J Pediatr Hematol Oncol* 24(3):211-214.

52. Portolani M*, et al.* (1997) Primary infection by HHV-6 variant B associated with a fatal case of hemophagocytic syndrome. *New Microbiol* 20(1):7-11.

53. Dockrell DH & Paya CV (2001) Human herpesvirus-6 and -7 in transplantation. *Rev Med Virol* 11(1):23-36.

54. Takahashi K*, et al.* (1989) Predominant CD4 T-lymphocyte tropism of human herpesvirus 6-related virus. *Journal of virology* 63(7):3161-3163.

55. Cermelli C*, et al.* (2003) High frequency of human herpesvirus 6 DNA in multiple sclerosis plaques isolated by laser microdissection. *J Infect Dis* 187(9):1377-1387.

56. Goodman AD, Mock DJ, Powers JM, Baker JV, & Blumberg BM (2003) Human herpesvirus 6 genome and antigen in acute multiple sclerosis lesions. *J Infect Dis* 187(9):1365-1376.

57. Berti R, Soldan SS, Akhyani N, McFarland HF, & Jacobson S (2000) Extended observations on the association of HHV-6 and multiple sclerosis. *J Neurovirol* 6 Suppl 2:S85-87.

58. Chan PK, Ng HK, Hui M, & Cheng AF (2001) Prevalence and distribution of human herpesvirus 6 variants A and B in adult human brain. *J Med Virol* 64(1):42-46.

59. Caselli E*, et al.* (2002) Detection of antibodies directed against human herpesvirus 6 U94/REP in sera of patients affected by multiple sclerosis. *J Clin Microbiol* 40(11):4131-4137.

60. Yao K*, et al.* (2008) Reactivation of human herpesvirus-6 in natalizumab treated multiple sclerosis patients. *PLoS One* 3(4):e2028.

61. Soldan SS, Leist TP, Juhng KN, McFarland HF, & Jacobson S (2000) Increased lymphoproliferative response to human herpesvirus type 6A variant in multiple sclerosis patients. *Ann Neurol* 47(3):306-313.

62. Rotola A*, et al.* (2004) Human herpesvirus 6 infects the central nervous system of multiple sclerosis patients in the early stages of the disease. *Mult Scler* 10(4):348-354.

63. Knox KK, Brewer JH, Henry JM, Harrington DJ, & Carrigan DR (2000) Human herpesvirus 6 and multiple sclerosis: systemic active infections in patients with early disease. *Clin Infect Dis* 31(4):894-903.

64. Leong HN*, et al.* (2007) The prevalence of chromosomally integrated human herpesvirus 6 genomes in the blood of UK blood donors. *J Med Virol* 79(1):45-51.

65. Ward KN, Thiruchelvam AD, & Couto-Parada X (2005) Unexpected occasional persistence of high levels of HHV-6 DNA in sera: detection of variants A and B. *J Med Virol* 76(4):563-570.

66. Jarrett RF*, et al.* (1988) Identification of human herpesvirus 6-specific DNA sequences in two patients with non-Hodgkin's lymphoma. *Leukemia* 2(8):496-502.

67. Strenger V*, et al.* (2010) Chromosomal integration of the HHV-6 genome as a possible cause of HHV-6 detection in cardiac tissues. *J Clin Pathol* 63(12):1129-1130.

68. de Lange T (2005) Shelterin: the protein complex that shapes and safeguards human telomeres. *Genes & development* 19(18):2100-2110.

69. Raynaud CM, Sabatier L, Philipot O, Olaussen KA, & Soria JC (2008) Telomere length, telomeric proteins and genomic instability during the multistep carcinogenic process. *Crit Rev Oncol Hematol* 66(2):99-117.

70. Riethman H (2008) Human telomere structure and biology. *Annu Rev Genomics Hum Genet* 9:1-19.

71. Azzalin CM, Reichenbach P, Khoriauli L, Giulotto E, & Lingner J (2007) Telomeric repeat containing RNA and RNA surveillance factors at mammalian chromosome ends. *Science* 318(5851):798-801.

72. Deng Z, Norseen J, Wiedmer A, Riethman H, & Lieberman PM (2009) TERRA RNA binding to TRF2 facilitates heterochromatin formation and ORC recruitment at telomeres. *Mol Cell* 35(4):403-413.

73. Hayflick L & Moorhead PS (1961) The serial cultivation of human diploid cell strains. *Exp Cell Res* 25:585-621.

74. Shay JW & Bacchetti S (1997) A survey of telomerase activity in human cancer. *Eur J Cancer* 33(5):787-791.

75. Bryan TM, Englezou A, Dalla-Pozza L, Dunham MA, & Reddel RR (1997) Evidence for an alternative mechanism for maintaining telomere length in human tumors and tumor-derived cell lines. *Nat Med* 3(11):1271-1274.

76. Dunham MA, Neumann AA, Fasching CL, & Reddel RR (2000) Telomere maintenance by recombination in human cells. *Nat Genet* 26(4):447-450.

77. Reddel RR (2000) The role of senescence and immortalization in carcinogenesis. *Carcinogenesis* 21(3):477-484.

78. de Lange T (2004) T-loops and the origin of telomeres. *Nat Rev Mol Cell Biol* 5(4):323-329.

79. Henson JD, Neumann AA, Yeager TR, & Reddel RR (2002) Alternative lengthening of telomeres in mammalian cells. *Oncogene* 21(4):598-610.

80. Tomaska L, Nosek J, Kramara J, & Griffith JD (2009) Telomeric circles: universal players in telomere maintenance? *Nat Struct Mol Biol* 16(10):1010-1015.

81. Hall CB*, et al.* (2004) Congenital infections with human herpesvirus 6 (HHV6) and human herpesvirus 7 (HHV7). *J Pediatr* 145(4):472-477.

82. Boyum A (1968) Separation of leukocytes from blood and bone marrow. Introduction. *Scand J Clin Lab Invest Suppl* 97:7.

83. Bandobashi K*, et al.* (1997) Human herpesvirus 6 (HHV-6)-positive Burkitt's lymphoma: establishment of a novel cell line infected with HHV-6. *Blood* 90(3):1200-1207.

84. Neipel F, Ellinger K, & Fleckenstein B (1991) The unique region of the human herpesvirus 6 genome is essentially collinear with the UL segment of human cytomegalovirus. *The Journal of general virology* 72 (Pt 9):2293-2297.

85. Southern EM (1975) Detection of specific sequences among DNA fragments separated by gel electrophoresis. *J Mol Biol* 98(3):503-517.

86. Collins CM, Medveczky MM, Lund T, & Medveczky PG (2002) The terminal repeats and latency-associated nuclear antigen of herpesvirus saimiri are essential for episomal persistence of the viral genome. *The Journal of general virology* 83(Pt 9):2269-2278.

87. Medveczky MM*, et al.* (1989) Herpesvirus saimiri strains from three DNA subgroups have different oncogenic potentials in New Zealand white rabbits. *Journal of virology* 63(9):3601-3611.

88. Gardella T, Medveczky P, Sairenji T, & Mulder C (1984) Detection of circular and linear herpesvirus DNA molecules in mammalian cells by gel electrophoresis. *Journal of virology* 50(1):248-254.

89. Rieder MJ, Taylor SL, Tobe VO, & Nickerson DA (1998) Automating the identification of DNA variations using quality-based fluorescence re-sequencing: analysis of the human mitochondrial genome. *Nucleic Acids Res* 26(4):967-973.

90. Kowalska A*, et al.* (2007) A new platform linking chromosomal and sequence information. *Chromosome Res* 15(3):327-339.

91. Vandesompele J*, et al.* (2002) Accurate normalization of real-time quantitative RT-PCR data by geometric averaging of multiple internal control genes. *Genome Biol* 3(7):RESEARCH0034.

92. Cote HC*, et al.* (2002) Changes in mitochondrial DNA as a marker of nucleoside toxicity in HIV-infected patients. *N Engl J Med* 346(11):811-820.

93. Medveczky P, Chang C-W, Oste C, & Mulder C (1987) Rapid vacuum driven transfer of DNA and RNA from gels to solid supports. *BioTechniques* 5(3):242-246.

94. Ochman H, Gerber AS, & Hartl DL (1988) Genetic applications of an inverse polymerase chain reaction. *Genetics* 120(3):621-623.

95. Britt-Compton B*, et al.* (2006) Structural stability and chromosome-specific telomere length is governed by cis-acting determinants in humans. *Hum Mol Genet* 15(5):725-733.

96. Baird DM (2005) New developments in telomere length analysis. *Exp Gerontol* 40(5):363-368.

97. Baird DM, Rowson J, Wynford-Thomas D, & Kipling D (2003) Extensive allelic variation and ultrashort telomeres in senescent human cells. *Nat Genet* 33(2):203-207.

98. Hall CB*, et al.* (2008) Chromosomal integration of human herpesvirus 6 is the major mode of congenital human herpesvirus 6 infection. *Pediatrics* 122(3):513-520.

99. Gompels UA & Macaulay HA (1995) Characterization of human telomeric repeat sequences from human herpesvirus 6 and relationship to replication. *The Journal of general virology* 76 (Pt 2):451-458.

100. Rieder CL & Palazzo RE (1992) Colcemid and the mitotic cycle. *J Cell Sci* 102 (Pt 3):387-392.

101. Graham FL, Smiley J, Russell WC, & Nairn R (1977) Characteristics of a human cell line transformed by DNA from human adenovirus type 5. *The Journal of general virology* 36(1):59-74.

102. Borenstein R & Frenkel N (2009) Cloning human herpes virus 6A genome into bacterial artificial chromosomes and study of DNA replication intermediates. *Proceedings of the National Academy of Sciences of the United States of America* 106(45):19138-19143.

103. Tang H*, et al.* (2010) Human herpesvirus 6 encoded glycoprotein Q1 gene is essential for virus growth. *Virology*.

104. Thomson BJ, Dewhurst S, & Gray D (1994) Structure and heterogeneity of the a sequences of human herpesvirus 6 strain variants U1102 and Z29 and identification of human telomeric repeat sequences at the genomic termini. *Journal of virology* 68(5):3007-3014.

105. Rapp JC, Krug LT, Inoue N, Dambaugh TR, & Pellett PE (2000) U94, the human herpesvirus 6 homolog of the parvovirus nonstructural gene, is highly conserved among isolates and is expressed at low mRNA levels as a spliced transcript. *Virology* 268(2):504-516.

106. Chang LK & Liu ST (2000) Activation of the BRLF1 promoter and lytic cycle of Epstein-Barr virus by histone acetylation. *Nucleic Acids Res* 28(20):3918-3925.

107. Lu F*, et al.* (2003) Chromatin remodeling of the Kaposi's sarcoma-associated herpesvirus ORF50 promoter correlates with reactivation from latency. *Journal of virology* 77(21):11425-11435.

108. Toth KF*, et al.* (2004) Trichostatin A-induced histone acetylation causes decondensation of interphase chromatin. *J Cell Sci* 117(Pt 18):4277-4287.

109. Chen J*, et al.* (2001) Activation of latent Kaposi's sarcoma-associated herpesvirus by demethylation of the promoter of the lytic transactivator. *Proceedings of the National Academy of Sciences of the United States of America* 98(7):4119-4124.

110. Yasukawa M*, et al.* (1999) Latent infection and reactivation of human herpesvirus 6 in two novel myeloid cell lines. *Blood* 93(3):991-999.

111. Martin ME*, et al.* (1991) The genome of human herpesvirus 6: maps of unit-length and concatemeric genomes for nine restriction endonucleases. *The Journal of general virology* 72 (Pt 1):157-168.

112. Severini A, Sevenhuysen C, Garbutt M, & Tipples GA (2003) Structure of replicating intermediates of human herpesvirus type 6. *Virology* 314(1):443-450.

113. Deng Z*, et al.* (2002) Telomeric proteins regulate episomal maintenance of Epstein-Barr virus origin of plasmid replication. *Mol Cell* 9(3):493-503.

114. Zhou J, Snyder AR, & Lieberman PM (2009) Epstein-Barr virus episome stability is coupled to a delay in replication timing. *Journal of virology* 83(5):2154-2162.

115. Im DS & Muzyczka N (1990) The AAV origin binding protein Rep68 is an ATP-dependent site-specific endonuclease with DNA helicase activity. *Cell* 61(3):447-457.

116. Henckaerts E*, et al.* (2009) Site-specific integration of adeno-associated virus involves partial duplication of the target locus. *Proceedings of the National Academy of Sciences of the United States of America* 106(18):7571-7576.

117. Samulski RJ*, et al.* (1991) Targeted integration of adeno-associated virus (AAV) into human chromosome 19. *EMBO J* 10(12):3941-3950.

118. Verma SC, Choudhuri T, Kaul R, & Robertson ES (2006) Latency-associated nuclear antigen (LANA) of Kaposi's sarcoma-associated herpesvirus interacts with origin recognition complexes at the LANA binding sequence within the terminal repeats. *Journal of virology* 80(5):2243-2256.

119. Verma SC, Lan K, Choudhuri T, & Robertson ES (2006) Kaposi's sarcoma-associated herpesvirus-encoded latency-associated nuclear antigen modulates K1 expression through its cis-acting elements within the terminal repeats. *Journal of virology* 80(7):3445-3458.

120. Lan K, Kuppers DA, Verma SC, & Robertson ES (2004) Kaposi's sarcoma-associated herpesvirus-encoded latency-associated nuclear antigen inhibits lytic replication by targeting Rta: a potential mechanism for virus-mediated control of latency. *Journal of virology* 78(12):6585-6594.

121. Barbera AJ*, et al.* (2006) The nucleosomal surface as a docking station for Kaposi's sarcoma herpesvirus LANA. *Science (New York, N.Y* 311(5762):856-861.

122. Rotola A*, et al.* (1998) U94 of human herpesvirus 6 is expressed in latently infected peripheral blood mononuclear cells and blocks viral gene expression in transformed lymphocytes in culture. *Proceedings of the National Academy of Sciences of the United States of America* 95(23):13911-13916.

123. Caselli E*, et al.* (2006) Human herpesvirus 6 (HHV-6) U94/REP protein inhibits betaherpesvirus replication. *Virology* 346(2):402-414.

124. Dhepakson P*, et al.* (2002) Human herpesvirus-6 rep/U94 gene product has single-stranded DNA-binding activity. *The Journal of general virology* 83(Pt 4):847-854.

125. Araujo JC*, et al.* (1995) Human herpesvirus 6A ts suppresses both transformation by H-ras and transcription by the H-ras and human immunodeficiency virus type 1 promoters. *Journal of virology* 69(8):4933-4940.

126. Mori Y*, et al.* (2000) Expression of human herpesvirus 6B rep within infected cells and binding of its gene product to the TATA-binding protein in vitro and in vivo. *Journal of virology* 74(13):6096-6104.

127. Thomson BJ, Efstathiou S, & Honess RW (1991) Acquisition of the human adeno-associated virus type-2 rep gene by human herpesvirus type-6. *Nature* 351(6321):78-80.

128. Hickman AB, Ronning DR, Perez ZN, Kotin RM, & Dyda F (2004) The nuclease domain of adeno-associated virus rep coordinates replication initiation using two distinct DNA recognition interfaces. *Mol Cell* 13(3):403-414.

129. Thomson BJ, Weindler FW, Gray D, Schwaab V, & Heilbronn R (1994) Human herpesvirus 6 (HHV-6) is a helper virus for adeno-associated virus type 2 (AAV-2) and the AAV-2 rep gene homologue in HHV-6 can mediate AAV-2 DNA replication and regulate gene expression. *Virology* 204(1):304-311.

130. James JA*, et al.* (2003) Crystal structure of the SF3 helicase from adeno-associated virus type 2. *Structure* 11(8):1025-1035.

131. Baralle D (2001) Chromosomal aberrations, subtelomeric defects, and mental retardation. *Lancet* 358(9275):7-8.

132. Biesecker LG (2002) The end of the beginning of chromosome ends. *Am J Med Genet* 107(4):263-266.

133. De Vries BB, Winter R, Schinzel A, & van Ravenswaaij-Arts C (2003) Telomeres: a diagnosis at the end of the chromosomes. *J Med Genet* 40(6):385-398.

134. Walter S*, et al.* (2004) Subtelomere FISH in 50 children with mental retardation and minor anomalies, identified by a checklist, detects 10 rearrangements including a de novo balanced translocation of chromosomes 17p13.3 and 20q13.33. *Am J Med Genet A* 128A(4):364-373.

135. Bowen T*, et al.* (1999) Linkage studies of bipolar disorder with chromosome 18 markers. *Am J Med Genet* 88(5):503-509.

136. Freimer NB*, et al.* (1996) Genetic mapping using haplotype, association and linkage methods suggests a locus for severe bipolar disorder (BPI) at 18q22-q23. *Nat Genet* 12(4):436-441.

137. Ottaviani A, Gilson E, & Magdinier F (2008) Telomeric position effect: from the yeast paradigm to human pathologies? *Biochimie* 90(1):93-107.

138. Gottschling DE, Aparicio OM, Billington BL, & Zakian VA (1990) Position effect at S. cerevisiae telomeres: reversible repression of Pol II transcription. *Cell* 63(4):751-762.

139. Tham WH & Zakian VA (2002) Transcriptional silencing at Saccharomyces telomeres: implications for other organisms. *Oncogene* 21(4):512-521.

140. Wyrick JJ*, et al.* (1999) Chromosomal landscape of nucleosome-dependent gene expression and silencing in yeast. *Nature* 402(6760):418-421.

141. Baur JA, Zou Y, Shay JW, & Wright WE (2001) Telomere position effect in human cells. *Science* 292(5524):2075-2077.

142. Luke B & Lingner J (2009) TERRA: telomeric repeat-containing RNA. *EMBO J*.

143. Mori T*, et al.* (2009) Transmission of chromosomally integrated human herpesvirsus 6 (HHV-6) variant A from a parent to children leading to misdiagnosis of active HHV-6 infection. *Transpl Infect Dis* 11(6):503-506.

144. Clark DA*, et al.* (2006) Transmission of integrated human herpesvirus 6 through stem cell transplantation: implications for laboratory diagnosis. *J Infect Dis* 193(7):912-916.

145. Daibata M, Taguchi T, Nemoto Y, Taguchi H, & Miyoshi I (1999) Inheritance of chromosomally integrated human herpesvirus 6 DNA. *Blood* 94(5):1545-1549.

146. Jeulin H*, et al.* (2009) Contribution of human herpesvirus 6 (HHV-6) viral load in whole blood and serum to investigate integrated HHV-6 transmission after haematopoietic stem cell transplantation. *J Clin Virol* 45(1):43-46.

147. Kamble RT*, et al.* (2007) Transmission of integrated human herpesvirus-6 in allogeneic hematopoietic stem cell transplantation. *Bone Marrow Transplant* 40(6):563-566.

148. Troy SB*, et al.* (2008) Severe encephalomyelitis in an immunocompetent adult with chromosomally integrated human herpesvirus 6 and clinical response to treatment with foscarnet plus ganciclovir. *Clin Infect Dis* 47(12):e93-96.

149. Daibata M, Taguchi T, Sawada T, Taguchi H, & Miyoshi I (1998) Chromosomal transmission of human herpesvirus 6 DNA in acute lymphoblastic leukaemia. *Lancet* 352(9127):543-544.

150. Hubacek P*, et al.* (2009) Prevalence of HHV-6 integrated chromosomally among children treated for acute lymphoblastic or myeloid leukemia in the Czech Republic. *J Med Virol* 81(2):258-263.

151. Chen M*, et al.* (1994) Human herpesvirus 6 infects cervical epithelial cells and transactivates human papillomavirus gene expression. *Journal of virology* 68(2):1173-1178.

152. Bannert N & Kurth R (2004) Retroelements and the human genome: new perspectives on an old relation. *Proceedings of the National Academy of Sciences of the United States of America* 101 Suppl 2:14572-14579.

153. Prusty BK, zur Hausen H, Schmidt R, Kimmel R, & de Villiers EM (2008) Transcription of HERV-E and HERV-E-related sequences in malignant and non-malignant human haematopoietic cells. *Virology* 382(1):37-45.

154. Duelli D & Lazebnik Y (2007) Cell-to-cell fusion as a link between viruses and cancer. *Nat Rev Cancer* 7(12):968-976.

155. Griffiths PD*, et al.* (1999) Human herpesviruses 6 and 7 as potential pathogens after liver transplant: prospective comparison with the effect of cytomegalovirus. *J Med Virol* 59(4):496-501.

156. Kidd IM*, et al.* (2000) Prospective study of human betaherpesviruses after renal transplantation: association of human herpesvirus 7 and cytomegalovirus co-infection with cytomegalovirus disease and increased rejection. *Transplantation* 69(11):2400-2404.

APPENDIX A: iHHV-6 SEQUENCING DATA

ORF U94 (U1102 141267 - 143197)

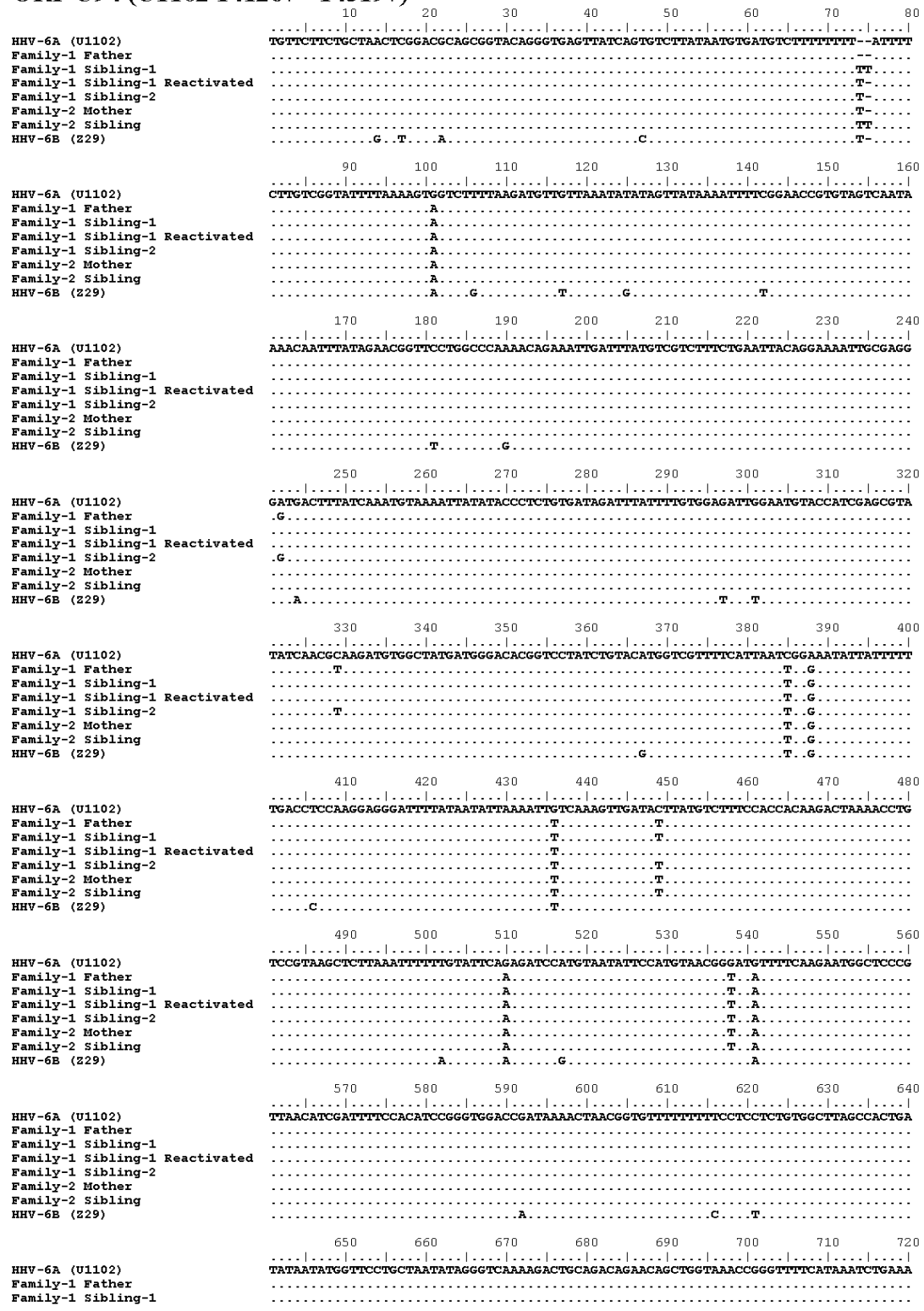

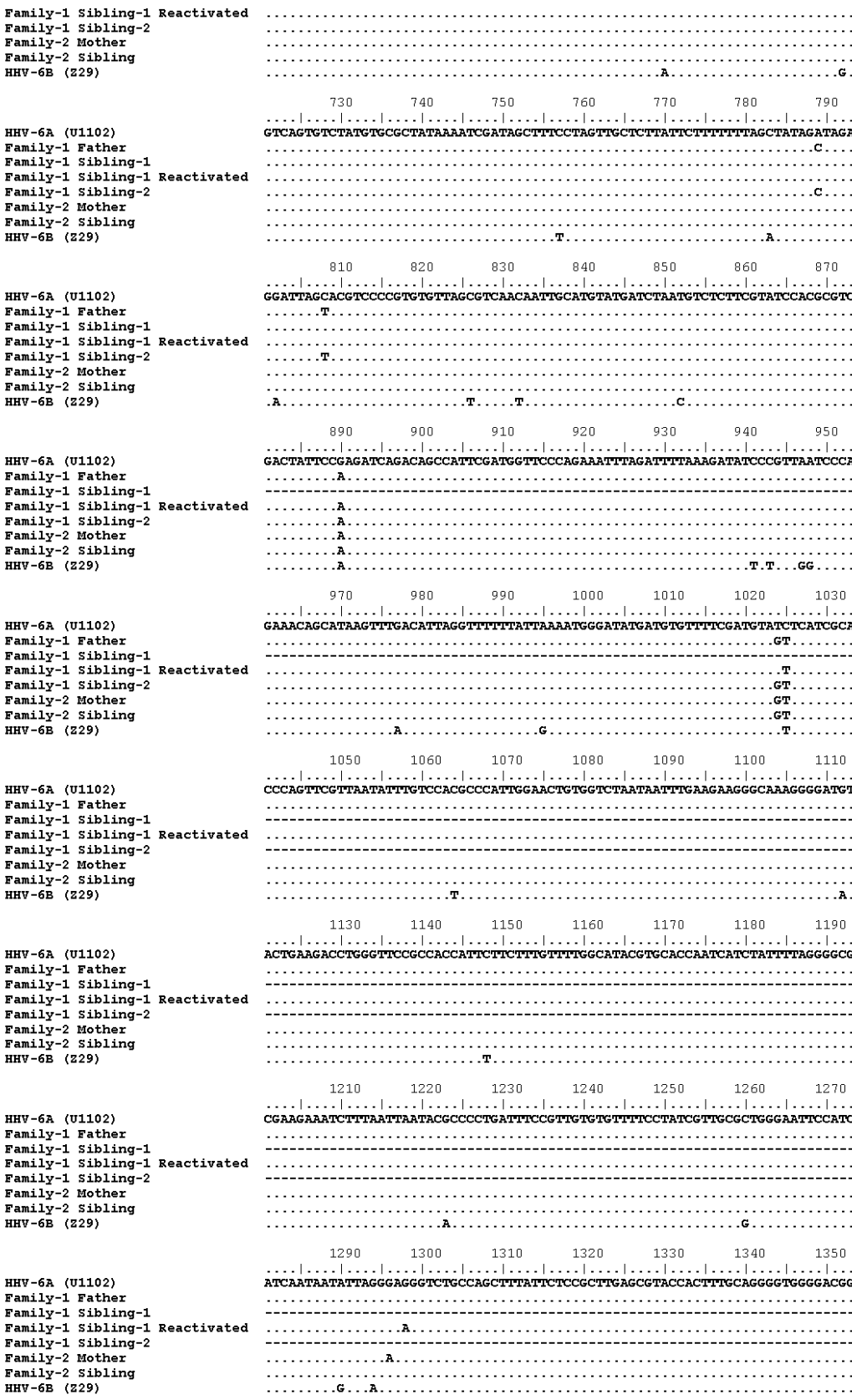
Family-1 Sibling-1 Reactivated
Family-1 Sibling-2
Family-2 Mother
Family-2 Sibling
HHV-6B (Z29)
730 740 750 760 770 780 790 800
HHV-6A (U1102) GTCAGTGTCTATGTGCGCTATAAAATCGATAGCTTTCCTAGTTGCTCTTATTCTTTTTTTAGCTATAGATAGAGCCCTAT
Family-1 Father
Family-1 Sibling-1
Family-1 Sibling-1 Reactivated
Family-1 Sibling-2
Family-2 Mother
Family-2 Sibling
HHV-6B (Z29)
810 820 830 840 850 860 870 880
HHV-6A (U1102) GGATTAGCACGTCCCCGTGTGTTAGCGTCAACAATTGCATGTATGATCTAATGTCTCTTCGTATCCACGCGTCTTCCG-T
Family-1 Father
Family-1 Sibling-1
Family-1 Sibling-1 Reactivated
Family-1 Sibling-2
Family-2 Mother
Family-2 Sibling
HHV-6B (Z29)
890 900 910 920 930 940 950 960
HHV-6A (U1102) GACTATTCCGAGATCAGACAGCCATTCGATGGTTCCCAGAAATTTAGATTTTAAAGATATCCCGTTAATCCCATCCTTTG
Family-1 Father
Family-1 Sibling-1
Family-1 Sibling-1 Reactivated
Family-1 Sibling-2
Family-2 Mother
Family-2 Sibling
HHV-6B (Z29)
970 980 990 1000 1010 1020 1030 1040
HHV-6A (U1102) GAAACAGCATAAGTTTGACATTAGGTTTTTTTATTAAAATGGGATATGATGTGTTTTCGATGTATCTCATCGCATACGTCT
Family-1 Father
Family-1 Sibling-1
Family-1 Sibling-1 Reactivated
Family-1 Sibling-2
Family-2 Mother
Family-2 Sibling
HHV-6B (Z29)
1050 1060 1070 1080 1090 1100 1110 1120
HHV-6A (U1102) CCCAGTTCGTTAATATTTGTCCACGCCCATTGGAACTGTGGTCTAATAATTTGAAGAAGGGCAAAGGGGATGTAACTTAG
Family-1 Father
Family-1 Sibling-1
Family-1 Sibling-1 Reactivated
Family-1 Sibling-2
Family-2 Mother
Family-2 Sibling
HHV-6B (Z29)
1130 1140 1150 1160 1170 1180 1190 1200
HHV-6A (U1102) ACTGAAGACCTGGGTTCCGCCACCATTCTTCTTTGTTTTGGCATACGTGCACCAATCATCTATTTTAGGGGCGTTCCCGT
Family-1 Father
Family-1 Sibling-1
Family-1 Sibling-1 Reactivated
Family-1 Sibling-2
Family-2 Mother
Family-2 Sibling
HHV-6B (Z29)
1210 1220 1230 1240 1250 1260 1270 1280
HHV-6A (U1102) CGAAGAAATCTTTAATTAATACGCCCCTGATTTCCGTTGTGTGTTTTCCTATCGTTGCGCTGGGAATTCCATCTAAAGCT
Family-1 Father
Family-1 Sibling-1
Family-1 Sibling-1 Reactivated
Family-1 Sibling-2
Family-2 Mother
Family-2 Sibling
HHV-6B (Z29)
1290 1300 1310 1320 1330 1340 1350 1360
HHV-6A (U1102) ATCAATAATATTAGGGAGGGTCTGCCAGCTTTATTCTCCGCTTGAGCGTACCACTTTGCAGGGGTGGGGACGGCAGTTTT
Family-1 Father
Family-1 Sibling-1
Family-1 Sibling-1 Reactivated
Family-1 Sibling-2
Family-2 Mother
Family-2 Sibling
HHV-6B (Z29)

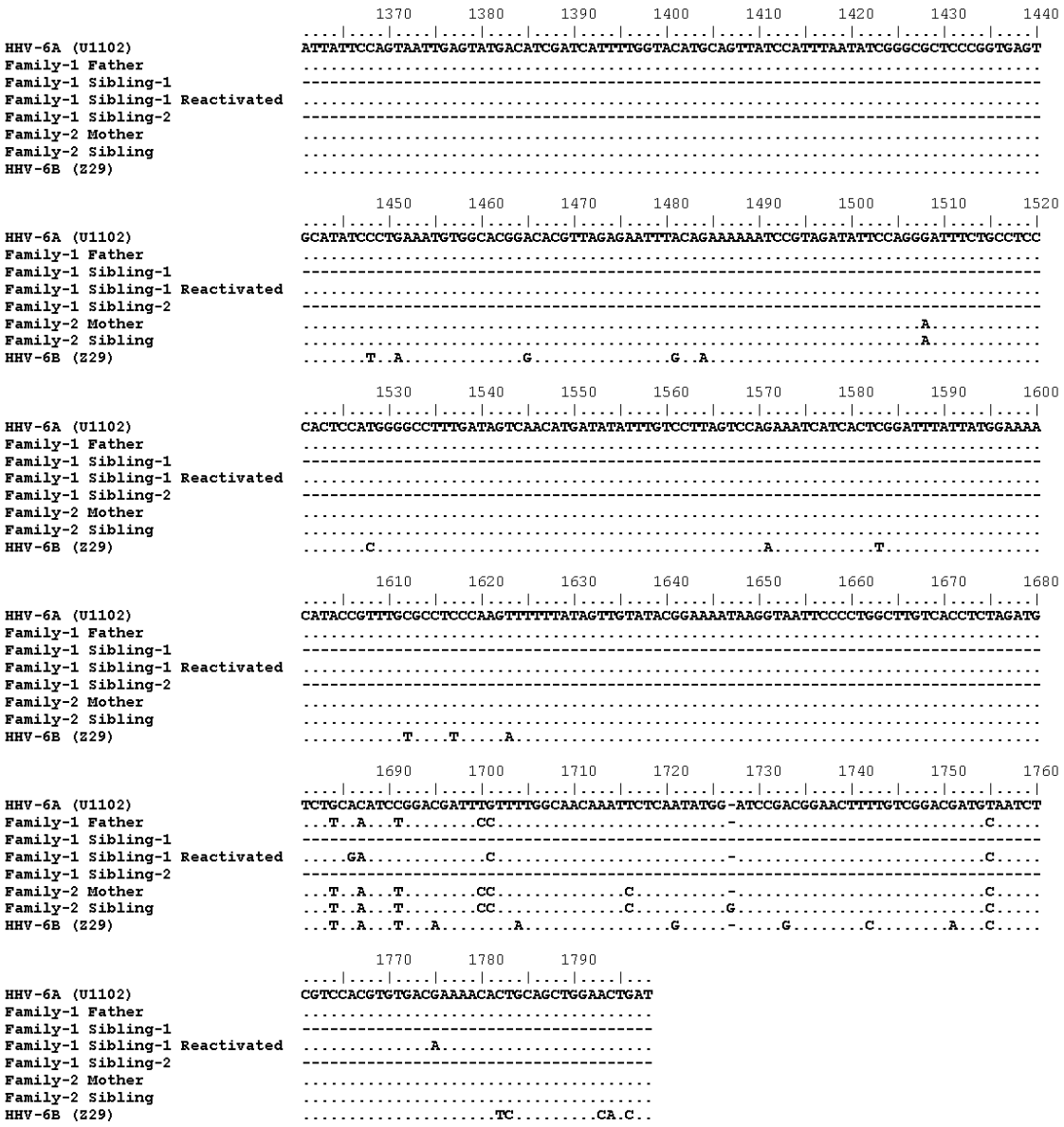
1370 1380 1390 1400 1410 1420 1430 1440
HHV-6A (U1102) ATTATTCCAGTAATTGAGTATGACATCGATCATTTTGGTACATGCAGTTATCCATTTAATATCGGGCGCTCCCGGTGAGT
Family-1 Father
Family-1 Sibling-1
Family-1 Sibling-1 Reactivated
Family-1 Sibling-2
Family-2 Mother
Family-2 Sibling
HHV-6B (Z29)
1450 1460 1470 1480 1490 1500 1510 1520
HHV-6A (U1102) GCATATCCCTGAAATGTGGCACGGACACGTTAGAGAATTTACAGAAAAAATCCGTAGATATTCCAGGGATTTCTGCCTCC
Family-1 Father
Family-1 Sibling-1
Family-1 Sibling-1 Reactivated
Family-1 Sibling-2
Family-2 Mother
Family-2 Sibling
HHV-6B (Z29)
1530 1540 1550 1560 1570 1580 1590 1600
HHV-6A (U1102) CACTCCATGGGGCCTTTGATAGTCAACATGATATATTTGTCCTTAGTCCAGAAATCATCACTCGGATTTATTATGGAAAA
Family-1 Father
Family-1 Sibling-1
Family-1 Sibling-1 Reactivated
Family-1 Sibling-2
Family-2 Mother
Family-2 Sibling
HHV-6B (Z29)
1610 1620 1630 1640 1650 1660 1670 1680
HHV-6A (U1102) CATACCGTTTGCGCCTCCCAAGTTTTTTATAGTTGTATACGGAAAATAAGGTAATTCCCCTGGCTTGTCACCTCTAGATG
Family-1 Father
Family-1 Sibling-1
Family-1 Sibling-1 Reactivated
Family-1 Sibling-2
Family-2 Mother
Family-2 Sibling
HHV-6B (Z29)
1690 1700 1710 1720 1730 1740 1750 1760
HHV-6A (U1102) TCTGCACATCCGGACGATTTGTTTTGGCAACAAATTCTCAATATGG-ATCCGACGGAACTTTTGTCGGACGATGTAATCT
Family-1 Father
Family-1 Sibling-1
Family-1 Sibling-1 Reactivated
Family-1 Sibling-2
Family-2 Mother
Family-2 Sibling
HHV-6B (Z29)
1770 1780 1790
HHV-6A (U1102) CGTCCACGTGTGACGAAAACACTGCAGCTGGAACTGAT
Family-1 Father
Family-1 Sibling-1
Family-1 Sibling-1 Reactivated
Family-1 Sibling-2
Family-2 Mother
Family-2 Sibling
HHV-6B (Z29)

Left Terminal Repeat (U1102 421-1474, 151654-152707)

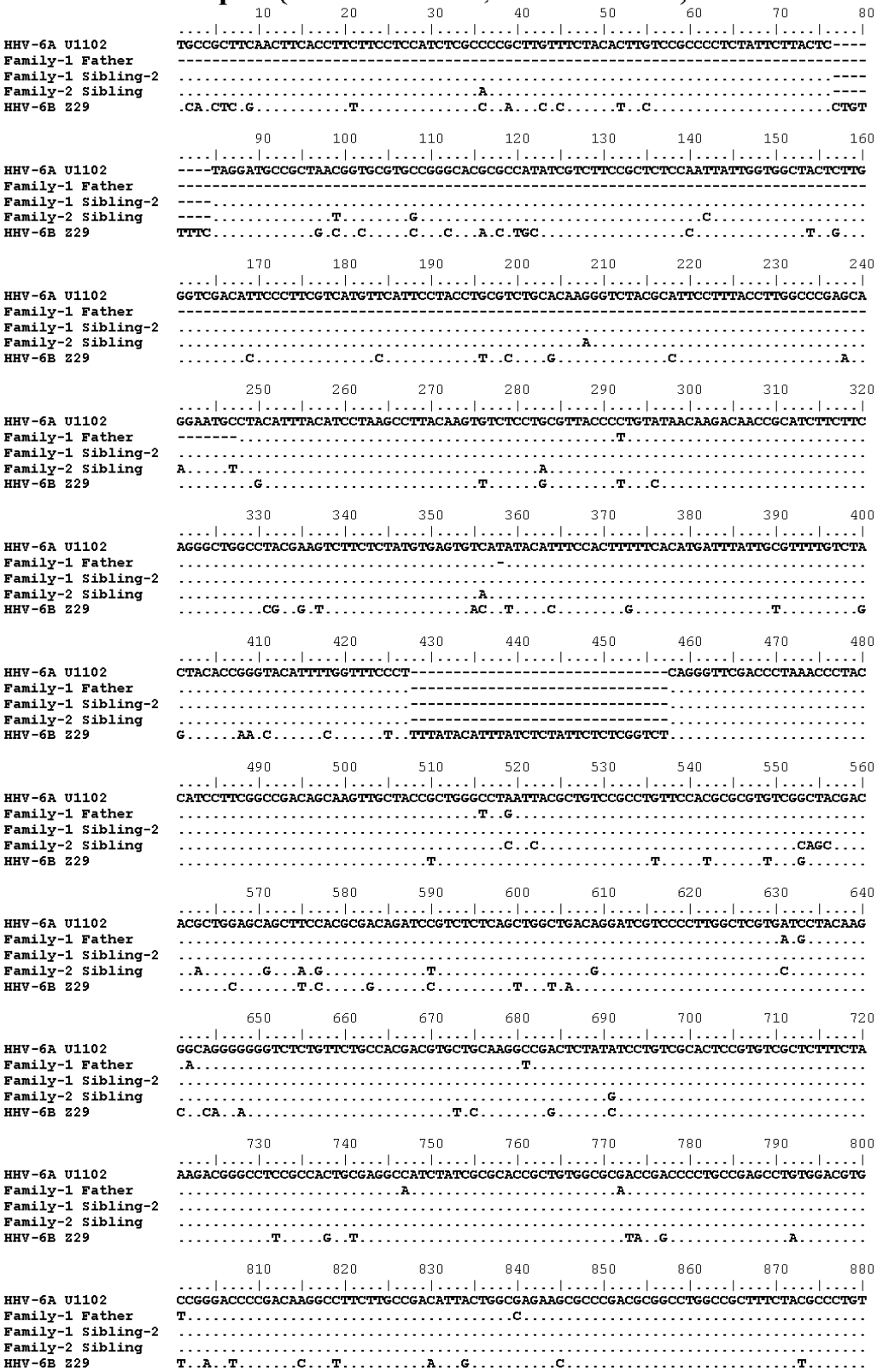

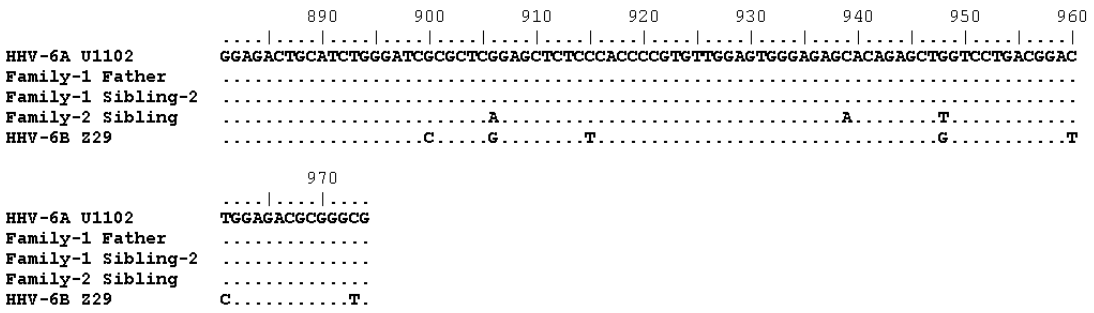

Fig. A1. Multiple sequence alignment of ORF U94 and direct repeat from chromosomally integrated and reactivated iHHV-6A. ORF U94 was amplified with primers U94L-1, U94L-2, U94R-1, and U94R-2; while the left repeat was amplified with primers LTR-1 and LTR-2 from genomic DNA isolated from chromosomally integrated family members. Alignments were completed with ClustalX 2.0 multiple sequence alignment software.

ABOUT THE AUTHOR

Jesse H. Arbuckle grew up in South Londonderry, Vermont and later obtained his Bachelor of Science degree in Biology with a minor in Chemistry from the University of Tampa in 2004. He started his research career in 2002 through 2006 by completing clinical research on the molecular epidemiology of nosocomial strains of methicillin-resistant *Staphylococcus aureus* at Tampa General Hospital in the Department of Pathology. In 2006, he entered the Ph.D. program in Medical Sciences at the University of South Florida College of Medicine in the Department of Molecular Medicine. He investigated the molecular biology of Human Herpesviruses 6A and 6B latency and telomere integration. During matriculation he obtained several travel grants to present his research at national and international conferences. He received the USF Golden Bull Award for academic excellence and was awarded first prize in oral and poster presentations at the USF College of Medicine Research Day and the SIPAIID symposium. He has currently published two manuscripts with first-authorships, one that was featured in the *Proceedings for the National Academia of Sciences* (2010) and another in *Microbes and Infection* (2011), both of which are based on his doctoral research. He was accepted to start his post-doctoral training in herpesvirology at The National Institute of Allergy and Infectious Diseases in the Molecular Genetics Section of Viral Diseases.